CONFERENCE PROGRAM

4TH International PEEK Meeting

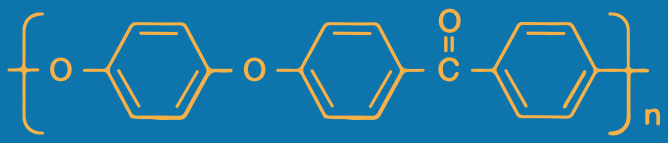

WASHINGTON, D.C.
April 25-26

2019

ORGANIZED BY

IRC IMPLANT RESEARCH CENTER

Exponent®

SPONSORED BY

Invibio BIOMATERIAL SOLUTIONS

Supporting the Future of Medical PEEK

Invibio is honored to support the 4th International PEEK Meeting and its mission to bring together the scientific and regulatory communities to present leading edge research on advancements in medical polyaryletherketone (PAEK) polymer technologies and clinical applications. We look forward to a productive and rewarding conference.

LEARN MORE ABOUT US AT:
invibio.com

Invibio
BIOMATERIAL SOLUTIONS

Stay at the Forefront of Medical PEEK Innovation

Online Reference for PEEK Implants

- Complimentary reference for polyaryletherketones used in medical devices
- Highlights recent developments in clinically relevant PEEK research
- Stimulate biomaterial investigations related to medical grade PEEK

REGISTER AT:
medicalpeek.org/register

Medical PEEK Lexicon

4TH International PEEK Meeting

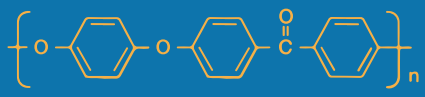

Dear Participant,

The purpose of the conference is to bring together engineers, scientists, regulators and clinicians from academia, industry and government agencies. Leading edge research on advancements in medical grade polyaryletherketone (PAEK) polymer technology and clinical applications will be presented:

- Additive manufacturing of PEEK and its composites
- Innovations in orthopedic bearings
- Bioactive PEEK composites
- Spinal rods and artificial disc applications
- Formulations for dental, trauma and arthroscopic implants
- Structural composites and woven fiber applications
- Biologic aspects of wear debris

Abstracts were evaluated by the Scientific Committee for inclusion in the program, either as a podium presentation or a poster.

Scientific Committee

Steven Kurtz, PhD
CONFERENCE ORGANIZER
Implant Research Center, Drexel University & Exponent, Inc.

Joanne Tipper, PhD
University of Technology Sydney

Jeremy Gilbert, PhD
Clemson University

Kate Kavlock, PhD
US FDA CDRH (Center for Devices and Radiological Health)

John Bowsher, PhD
US FDA CDRH

SPONSORED BY

Invibio
BIOMATERIAL SOLUTIONS

Invibio
BIOMATERIAL SOLUTIONS

Meeting Future Needs of Medical Device Manufacturers, Healthcare Professionals and Patients

Invibio is a proven partner that can add value to all stages of a medical device product lifecycle.

Pre-launch

MARKET RESEARCH to determine the challenges

IMPACT ON HEALTH ECONOMICS for PEEK-OPTIMA™ Polymer potential economic outcomes

DEVELOP MATERIALS AND COMPONENTS using multiple approaches

PERFORMANCE VALIDATION to define performance criteria and address risk

Launch and beyond

REGULATORY SUPPORT AND EDUCATION with global trusted relationships

KOL ENGAGEMENT for educational activities

CLINICAL EVIDENCE PROGRAMS to develop evidence-based medicine for PEEK-OPTIMA Polymer devices

CLINICAL RELATIONS for commercial support

Invibio.com

Copyright © 2019 Invibio Ltd. INVIBIO™, PEEK-OPTIMA™, JUVORA™, INVIBIO BIOMATERIAL SOLUTIONS™ are trademarks of Victrex plc or its group companies. All rights reserved.

a victrex company

4TH INTERNATIONAL PEEK MEETING AGENDA

Thursday Morning, April 25

WELCOME

8:00 am	On-site Registration Opens	
9:00 am	Welcome, Opening Remarks & Advances Since 2017	*Steve Kurtz, PhD*

SESSION I: Processing and Properties of PAEK and PAEK Composites

Moderators: Clare Rimnac, PhD, and Hany Demian, FDA

9:15 am	**Invited Talk 1:** Recent Developments in Understanding the Fatigue Behavior of PEEK Materials	*Clare Rimnac, PhD*
9:35 am	**Podium Talk 1:** Fractography of PEEK Filled Materials from Tensile, Impact, and Fatigue Crack Propagation Testing	*MariAnne Sullivan, PhD*
9:50 am	**Podium Talk 2:** The nanomechanical properties of annealed PEEK with PITCH-based and PAN-based carbon fibers: the effect of annealing and indentation tip diameter	*Sofia E Arevalo*
10:05 am	**Podium Talk 3:** Next Generation VESTAKEEP® PEEK	*Balaji Prabhu*
10:20 am	**Coffee Break**	

SESSION II: Engineering PEEK Bioactivity

Moderators: Noreen Hickock, and Michele Marcolongo

10:50 am	**Podium Talk 4:** Enhancements to Cell Proliferation, Bone Tissue Production, Biofilm Formation Resistance, and Radiolucency Observed *in vitro* when Silicon Nitride-type Materials are Compounded into PEEK	*Ryan M. Bock, PhD*
11:05 am	**Podium Talk 5:** Silver Carboxylate Coating Prevents Adherence of Multi Drug Resistant *Serratia marcescens* on Polyetherether Ketone	*Andrea Gilmore*
11:20 am	**Podium Talk 6:** A novel polyetheretherketone-zeolite composite reduces long term inflammatory response in an ovine cervical fusion model	*Siriam Sankar*
11:35 am	**Podium Talk 7:** Best osseointegrative surface characteristics of PEEK implants due to an evolutionary surface functionalization technique MBT (Mimicking Bone Technology)	*Dietmar Schaffarczyk*
11:50 am	**Podium Talk 8:** Results of In-vivo Testing of a Novel Macro-Scale Osseointegration Surface Morphology	*Greg Causey, PhD*
12:05 pm	**Short Podium Talks**	*Selected Poster Presenters*
12:30 pm	**Lunch & Poster Session 1**	

4TH INTERNATIONAL PEEK MEETING AGENDA

Thursday Afternoon, April 25

SESSION III: Additive Manufacturing of PAEKs

Co-Moderators: Matthew Di Prima, PhD, FDA, and Steve Kurtz, PhD

2:00 pm	**Invited Talk 2:** Update on regulating 3D-printed medical products	*Matthew Di Prima, PhD*
2:20 pm	**Podium Talk 9:** Characterization of PEEK filaments for Fused Filament Fabrication (FFF)	*Manuel Garcia-Leiner, PhD*
2:40 pm	**Podium Talk 10:** Developments in PAEKs for Additive Manufacture	*Robert McKay*
2:55 pm	**Podium Talk 11:** Apium M220 medical device manufacturing machine	*Uwe Popp, PhD*
3:10 pm	**Podium Talk 12:** 3D Printing Of Medical Products with PEEK Using FLM Technology	*Stefan Leonhardt, PhD*
3:25 pm	**Afternoon Coffee Break**	

SESSION IV: 3D Printed Orthopedic and Spinal Implants

3:45 pm	**Podium Talk 13:** Effect of Pore Size on Bone Regeneration of 3D-printed Porous PEEK Implant in Critical Size Bone Defects	*Kai Xie, MD*
4:00 pm	**Podium Talk 14:** Comparison of different FFF PEEK printer generations and nozzle sizes for FFF printed PEEK spinal cages	*Cemile Basgul*
4:15 pm	**Podium Talk 15:** PEEK laser sintered intervertebral lumbar cages: process and properties	*Oana Ghita, PhD*
4:30 pm	**Podium Talk 16:** In Vitro Response to FFF Printed Porous PEEK Surfaces	*Hannah Spece*
	Day 1 Meeting Adjourns (Time??)	
6:00 pm	**Reception and Dinner Begins**	

4TH INTERNATIONAL PEEK MEETING AGENDA

Friday Morning, April 26

8:00 am	On-site Registration Opens, Breakfast	

PAPER SESSION V: Spinal Applications of PAEK

Session Chairpersons: Katherine Kavlock, PhD, FDA, and Brennan Torstrick, PhD

9:00 am	**Podium Talk 17:** Anterior Lumbar Interbody Fusion; A prospective, unmasked, non-randomized study of 240 patients utilizing a PEEK® Optima ALIF cage	*Matthew Scott-Young, MSSB, FRACS, FAOrthA*
9:15 am	**Podium Talk 18:** Effects of Toggling Loading on Pullout Strength of Modified Unilateral Spinal Constructs with PEEK and Titanium Rods	*Y. Uslan*
9:30 am	**Podium Talk 19:** Effect of Porous Orthopaedic Implant Material and Structure on Load Sharing with Simulated Bone Ingrowth: A Finite Element Analysis Comparing Titanium and PEEK	*David Safranski, PhD*
9:45 am	**Podium Talk 20:** Impaction Durability of Porous PEEK and Titanium-coated PEEK Interbody Fusion Devices	*Brennan Torstrick, PhD*
10:00 am	**Morning Coffee Break**	

PAPER SESSION VI: Novel Clinical Applications of PEEK

Session Chairpersons: John Bowsher, PhD, FDA, and Philip Hyde, PhD

10:30 am	**Podium Talk 21:** Orthodontic Thermoactive Archwire - PEEK	*Alan Rodrigues*
10:45 am	**Podium Talk 22:** Wear Performance of an All-Polymer Total Knee Replacement	*Raelene Cowie, PhD*
11:00 am	**Podium Talk 23:** The quantification and characterisation of the wear debris produced from Poly-ether-ether-ketone (PEEK) based bearing couples from a multi-directional motion pin-on-plate test rig	*Kathryn Chamberlain, PhD*
11:15 am	**Podium Talk 24:** Medical Imaging of an All-polymer Total Knee Arthroplasty	*Adam Briscoe, PhD*
11:30 am	**Podium Talk 25:** The Role of Contact Mechanics on the Fretting Corrosion Performance of PEEK-Metal Taper Junctions	*Stephanie Smith*
11:45 pm	**Meeting Adjourn**	

4TH International PEEK Meeting

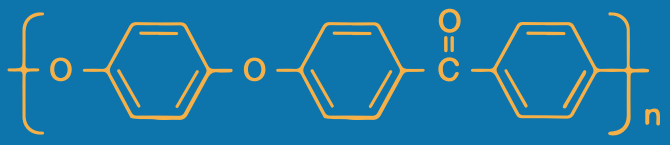

WASHINGTON, D.C.
April 25-26

2019

ABSTRACTS

ABSTRACTS

Recent Developments in Understanding the Fatigue Behavior of PEEK Materials

Rimnac, CM[1] and Sobieraj, MC[2]
[1]Case Western Reserve University, Cleveland, OH
[2]Geisinger Wyoming Valley Medical Center Wilkes-Barre, PA
clare.rimnac@case.edu

Introduction: In its use in medical devices, it is important to understand how PEEK behaves in terms of resistance to fracture under fatigue conditions given that most orthopaedic, dental, and cardiovascular components can be expected to be subjected to tens of millions of loading cycles during in vivo use.

This presentation will review recent efforts to better understand the fatigue behavior of PEEK materials as affected by intrinsic and extrinsic factors.

Fatigue of PEEK under S-N and ε-N Conditions: Little has been published in recent years on the smooth specimen stress-life (S-N) behavior of PEEK, while there has been increasing interest in the strain-life (ε-N) behavior. With regard to S-N behavior, Abbasnezhad et al [1] showed that both increasing stress amplitude and increasing test frequency (≥10 Hz) significantly reduced specimen lifetime. In contrast, Shrestha and coworkers [2] performed fully reversed strain-life (ε-N) tests and found that lower test frequencies (range: 0.25-2Hz) may be associated with decreased fatigue life of PEEK.

Shrestha and coworkers [3] have also investigated the effects of load history and sequence on the deformation and fatigue of PEEK using ε-N testing conditions. They tested under both fully reversed loading (strain ratio = -1) and pulsating tension loading (strain ratio = 0). For fully reversed loading they found that preloading a specimen at a different strain amplitude for a given number of cycles extended the fatigue life. Interestingly, it did not seem to matter whether the preloading was at a higher strain or a lower strain than the final strain amplitude or whether there were multiple cycles of preloading. In pulsating tension tests, preloading had minimal effect with a trend toward shorter lives when preloaded.

Simsiriwong et al [4] have investigated the effects of microstructural inclusions on the fatigue life of PEEK utilizing uniaxial, fully reversed, ε-N fatigue tests. The authors correlated their analysis of the fracture surfaces to a multi-staged fatigue model. Based on their fracture surfaces they concluded that, at higher strains, a physically small crack growth regime was where the main portion of fatigue lifetime was spent. As the cyclic strain was reduced, this transitioned to the majority of the lifetime being spent in the growth of a microstructurally small crack and to an incubation period. The model they developed suggested that in the long lifetime regime the majority of the lifetime was spent in incubation of a crack, as would be expected.

Shrestha et al [3] also investigated the cyclic deformation of PEEK in fully reversed strain controlled testing as well as the effects of mean strain on PEEK fatigue [5]. Under multiple strain levels and multiple strain ratios, including fully reversed, they found significant stress relaxation in PEEK, with the mean stress approaching zero at higher cycles. This softening correlated to increased temperature of the specimen due to generation of hysteresis energy. As the mean stress stabilized at a new value, the specimen temperature stabilized as well. They showed that the rate of stress relaxation was significantly dependent on both the strain amplitude and the strain ratio. Notably, they showed that larger inclusions (particles or void-like defects) generally resulted in a shorter fatigue lifetime. Additionally, void-like defects caused a greater decrease in fatigue lifetime then similarly sized particle inclusions.

Taken together, these fundamental fatigue studies suggest that investigation into the clinical relevance of intrinsic factors (beyond molecular weight and crystallinity) such as inclusions and defects, and extrinsic factors such as frequency, preloading and mean strain effects on the fatigue behavior of PEEK materials may be warranted given that these factors may affect design criteria with regards to the anticipated cyclic lifetime of PEEK devices during in vivo use.

Surface Porous Manufactured PEEK and Fatigue: For the purpose of improved osseointegration, Evans et al [6] have developed a surface porous PEEK (PEEK-SP). They compared the performance of this material to injection molded PEEK (PEEK-IM). Under cyclic loading conditions, PEEK-SP was generally found to have lower fatigue strength than PEEK-IM. In a follow-up study of PEEK-SP, the group evaluated the effect of pore size on fatigue as well as endurance limit using S-N testing [7]. They found that increasing the surface porosity decreased the fatigue strength of PEEK-SP. Additionally, the decreasing fatigue strength of PEEK-SP with increasing pore size was more pronounced at higher lifetimes (lower cyclic stresses).

Summary: Though there have been recent contributions to the literature on the fatigue behavior of PEEK materials, much work remains to be done to understand the fatigue fracture behavior of medical-grade PEEK blends and composites for medical devices, particularly for porous and additively manufactured constructs.

Acknowledgements: Wilbert J. Austin Professor of Engineering Chair (CMR).

References: [1] Abbasnezhad N et al. Int J Fat, 2018; **[2]** Shrestha R et al. Int J Fat, 2016; **[3]** Shrestha R et al. Polym Test, 2016; **[4]** Simsiriwong J et al, JMMBM, 2015; **[5]** Shrestha R et al. Polym Test, 2016; **[6]** Evans NT et al. Acta Biomat, 2015; **[7]** Torstrick FB et al. CORR, 2016.

Fractography of PEEK Filled Materials from Tensile, Impact, and Fatigue Crack Propagation Testing

Sullivan, M., Pentecost, A., and Siskey, R.[1]
[1]Exponent, Philadelphia, PA
msullivan@exponent.com

Introduction: Polyetheretherketone (PEEK) materials are utilized in industries such as aerospace or automotive because of the material's higher strength-to-weight ratio. In biomedical applications, strength and visualization on x-ray make PEEK an ideal biomaterial. PEEK mechanical properties can also be tailored based on filler content such as carbon or glass fibers. In this work, mechanical properties were evaluated on industrial PEEK materials (neat PEEK, carbon fiber reinforced PEEK, and glass fiber reinforced PEEK), and fracture surfaces were examined. Additionally, anisotropy of the materials was studied. In general, the fracture features of PEEK under different failure modes has not been extensively published. The lack of documentation around typical fracture features makes failure analyses of these materials difficult. With PEEK materials continuously subjected to nonstandard loading conditions and new environments, it is imperative to understand how the components may fracture to avoid catastrophic failure and identify trends in failure modes.

Methods and Materials: Samples of industrial PEEK were prepared with general machining techniques from raw materials purchased in plaques from Solvay. Neat PEEK, 30% carbon fiber reinforced PEEK, and 30% glass fiber reinforced PEEK were studied. ASTM standards were used as guidance for tensile, impact, and fatigue crack propagation testing. Dogbone samples were tested per ASTM D638. ASTM D256 was used for Izod impact samples at room temperature and low temperature. Fatigue crack propagation of polymers and composites is not strictly defined by ASTM standards, but testing was completed in the spirit of ASTM E399 and ASTM E647. A laser was utilized to measure crack length during testing, which is a novel test method for fatigue crack propagation to generate da/dN versus delta K curves and to predict delta K inception values. After testing, samples were imaged using optical and scanning electron microscopy (SEM) to view the fracture surfaces.

Results: Mechanical properties of all three PEEK materials were collected from each test method. Neat PEEK samples behaved differently than the filled PEEK samples. Filled PEEK exhibited higher strength and lower impact resistance. In general, fatigue crack propagation data for PEEK samples exhibited increased fatigue performance with additional filler content. Fatigue testing resulted in a fracture surface for neat PEEK that presented as beach marks. The fatigue testing of filled PEEK did not exhibit beach marks on the macroscale. Viewing the samples at the microscale using SEM revealed fiber pull-out, which was especially noticeable in samples that exhibited directionality of their filler materials. SEM images of all samples of each material type and failure mode are shown in Figure 2.

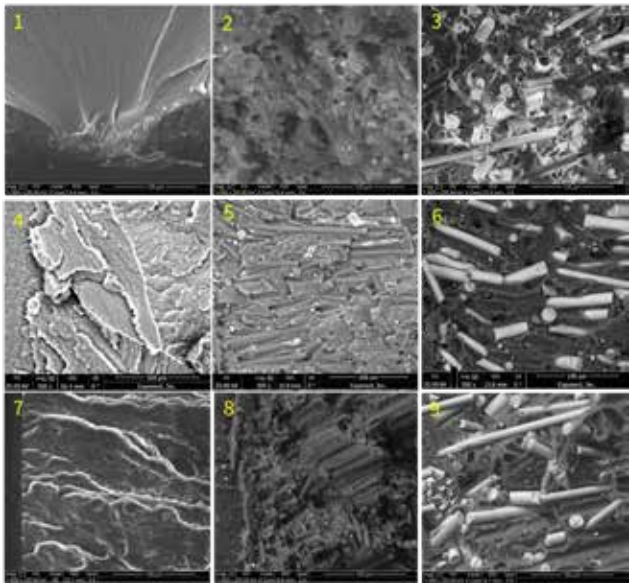

Figure 1. Columns indicate material type (neat PEEK is first column, carbon fiber reinforced PEEK is second column, and glass fiber reinforced PEEK is third column) while rows indicate failure mode (first row (1-3) are tensile samples, second row (4-6) are impact samples, and third row (7-9) are fatigue crack propagation samples),

Discussion: This work studied neat PEEK, carbon fiber reinforced PEEK, and glass fiber reinforced PEEK to confirm mechanical properties and to create an atlas of fractography images based on certain failure modes. Tensile, impact and fatigue crack propagation samples revealed differences in deformation on multiple length scales. With this work, a better understanding of failure modes of PEEK materials with and without filler has been established. Examining these fracture surfaces provides example failed surface morphologies that can be used to aid in failure analyses of these materials in environments that have not been thoroughly studied. It is especially important in the age of tailored materials created by various manufacturing processes, such as additive manufacturing and 3-D printing, that the failure mechanisms are understood to prevent catastrophic failures with the materials in use. While this work focused on the use of industrial PEEK forms, the fracture morphologies and methods should be reasonably representative of medical forms. It is the intention to verify this hypothesis using medical grades of PEEK in the future.

The nanomechanical properties of annealed PEEK with PITCH-based and PAN-based carbon fibers: the effect of annealing and indentation tip diameter

Arevalo, SE[1] , Raes, SP[2], Pruitt, L[1]
[1]University of California Berkeley, Berkeley, CA
[2]Eindhoven University of Technology, Eindhoven, Netherlands
searevalo94@berkeley.edu

Introduction:

The emergence of polyetheretherketone (PEEK) in orthopedics began in the 1980s, in the form of spinal cages for lumbar spinal fusion [1]. PEEK is a linear semicrystalline polymer that belongs to the polaryletherketone polymer family that offers strength, stiffness, toughness, radiolucency, biocompatibility as well as resistance to harsh *in vivo* conditions [1]. Owing to the desirable properties and success in spinal implants, PEEK is a strong contender to replace metal components used in modern total joint replacements (TJR).

PEEK provides a more suitable modulus match to bone than metal components used in contemporary TJR and may mitigate premature failures resulting from bone resorption, stress shielding and subsequent aseptic loosening [1]. Another interest for using PEEK is the ability for *in vivo* monitoring to assess the integrity of the implant [2]. Furthermore, PEEK offers potential resolution to other challenges plaguing metal implants including corrosion-induced failures as well as wear of the metal that can create particulate debris and metal ion release. Such complications with metals may lead to inflammation, metallosis, and eventual loosening of the implant [3].

The incorporation of carbon fibers into the PEEK matrix provides opportunities for expanding its applications to articulating load-bearing systems. The two main types of carbon fibers are polyacrylicnitrile (PAN) and PITCH. The latter are obtained from the polymerization of petroleum or coal-tar pitch [4]. The current gold standard in orthopedics for articulating load-bearing systems is ultra-high molecular weight polyethylene (UHMWPE) [3]. Yet, wear remains a limiting factor affecting the longevity of UHMWPE implants [3]. Recent studies show that PEEK composites (PAN-CF PEEK or PITCH-CF PEEK) offer higher wear resistance than UHMWPE when the polymers articulate against ceramics under the same tribological conditions [5].

An expansive body of literature exists on the tribological and mechanical performance of PEEK. Wear studies, such as those of Wang et al., show potential application of PEEK composites in hip and knee bearings [6]. Conversely, there is a paucity of research that addresses the nanomechanical and nanotribological properties of PEEK. Nanomechanical surface properties may offer insight into the wear mechanisms and may serve as a screening tool when assessing surface treatments, environmental conditions, sterilization techniques or different types of carbon fibers utilized with PEEK implants. Notably, PEEK modified by mesh-assisted plasma immersion ion implantation is shown to alter the viscoelastic properties of the near-surface region [7] while immersion in various solvents changes nanomechanical properties of PEEK [8]. Similarly, Molazemhosseini et al [9] notes an increase in hardness and elastic modulus from the addition of fibers (short carbon fibers and nanosilica) into the PEEK matrix. Godara also observes an effect on the structural integrity of medical grade PEEK with carbon fibers resulting from different sterilization techniques [10].

Though earlier studies make use of nanoindentation techniques to measure the surface properties (reduced modulus), this is the first study to investigate the effects of heat treatment for two different temperatures (200 °C and 300 °C) on the surface properties of PAN-CF PEEK and PITCH-CF PEEK. Additionally, we address the influence of different nanoindentation diameter tips on the nanomechanical measurements.

Methods and Materials:

Materials

The three material groups are: unfilled formulations of PEEK, PAN-based carbon fibers in PEEK, and PITCH-based carbon fibers in PEEK. Each material group contains three different heat treatment conditions: no heat treatment, 200 °C, and 300 °C.

Specimen surface preparation

Surface roughness may lead to erroneous material property measurements. For this reason, we utilize a multi-step polishing protocol to minimize the surface roughness on the PEEK samples [11]. The first step polishes the sample using a series of coarse grit (800, 1200, 2000, 2500) silicon carbide polishing papers. This is followed by an ultra-fine polishing using sequentially finer grit sizes of silicon carbide papers: 3000, 5000, 7000. The final polishing step is the lapping finish, which uses aluminum oxide sand paper of 1μm grit size to get a smooth surface finish. All polishing is done using a lapper (South Bay Technology) at an RPM range of 160-50 under hydrated conditions. A custom 3D-printed jig holds the samples in place during polishing to ensure even polishing.

Nanoindentation-Testing Parameters & Data Analysis

A TI 900 TriboIndenter (Hysitron, Minneapolis, MN) performs indentations at ambient temperature using three different types of tips: a 20 μm conospherical diamond tip, a 400 μm sapphire, and a 1mm sapphire flat punch. The indentations implement a load-control methodology for a maximum load of 1000 μN.

The nanoindenter follows a trapezoidal load function, in which the tip penetrates the sample at a loading rate of 100 μN/s until it reaches the maximum load, it then holds the maximum load for 10-seconds, after which the tip withdraws from the sample at the same rate as loading.

Each sample comprises of a total of 80 indentations, twenty indentations per region on the sample for four different locations. Owing to the limitations from the specimen dimensions, flat punch testing can only accommodate 15 indentations per sample (five per region for three different locations). The distance between each indentation is twice the diameter of the tip as this prevents the plastic zone from influencing the nearby indentations [12].

Flat punch and conospherical tips

The stiffness of the material emanates from the unloading region of the load-displacement curve. Following the Oliver and Pharr method, a power-law relation (Equation 1) fits to the 20-95% range of the unloading curve [13]. The derivative of the power law, the stiffness (Equation 2), relates to the contact area (Equation 3) and reduced modulus. The equation for calculating stiffness of a flat punch indentation is the maximum applied load over the elastic displacement and uses Equation 2 to calculate the reduced modulus.

$$P = \alpha(h - h_f)^m \qquad \text{Equation 1}$$

$$S = \frac{dP}{dh} = \frac{2\sqrt{A_c(h_c)}}{\sqrt{\pi}} E_r \qquad \text{Equation 2}$$

$$A_c = \pi(2Rh_c - h^2)_c \qquad \text{Equation 3}$$

The Interquartile range (IQR) identifies the outliers for removal based on the cutoff equation (Equation 4).

$$cutoff = Q_3 + 1.5(Q_3 - Q_1) \qquad \text{Equation 4}$$

Results:

Table 1 shows the modulus, while Figure 1 highlights the load displacement behavior of several PEEK formulations.

Table 1: Nanomechanical properties for all material groups tested using three different tips. Elastic modulus is calculated assuming 0.40 Poisson's ratio.
Tip 1 = 20 um, Tip 2 = 400 um, Tip 3 = 1 mm flat punch.

		Tip 1		Tip 2	Tip 3
Material Group	**Heat Treatment**	**E** [GPa] med. Std.	**H** [MPa] med. Std.	**E** [GPa] med. Std.	**E** [GPa] med. Std.
Unfilled	Control	4.58 0.95	260 107	6.31 2.20	5.17 0.87
	200	3.96 0.82	229 70.9	7.45 1.99	5.02 0.44
	300	5.79 0.93	268 103	9.54 1.52	5.89 0.48
PAN-CF	Control	6.36 1.71	262 91.1	4.45 1.18	10.2 0.64
	200	6.06 3.85	292 225	6.48 3.11	10.4 2.38
	300	7.57 3.98	294 249	9.82 3.27	10.6 3.42
PITCH-CF	Control	5.42 1.97	220 136	7.40 2.58	8.90 1.84
	200	5.70 2.18	222 86.4	7.66 2.22	10.1 1.11
	300	6.79 2.70	300 200	9.08 2.81	10.9 0.94

Discussion:

From the indentations we draw the following conclusions:

1. A smaller indentation tip is able to better capture the modulus of the individual components (fiber and the matrix); whereas, larger diameter tips indent over an expanded area containing a mixture of fibers and matrix. The smaller tip becomes necessary when comparing the behavior of each individual constituent across formulations. Our results indicate that the PAN carbon fiber exhibits less plasticity than PITCH carbon fibers.
2. The PAN-based carbon fibers experience minimal plastic deformation (Figure 1) and reveal a reduction in hysteresis in load-displacement curve. The large standard deviation for the PAN-based carbon fiber materials, for the 20 μm tip, stem from the large difference in modulus between fiber and matrix.
3. The results of the 20 μm conospherical tip indentations show that the PITCH-CF and PEEK resin heat treated at 300°C results in an increase in reduced modulus (relative to the control groups). The increase in reduced modulus suggests that elevating the temperature may enhance crystallization of the resin [14].
4. A difference in modulus with increase in tip diameter results from the changes in contact stresses beneath the indenter. The reduced modulus and hardness for unfilled PEEK (obtained with the 20 μm radius nanoindentation tip) agrees with literature [14]. However, this is the first known study to measure the modulus for PAN-based and PITCH-based PEEK across a range of heat treatments.
5. There is a need for developing a standard nanoindentation method that enables comparison of materials across different researchers as nanoindentation emerges as a viable characterization tool.

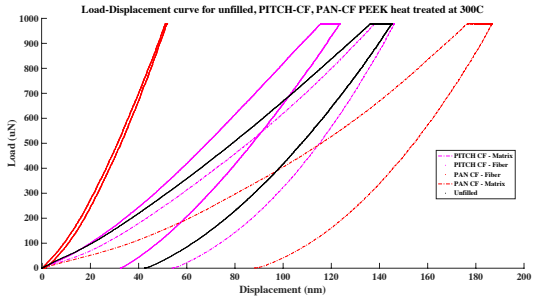

Figure 1: The Load-displacement curve shows the tip is able to differentiate between a fiber and the matrix for PEEK with PITCH-CF, and PEEK with PAN-CF heat treated at 300 °C. The black load-displacement curve corresponds to unfilled PEEK.

References:

[1] Kurtz S. PEEK Biomaterials Handbook. 1st ed. 2018.
[2] Kurtz SM.UHMWPE Handbook. 2009; 341-353.
[3] Kurtz SM. *Biomaterials*. 2007; 28 (32):4845-4869.
[4] Arai Y. (2016) Pitch-Based Carbon Fibers. In: The Society of Fiber Science and Techno J. (eds) High-Performance and Specialty Fibers. Springer, Tokyo
[5] Scholes S. Proc of the Inst of Mech Eng, Part H: Journal of Engineering in Medicine. 2007; 221 (3): 281-289.
[6] Wang A. Wear. 1999; 225-229:724-727.
[7] Powles R. Surf and Coat Tech. 2007; 201 (18): 7961-7969.
[8] Iqbal T. Journal of Applied Polymer Science 130 (6): 4401-4409.
[9] Molazemhosseini A. Polymer Testing. 2013; 32 (3): 525-534.
[10] Godara A. Acta Biomaterialia. 2007; 3 (2): 209-220.
[11] Paes-Junior T. Adv in Mat Sci and Eng. 2017; 2017:1-6.
[12] Kramer, D. Journal of Materials Research. 16 (11): 3150-3157.
[13] Ebenstein D. J of Mat Res. 2011; 26(08): 1026-1035.
[14] Voyiadjis G. Polymer Testing. 2017; 61: 57-64.

Next Generation VESTAKEEP® PEEK

Authors: Balaji Prabhu[1], Dr. Andrew Wood[1], Dr. Suneel Bandi[2], Mark Knebel[2], Kenneth Ross[2], Dr. Harsh Patel[1], Dr. Subhadip Bodhak[1], Dr. Mahrokh Dadsetan[1],

1. Evonik Industries, Medical Device Competence Center,
2. Evonik Industries, High Performance Polymers,

Polyetheretherketone (PEEK) continues to see increased interest in medical device applications largely due to bone-like mechanical properties and biocompatibility. PEEK based implants have garnered clinical acceptance for a number of indications, particularly in the orthopaedic and spinal devices space. In the case of spinal applications, PEEK's bioinert nature can lead to the formation of fibrous tissue around the implant, which can result in implant subsidence. Evonik has developed next-generation VESTAKEEP® PEEK with superior osteoconductivity for improving initial osteoblast cell attachment, which inhibits the formation of fibrous tissue around implant, followed by superior bone remodeling and bone apposition required for long-term implant stability. Additionally, the superior mechanical properties of new VESTAKEEP® PEEK will support implant performance in load-bearing application such as spinal and fixation devices. Process optimization of these newly developed materials make them viable candidates for both conventional and new processing technologies like 3d printing in the medical device field.

Key words: Polyetheretherketone, osteoconductivity, bone apposition, mechanical properties

Enhancements to Cell Proliferation, Bone Tissue Production, Biofilm Formation Resistance, and Radiolucency Observed *in vitro* when Silicon Nitride-type Materials are Compounded into PEEK

Ryan M. Bock[1], Wenliang Zhu[2], Elia Marin[3], Alfredo Rondinella[3], Francesco Boschetto[3], Bryan J. McEntire[1], B. Sonny Bal[1,4], and Giuseppe Pezzotti[3,5-7]

[1]SINTX Technologies, Salt Lake City, UT, USA; [2]Department of Medical Engineering for Treatment of Bone and Joint Disorders, Osaka University, Osaka, Japan; [3]Ceramic Physics Laboratory, Kyoto Institute of Technology, Kyoto, Japan; [4]Department of Orthopaedic Surgery, University of Missouri, Columbia, MO, USA; [5]Department of Orthopedic Surgery, Tokyo Medical University, Tokyo, Japan; [6]Center for Advanced Medical Engineering and Informatics, Osaka University, Osaka, Japan; [7]Department of Molecular Cell Physiology, Graduate School of Medical Science, Kyoto Prefectural University of Medicine, Kyoto, Japan

rbock@sintx.com

Introduction: Biomaterials used in spinal fusion surgery can exhibit differentiated performance by supporting appositional bone ingrowth and resisting bacterial colonization. Although polyetheretherketone (PEEK) is widely used as an interbody spacer material, it exhibits poor osseointegration and lacks resistance to bacterial colonization due to its hydrophobicity. In contrast, silicon nitride (Si_3N_4) monoliths have shown enhanced osteogenic and antimicrobial behavior. Therefore, it was hypothesized that incorporation of Si_3N_4 into a PEEK matrix would improve PEEK's inherently poor ability to bond with bone and also impart resistance to biofilm formation.

Methods and Materials: Three different silicon nitride-type materials, (i) raw α-Si_3N_4 powder; (ii) a spray-dried powder mixture subjected to liquid phase sintering and hot isostatic pressing to form granules of β-Si_3N_4; and (iii) a pulverized melt-derived silicon yttrium aluminum oxynitride (SiYAlON) mixture, were dispersed via compounding within a PEEK polymer matrix to form 15% by volume (vol.%) ceramic-polymer composites. The powder feedstocks and resulting composites were characterized using XRD, SEM, and EDS. Cell proliferation and bone tissue formation were assessed by exposing specimens to 5 x 10^5/ml SaOS-2 osteosarcoma cells within an osteogenic medium (50 µg/mL ascorbic acid, 0.1 M glycerol, 0.01 M hydrocortisone, and 10% fetal bovine serum in Dulbecco's modified Eagle medium) for 7 days. Antibacterial behavior was determined by inoculating samples with 1 x 10^7 CFU/ml of *Staphylococcus epidermidis* (*S. epi*.) in a 1 x 10^8/ml brain heart infusion agar culture for 24 h. After staining with PureBlu™ Hoechst 33342 or with DAPI and CFDA for SaOS-2 cell proliferation or bacterial presence, respectively, samples were examined with a confocal fluorescence microscope using a 488 nm Krypton/Argon laser source. Hydroxyapatite (HAp) deposition was measured using a laser microscope. Raman spectra were collected for samples in backscattering mode using a triple monochromator with a 532 nm excitation source ($Nd:YVO_4$ diode-pumped solid-state laser).

Results: PEEK composites containing α-Si_3N_4, β-Si_3N_4, or the SiYAlON showed significantly greater SaOS-2 cell proliferation (>600%, $p<0.003$, *cf.*, Fig. 1(a)) and HAp deposition (>100%, $p<0.003$, *cf.*, Fig. 1(b)) relative to monolithic PEEK. The largest increase in cell proliferation was observed with the SiYAlON composite, while the greatest amount of HAp was found on the β-Si_3N_4 composite. Following exposure to *S. epi.*, the composite containing the β-Si_3N_4 powder showed an order of magnitude reduction in adherent live bacteria ($p<0.003$, *cf.*, Fig. 1(c)) as compared to monolithic PEEK. The β-Si_3N_4 composite exhibited ideal radiolucency while the SiYAlON composite was more radiopaque than a β-Si_3N_4 monolith and nearly as radiopaque as a Ti alloy (Fig. 1(d)).

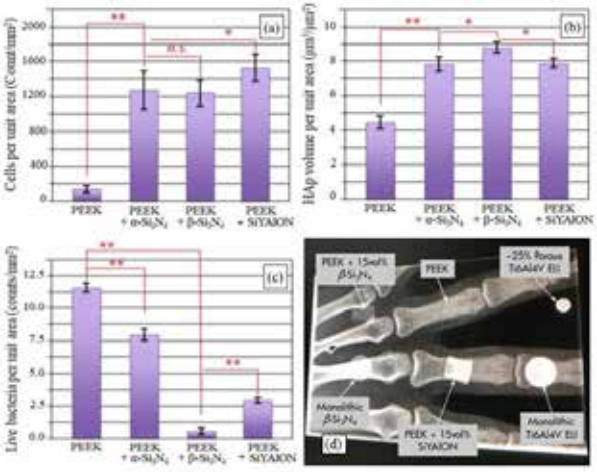

Figure 1. SaOS-2 cell (a) and HAp volume (b) areal density following 7 day exposure to biomaterials. Live bacteria areal density (c) on biomaterials following 24 hour *S. epi.* exposure. X-ray radiograph (d) of biomaterial specimens underneath metacarpal and carpal bones of a human hand.

Discussion: The addition of 15 vol.% of specific Si_3N_4–type powders to PEEK showed enhanced SaOS-2 cell adhesion, proliferation, and HAp deposition when compared to monolithic PEEK. These same composites also showed resistance to *S. epi.* adhesion and biofilm formation. It is interesting to note that the composite containing α-Si_3N_4 exhibited the worst bacterial resistance (*i.e.*, ~100% higher than monolithic PEEK by one measure), suggesting that the bacteriostatic effectiveness of Si_3N_4 bioceramics is apparently dependent upon the presence of selective sintering additives, *viz.* yttria and alumina, and subsequent thermal processing. Although improvements in osteoconductivity have been previously observed by compounding or coating PEEK with HAp, titanium, or tantalum, these approaches did not provide antimicrobial properties. Compounding PEEK with Si_3N_4 represents a significant advancement due to its ability to provide both improved bone apposition and resistance to biofilm formation.

Silver Carboxylate Coating Prevents Adherence of Multi Drug Resistant *Serratia marcescens* on Polyetherether Ketone

Gilmore, Andrea J. [1] Dioscaris Garcia, PhD [123] Christopher, Born, MD [123]
[1]Brown University, Providence RI, USA [2]Diane Weiss Center for Orthopedic Trauma Research, [3]Rhode Island Hospital, Providence, RI
andrea_gilmore@brown.edu

Introduction: Hospital acquired infections annually affect more than two million patients in the US and cause more than 100, 000 deaths.[1] Moreover infection rates in biomedical implants can be as high as 4% and can cost up to $50,000 to fix.[1] A rising contributor to these infections is the opportunistic pathogen *Serratia marcescens.* Human infections by this pathogen were not recognized until the latter half of the 20th century[2], but have quickly become a significant concern. *S. marcescens* is a gram-negative bacterium commonly associated with chronic orthopedic wounds, specifically in the spine. These infections are comprised of biofilms, which complicate treatment of surgical site infections (SSIs)[3] due to their physical resistance to antibiotics and debridement. In recent years, the use of silver as an antimicrobial agent has received attention for its ability to combat biofilm formation through its long lasting release, broad antibacterial spectrum, and low incidence of antibiotic resistance.[4] *S. marcescens* lacks much understanding and scientific consensus, and therefore, has been dismissed as a significant pathogen in need of clinical attention. Our research suggests that *S. marcescens* may be far more prevalent than suggested in the literature. This study aims to test the efficacy of a silver carboxylate complex delivered via a titanium dioxide-polydimethyl siloxane against S. marcescens on spinal polyetherether ketone (PEEK).

Methods and Materials:

Cell Culture: *S. Marcescens* was obtained as a pure and frozen culture from ATCC and stored at -80°C. The pathogen was streaked onto agar plates with media comprised of Tryptic Soy Broth (TSB) and tobramycin and incubated for 24 hours at 37°C.

Implant Biomaterials: Polyetheretherketone (PEEK) spinal implant biomaterials were machined into 2.5 mm semi-circular rods via electron discharge machining or (EDM) and submitted to an extensive cleaning procedure.

Preparation of Antimicrobial Silver Doped TiO_2–PDMS Coating: Variable ratios of titanium dioxide (TiO_2) polydimethylsiloxane (PDMS) mixes doped with various concentrations ionic silver carboxylate were prepared. 100% silver and uncoated implant trials served as positive and negative controls. Chemistry was applied via dip-coating.

Inoculation of Bacteria: *S. Marcescens* inoculated at a concentration of 10^7 CFU/ml through the use of optical density measurement. The implants were then inoculated with this concentration of *S. Marcescens* and allowed to adhere for 4 hours. After completion of the 4 hours, the samples were rinsed with Phosphate Buffer Solution (PBS) and allowed to proliferate for 20 hours.

Confocal Microscopy: The PEEK implants were fixed in formalin overnight and then tagged with an antibody LPS and anti-LTA 1° for gram-negative *S. marcescens.* The implants were then conjugated with a FITC 2° anti-body for imaging at 120x.

Scanning Electron Microscopy Imaging: Samples were fixed in glutaraldehyde via a sodium cacodylate (NaCaCo) buffer. Samples were visualized via a ThermoFisher Scientific Apreo VS SEM at 5,000x magnification. Images were then analyzed for biofilm colonization with NIH program, ImageJ.

Antimicrobial Testing via Dose Curve Response: 96 well plates were coated with various silver concentrations to test the antimicrobial resistance of silver to *S. marcescens.* This was completed; for 50x, 75x, and 95x TiO_2:PDMS. 200 µl of 10^7 CFU/ml.

Results: From the results posed, this project found that 95% TiO_2-5% PDMS doped with 10X ionic silver coating was the best coating for preventing bacterial adherence. Moreover, the dose response curve for *S. marcescens* concluded that 1X silver concentration was sufficient for killing *S. marcescens* for the 50% concentration, and minimal silver dopage was able to kill the pathogen for the 75% and 95% concentrations. SEM imaging concluded that for the 50% x silver concentration, the number of CFUs per implant decreased as silver concentration increased, with a significant drop at 10x conc. Likewise, the 75% concentration displayed less overall CFUs than the 50% concentration and also consistently decreased in number of CFU as silver concentration increased. However, for 75 0x and 75 1x the CFU's were about equal, with again a large drop at 10x. The 95% concentration followed the same trends except for the large decrease in CFU occurring at the 1x concentration, as well as the least amount of overall CFU's at the 95 10x concentration.

Discussion: Surgical Site Infections (SSI's) cause serious harm to patients. As bacteria such as *S. marcescens* adapt and develop drug resistant characteristics, new antimicrobial methods for preventing biofilm formation must be explored. This project showed the effectiveness of the titanium dioxide and PDMS matrix infused with ionic silver mix on combating the adherences of bacteria on orthopedic materials. Further research of this project will include the incorporation and experimental studies on more implants such as Titanium Alloy and Cobalt Chromium. Also, other imaging techniques, such as Confocal Microscopy could be utilized in order to get a more accurate representation of bacterial coverage on each implant. Lastly, it would be beneficial to look at the

interaction of the coatings with the specific implant topographies and its effect on bacterial adherence.

References:

1. Taheri, S. and A. Cavallaro, et. al. “Substrate independent silver nanoparticle based antimicrobial coatings”. *Biomatierals.* May 2014. 35(16). 4601-4609. doi: 10.1016/j.biomaterials.2014.02.033

2. Huang Liou, Bo., Ruay-Wang Duh., Yi-Tsung Lin, Tsai-Ling Yang Lauderdale, and Chang-Phone. “A multicenter surveillance of antimicrobial resistance in Serratia marcescens in Taiwan”. [Internet]. *Journal of Microbiology and Infection,* Volume 47 Issue 5, October 1, 2014. 387-393.

3. Rabin, Nira, Yue Zheng, Clement Opoku-Thmeng, Yixan Du, Eric Bonso, Herman O Sintim, “Biofilm formation mechanisms and target for developing antibiofilm agents” *Future Medical Chemistry.* 2015. *7(4).* 493-512. doi: 10.4155/FMC.

4. Zhang, W., S. Wang, S. Ge, J. Chen, P Ji. “The relationship between substrate morphology and biological performances of nano-silver-loaded dopamine coatings on titanium surfaces.” *R Soc Open Sci.* April 11, 2018. *5(4).* 172310. doi: 10.1098/rsos.172310.

A novel polyetheretherketone-zeolite composite reduces long term inflammatory response in an ovine cervical fusion model

Sankar, Sriram[1]; Crudden, Joseph[1]; Johns, W.Derrick[1]; Swink, Isaac [2]; Carbone,Jake[2]; Yu,Alexander[2];Cheng,Boyle[2]
[1]DiFusion Technologies Inc., Austin, TX-USA [2] Department of Neurosurgery Spine Biomechanics Lab, Allegheny General Hospital, Pittsburgh, PA-USA.
sankar@difusiontech.com

Introduction

Osteoimmunology, the study of the relationship between the musculoskeletal system and immune system, has emerged as an important aspect of biomaterial research, providing new tools for understanding and manipulating cellular interactions at the bone implant interface. For example, osteoimmunolgy techniques could be used to better understand the mechanism of fibrous capsule formation commonly seen with PEEK implants. PEEK, being hydrophobic, elicits a foreign body initiated immune response, involving the long-term release of pro-inflammatory cytokines and pain markers such as IL-1β and IL-6, which are associated with increased fibrous encapsulation and poor bone response.

A novel PEEK-zeolite composite, (ZFUZE^{TM}) has been developed to address the issue of fibrous encapsulation associated with PEEK implants. The incorporation of zeolite, a super-hydrophilic inorganic ceramic into PEEK, creates a novel negatively charged hydrophilic PEEK composite. The expression of these cytokine markers is evaluated in a non-plated cervical ovine fusion model for both materials.

Hypothesis: The new PEEK-zeolite composite is expected to elicit favorable cytokine expression, resulting in improved cellular/new bone response and reduced fibrous encapsulation compared to PEEK; ultimately resulting in better fusion outcomes. Analysis was focused on IL-1, IL-6, and TNF-α cytokine expression levels, biomechanical stability, histopathological examination, and radiographic results.

Methods and Materials

Fourteen skeletally mature Mondtale sheep were implanted with PEEK or PEEK-zeolite interbody cages at the C2-C3 and C4-C5 index levels and survived to 12 or 26 weeks, as approved by the IACUC Committee. At the time of sacrifice index level functional spinal units (FSU), major organs, lymph nodes, and muscle tissues were collected.

FSU were immediately mounted and range of motion (ROM) was measured using a Bose Spine Tester by applying 2.0 Nm moments in Flexion extension (FE), Lateral Bending (LB) & Axial Torsion (AT).

Micro-CT and radiographic images were then obtained to assess the fusion mass Fusion was graded on a 1-5 scale based off bridging trabecular bone and cortication of peripheral edges of the fusion mass.

Subsequently, histopathological examination was carried out after fixation with formalin alongside other organ samples and the FSU's were evaluated for new bone formation, inflammation and fibrous tissue formation.

For immunohistochemistry (IHC), muscle tissue from the spinal column at the operative level was collected and used for a quantitative analysis of various inflammatory markers. Slides were prepared from these spinal tissue samples as well as positive and negative control tissues. Lymph nodes and muscle tissues distant from the surgical site were collected during necropsy and served as the positive and negative controls respectively. The levels of inflammatory cytokines interleukin-1 beta (IL-1β), interleukin-6 (IL-6), and tumor necrosis factor alpha (TNF-α) were quantified in these tissues based on the intensity of fluorescence in each slide. Primary antibodies for IL-1β, IL-6, and TNF-α were purchased from antibodies-online.com, had ovine reactivity, and rabbit was the host species in all three cases. The secondary antibodies chosen, Donkey anti-rabbit IgG-Dr Light 488, were also purchased from antibodies-online.com, and were chosen to prevent cross-reactivity between species.

Results and Discussion

Histology: Histomorphometry showed statistical difference in percent(%) new bone formation at C2-C3 sites for PEEK-Zeolite; which showed 31% ± 10% compared to 7% for PEEK at 26 weeks; at C4-C5 sites PEEK-Zeolite showed 57% new bone compared to 40% ± 3% for PEEK at 26 weeks. On fibrous tissue response; PEEK-Zeolite was associated with minimal fibrosis at week 26 compared to PEEK

Biomechanics: ROM revealed no statistical difference between PEEK-Zeolite and PEEK after 12 and 26 weeks.

Immunohistochemistry (IHC):
Intensity values for each sample were normalized by dividing the measured intensity by the average intensity of the negative control samples. Raw and normalized IHC data can be viewed in the table and graph below. Using normalized values which represent the intensity as a percentage of the negative control, an independent T-test were performed to compare cytokine expression at both 12 and 26 week time points

Normalized Cytokine Expression Levels							
		12 Weeks			26 Weeks		
Cytokine	Material	N	Mean	Std. Dev	N	Mean	Std. Dev
IL-1	PEEK-Zeolite	5	0.226	0.277	7	0.024	0.009
	PEEK	5	1.374	0.487	6	0.602	0.231
IL-6	PEEK-Zeolite	5	1.144	0.809	7	0.713	0.436
	PEEK	5	1.660	0.612	6	1.403	0.742
TNF-a	PEEK-Zeolite	5	0.488	0.201	7	0.478	0.266
	PEEK	5	0.521	0.312	6	0.695	0.413

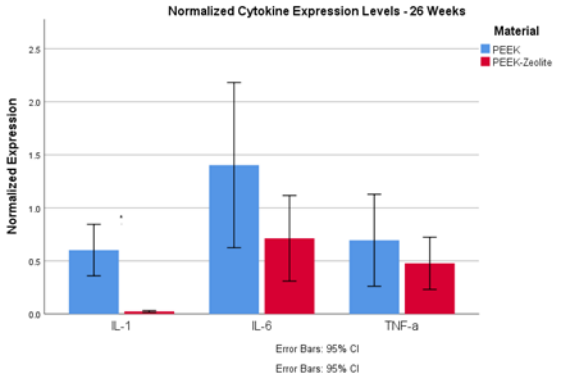

Expression of IL1-β was found to be significantly lower in PEEK-zeolite samples at 12 weeks (M=0.23, SD=0.28) than standard PEEK samples at 12 weeks (M=1.37, SD=0.49) t(8)=-4.582, p=0.002. PEEK-zeolite composite samples were also found to have significantly lower IL1-β expression at 26 weeks (M=0.02, SD=0.009) when compared to standard PEEK samples (M=0.60, SD=0.23) t(11)=--6.667, p<0.001. While there was no statistically significant difference in expression of IL-6 or TNF-α, it should be noted that PEEK-zeolite composite samples trended lower in all cases compared to PEEK as seen above.

Understanding the mechanisms driving bone-implant interactions will allow for the development of materials and implants with improved clinical success. Interleukin-1 beta and interleukin-6 are both produced by osteoblasts and associated with inflammation, fibrous capsule formation, and bone resorption. Tumor necrosis factor alpha is responsible for stimulating osteoclast formation while simultaneously preventing osteoblast differentiation and collagen formation. While the results of in-vitro osteoimmunology studies have not always translated to in vivo studies, the relative quantification of key cytokines in vivo may provide findings more closely aligned with a clinical scenario. The current study showed a novel PEEK-zeolite composite elicits reduced pro-inflammatory cytokine excretion when compared to standard PEEK implants. Specifically, the tissues surrounding PEEK-zeolite composite implants had significantly lower levels of IL1-β and IL-6. These results may explain the increased bone growth and reduced fibrous tissue formation as seen in histology

Micro-CT imaging

Images shown below at 12 and 26 weeks for both PEEK-Zeolite (ZFUZE™) and PEEK show no plating to help with stabilization and no corpectomy to expose the vascular tissue under the endplates. PEEK-Zeolite (ZFUZE™) definitively outperforms PEEK with respect to new bone formation, quality of new bone and extent of fibrosis. We believe that the osteoconductivity demonstrated by ZFUZE could potential result in better fusion, and that implants made with this novel composite will enable surgeons to deliver better patient outcomes

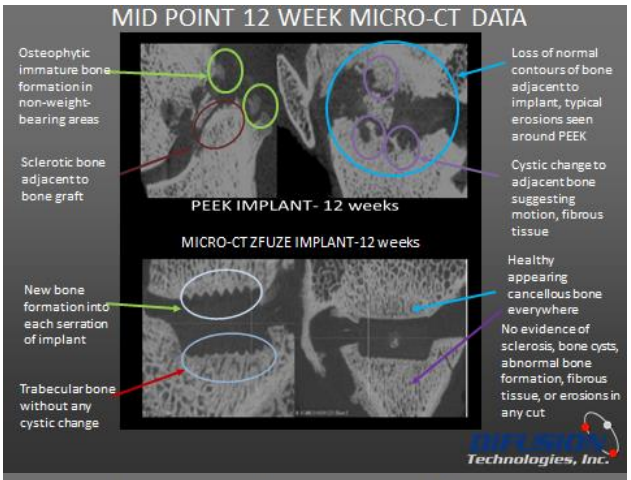

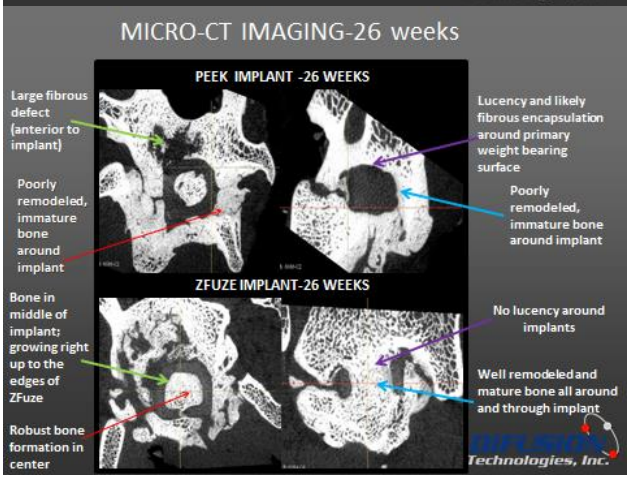

Conclusion

PEEK-Zeolite (ZFUZE™) sites show significant reduction in IL1β and reduced IL-6 expression levels; increased new bone growth and reduced fibrotic response at 26 weeks compared to PEEK devices. We believe that the suppression of these long term degenerative markers resulted in favorable bone response and reduced fibrous encapsulation. Along with previously presented data; which showed increased in vitro osteoblastic activity and enhanced invivo osteoconduction in a rabbit critical defect model; these findings suggest that PEEK-Zeolite (ZFUZE™) could potentially be an attractive alternative to standard PEEK as a spine biomaterial for interbody devices.

Best osseointegrative surface characteristics of PEEK implants due to an evolutionary surface functionalization technique MBT (Mimicking Bone Technology)

Cölfen, H[1]; **Rechenberg**, B[2]; **Schaffarczyk**, D[3]; **Schwitalla**, A [4]
[1]University of Constance, Germany
[2]ETH, University of Zurich, Switzerland
[3]stimOS GmbH, Constance, Germany
[4]Charité Universitätsmedizin, University Berlin, Germany

[3]*Corresponeding author: zyk@stimos.net*

Introduction. While implant materials such as polymers (PEEK) are known for their good mechanical characteristics, they are also known for being bio-inert. Cells do not adhere properly to these materials. As a result, surgeons observe patients' pain and inflammatory reactions after surgery. Adverse effects even include implant loosening and expensive and painful re-operations cannot be avoided. To enhance the biological performance of PEEK implants, these materials are often mixed with HA (invibio) or coated with Titanium (Ti). But the high risk for patients with these kinds of Ti-PEEK composites are abrasion and delamination of Ti-nanoparticels, as Ti and TiO_2 is suspected to be toxic and carcinogenic.

In the case of medical implants and prostheses, wear debris and ions release produced due to the loss of material by bio-tribocorrosion of implant surfaces have been related to tissue inflammatory reactions[3-5,6]. The presence of metallic ions and particles in human tissues induces the activation of macrophages, neutrophils, and T-lymphocytes with elevation of cytokines and metallic proteinases that can promote bone resorption[7–10]. Coalescence of particles of all classes (including titanium particles) originating from implants are often seen in the vesicles of macrophage cytoplasm in the liver, spleen, and para-aortic lymph nodes[10–19].

Titanium particles found in the lymph nodes ranged from 0.1 µm up to 50 µm, while in the liver and spleen the particles ranged from 10 µm[11]. An association between ultrafine TiO_2 (UF-TiO_2) (<100 nm in diameter) particles and adverse biologic effects have been reported in the literature[2,3]. Garabrant et al.[2] reported that 50 % of titanium metal production workers exposed to TiO_2 particles suffered from respiratory symptoms, followed by injury of pulmonary function[20]. In agreement with previous studies in rats[12,15,16], recent studies in cultured human cells have also shown genotoxicity and cytotoxicity effects of UF-TiO_2[1].

These scientific publications and the results presented herein led the authors consider the possible biological adverse effects of TiO_2 particles (<100 nm in diameter) produced during bio-tribocorrosion mechanisms of Titanium or Titanium coatings in the human body. To avoid risks for the patients associated with the use of Titanium or Titanium composites the authors developed and analyzed a new surface modification technique called Mimicking Bone Technology (MBT) invented to add best osseointegrative characteristics to pure PEEK surfaces. This MBT technology is patented / patent pending worldwide.

Titanium Plasma Spray Coating: High Risk of Wear Debris

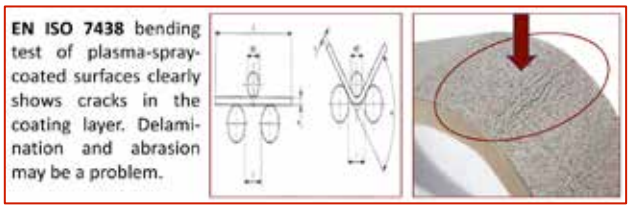

Pic. 1: Titanium coated PEEK surfaces tested by stimOS.

MBT Technology: Unique Surface Modification for PEEK Implants

The surface modification technique presented in this paper is not a coating technique but an evolutionary bio-chemically covalently joined surface functionalization resulting in unique, bone-identic and mineralized PEEK^{MBT} implant surfaces eliminating the risks of abrasion, wear debris and TiO_2 diffusion.
As the MBT surface modification is designed on a biomimetic basis, it includes the most advantageous properties of surface topography, surface chemistry and physicochemical parameters and combines it with state-of the art chemical strategies for the improvement of the longevity of the implant within the host. Therefore, from the point of view of inorganic surface modifications, implant surface designs and surface topographies should also incorporate all the relevant scales that interact with the surrounding cells. Also, it has been suggested that only a very specific surface topography with a roughness value between 1 and 1.5 µm provides an optimal surface for bone integration9. stimOS' engineered PEEK^{MBT} surface meets this range.

Material and methods. To demonstrate the superior performance of PEEK^{MBT} surfaces, in vitro cell tests and in vivo animal models have been developed and used to compare the characteristics of various implant surfaces, such as PEEK, HA enhanced PEEK (invibio), PEEK^{MBT} (stimOS) and Titanium.

Results. MBT surface modifications are process-validated technologies. The technology has been subject of

statistically significant comparative in-vitro cell tests performed by the faculty of biology (University Constance) showing superior results regarding cell adhesion, cell viability and cell proliferation compared to PEEK, Titanium and HA-enhanced PEEK materials. PEEK^{MBT} surface turned out to be the most suitable candidate for healing into the bone tissue among all tested materials due to high osteoblast proliferation and cell adhesion, and due to the most intensive formation of mineralized bone nodules (follow up 12h / 24h).

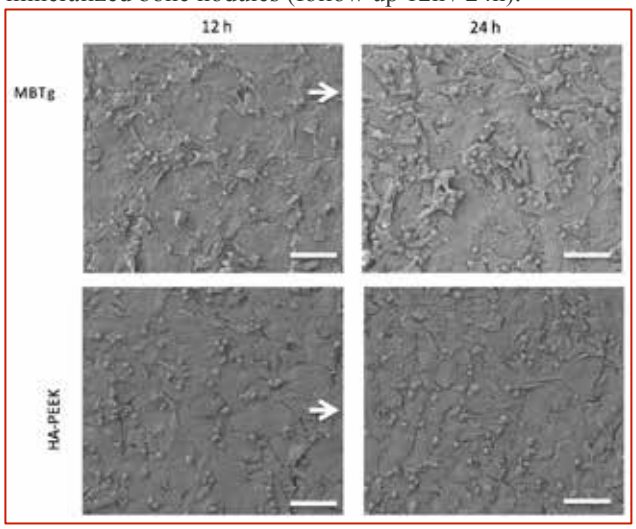

Pic 2: HA enhanced PEEK (invibio) material surface compared with PEEK^{MBT} surface (stimOS). Superior formation of mineralized bone nodules on stimOS PEEK^{MBT} surface.

To confirm the outstanding results achieved in in-vitro cell tests, an animal model was conducted - together with the University of Zurich and Charité Berlin - to demonstrate that stimOS MBT implant surface modification has evolutionary unique characteristics designed to support early bone formation and proper implant anchorage.

The animal model proofs that stimOS PEEK^{MBT} materials can be described as biocompatible, cell-attractive, osseointegrative and can be associated with anti-inflammatory material characteristics.

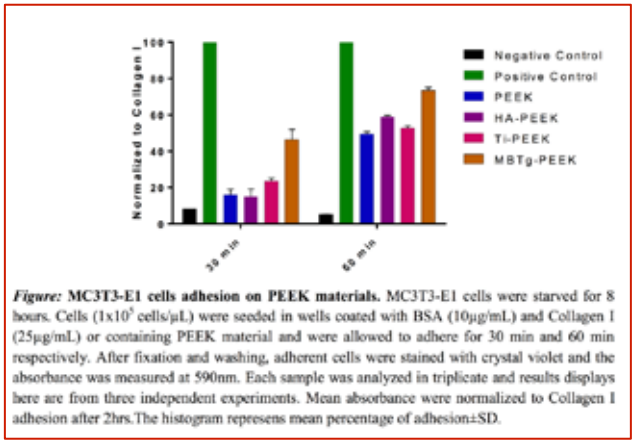

***Figure:* MC3T3-E1 cells adhesion on PEEK materials.** MC3T3-E1 cells were starved for 8 hours. Cells ($1x10^5$ cells/µL) were seeded in wells coated with BSA (10µg/mL) and Collagen I (25µg/mL) or containing PEEK material and were allowed to adhere for 30 min and 60 min respectively. After fixation and washing, adherent cells were stained with crystal violet and the absorbance was measured at 590nm. Each sample was analyzed in triplicate and results displays here are from three independent experiments. Mean absorbance were normalized to Collagen I adhesion after 2hrs.The histogram represens mean percentage of adhesion±SD.

Conclusion. Intensive testing in vitro and in vivo demonstrated safety and performance of the unique biochemical implant surface PEEK^{MBT}. Test set up was chosen to compare MBT material surfaces against Titanium and HA-enhanced PEEK materials. PEEK^{MBT} showed osseointegrative characteristics that are significant superior to PEEK, HA-enhanced PEEK and Titanium, known as the golden standard for orthopedic and dental implant materials.

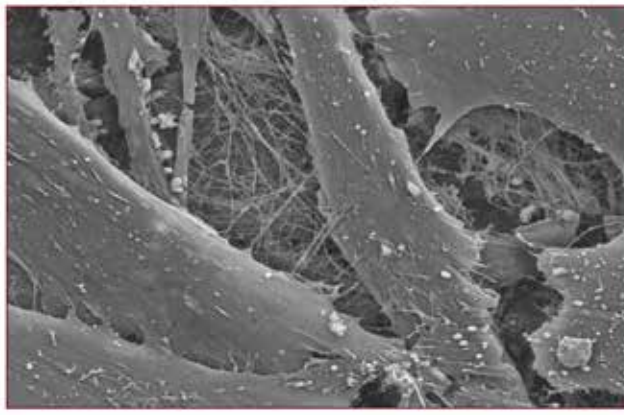

Pic. 3 - stimOS PEEK^{MBT}:Secretion of a large amount of extra-cellular collagen matrix and start of mineralization after already 12 hours – cells grow in several compact layers and the calcification process started.

The animal model (sheep) and in vitro cell tests demonstrated the overall biocompatibility of the new developed surface modification MBT.

Literature

1. Mints, D.; Elias, C.; Funkenbusch, P.; Meirelles, L.; Integrity of Implant Surface Modifications After Insertion. DOI: **10.11607/jomi.3259**
2. Garabrant DH, Fine LJ, Oliver C, Bernstein L, Peters JM (1987) Abnormalities of pulmonary function and pleural disease among titanium metal production workers. Scand J Work Environ Health 13:47?51
3. Wang JJ, Sanderson BJS, Wang H (2007) Cyto- and geno- toxicity of ultrafine TiO2 particles in cultured human lym- phoblastoid cells. Mutat Res 628:99?106
4. Manaranche C, Hornberger H (2007) A proposal for the clas- sification of dental alloys according to their resistance to cor- rosion. Dent Mater 23:1428?1437
5. Broggini N, McManus LM, Hermann JS, Medina R, Schenk RK, Buser D, Cochran DL (2006) Peri-implant inflammation defined by the implant-abutment interface. JDent Res 85:473?478
6. Broggini N, McManus LM, Hermann JS, Medina RU, Oates TW, Schenk RK, Buser D, Mellonig JT, Cochran DL (2003) Persistent acute inflammation at the implant-abutment interface. JDent Res 82:232
7. Buscher R, Tager G, Dudzinski W, Gleising B, Wimmer MA, Fischer A (2005) JBiomed Mater Res B 72B:206
8. Haynes DR, Rogers SD, Hay S et al (1993) The differences in toxicity and release of bone-resorbing mediators induced by ti- tanium and cobalt-chromium wear particles. JBone Joint Surg A 75:825?834
9. Maloney WJ, Lane Smith R, Castro F, Schurman D (1993) Fi- broblast response to metallic debris in vitro. JBone Joint Surg A 75:835?844
10. Kumazawa R, Watari F, Takashi N, Tanimura Y, Uo M, Totsuka Y (2002) Effects of Ti ions and particles on neutrophil function and morphology. Biomaterials 23:3757?3764
11. Case CP, Langkamer VG, James C, Palmer MR, Kemp AJ, Heap PF, Solomon L (1994) Widespread dissemination of metal de- bris from implants. JBone Joint Surg B 76:701?712
12. Urban RM, Jacobs JJ, Tomlinson MJ, Gavrilovic J, Black J, Peoc?h M (2000) Dissemination of wear particles to the liver, spleen, and abdominal lymph nodes of patients with hip or knee replacement. JBone Joint Surg Am 82:457
13. Goodman SB (2007) Wear particles, periprosthetic osteolysis and the immune system. Biomaterials 28:5044?5048
14. Ozakaki Y (2001) A New Ti?15Zr?4Nb?4Ta alloy for medical applications. Curr Opin Sol St Mater Sci 5:45?53
15. Afaq F, Abidi P, Matin R, Rahman Q (1998) Cytotoxicity, pro- oxidant effects and antioxidant depletion in rat lung alveolar macrophages exposed to ultrafine titanium dioxide. J Appl Toxicol 18:307?312
16. Baggs RB, Ferin J, Oberdorster G (1997) Regression of pulmonary lesions produced by inhaled titanium dioxide in rats. Vet Pathol 34:592?597
17. Harvey, A. G.; Hill, E. W.; Bayat, A., Designing implant surface topography for improved biocompatibility. **Expert review of medical devices** *2013*,**10**(2), 257-267.
18. Le Guéhennec, L.; Soueidan, A.; Layrolle, P.; Amouriq, Y., Surface treatments of titanium dental implants for rapid osseointegration. **Dent Mater** *2007*,**23**(7), 844-854.
19. Bauer, S.; Schmuki, P.; von der Mark, K.; Park, J., Engineering biocompatible implant surfaces: Part I: Materials and surfaces. **Progress in Materials Science** *2013*,**58**(3), 261-326.
20. Bettinger, C. J.; Langer, R.; Borenstein, J. T., Engineering Substrate Topography at the Micro- and Nanoscale to Control Cell Function. **Angewandte Chemie International**, Edition 2009, **48** (30), 5406-5415.
21. Martin, J.; et al., Effect of titanium surface roughness on proliferation, differentiation, and protein synthesis of human osteoblast- like cells (MG 63). **Journal of Biomedical Materials Research Part A** *1995*,**29**(3), 389-401.

Results of In-vivo Testing of a Novel Macro-Scale Osseointegration Surface Morphology

Causey, GC[2], Price, J[2], Picha, GJ[2], Pelletier, M[1], Wang, T[1], Walsh, WR[1]
[1]UNSW Australia, [2]Applied Medical Technology, Inc. Brecksville, OH. *(greg.causey@appliedmedical.net)*

Introduction: Initial stability and secondary biological fixation are crucial requirements of any surface morphology for implant fixation. Implant systems have utilized a variety of macro, micro, and nano scale features in an attempt to maximize implant integration. With few exceptions, most research and development has focused on metallic surface finishing techniques and coatings or 3D porous implants. We have developed a surface morphology consisting of an open array of macro scale pillars. The surface is uniquely differentiated from other porous surfaces in that the discontinuous array of pillars enables the ingrowth of a continuous and interconnected bony volume. In-vivo testing has been performed in canine and ovine models exploring a variety of pillar configurations and implant materials. Here, we present the µCT, histology, and mechanical push-out testing results for PEEK, HA PEEK, and Ti PVD (Physical Vapor Deposition) coated PEEK implant materials and compared results with Titanium implants of similar surface morphologies.

Methods and Materials: Three in-vivo studies have been performed using a tibial/femoral bone defect model. All studies were cleared thru the appropriate IACCUC/ethical review boards. All studies utilized square profile pillars. All implant description, geometry, and material are shown in Table 1.

Study 1 utilized 5 male mongrels and 5 rectangular implant groups manufactured from PEEK or Titanium at a 6 week endpoint. This study examined the effects of intrapillar spacing on bone ingrowth. A smooth PEEK implant was used as the negative control. Histology and push-out testing was performed.

Study 2 utilized 8 adult ovine wethers and 4 cylindrical implant groups at 4 and 12 week endpoints. A smooth Ti implant with a grit blast finish was used as the control. Radiography, µCT, histology, histomorphometry and push-out testing was performed.

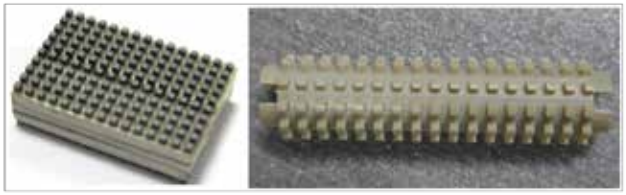

Figure 1: Canine and Ovine Implants (not to relative scale)

Study 3 followed the same protocol as study 2 with 12 adult ovine wethers and 6 cylindrical implant groups at 6 and 12 week endpoints. This study examined the effects of materials which included Titanium, PEEK, HA PEEK, and ultrahigh molecular weight polyethylene (UHMWPE). One PEEK sample was coated with a thin layer of Titanium via a PVD process (3-5 micron thick coating). Figure 1 shows examples of the canine and ovine test implants.

One key metric when considering the pillar morphology is the concept of surface void volume, a measure of the open and available space for bony ingrowth in and around the pillars. It is measured as a percentage of the space bounded by the base and tops of the pillars not occupied by the pillars themselves. The void volume is a function of pillar geometry and spacing and is not dependent on material. The void volume defines the ratio of bone to implant in the ingrowth zone. Void volumes for the studies varied from 0% for flat surfaces to over 85% for some pillar configurations.

Results: No adverse events were encountered in any study. All animals reached study endpoints. Healing and bony ingrowth progressed with time for all implants in all studies.

Study Animal	Pillar Size	Pillar Height	Pillar Spacing	Material	Void Volume
Canine	N/A	N/A	N/A	PEEK	0%
	400	500	100	PEEK	36%
	400	500	200	PEEK	56%
	400	500	400	PEEK	75%
	400	500	400	Ti	75%
Ovine	N/A	N/A	N/A	Ti	0%
	400	500	400	Ti	77%
	400	1000	400	Ti	80%
	400	500	600	Ti	85%
Ovine	400	1000	400	PEEK	80%
	750	750	665	PEEK	77%
	750	750	665	HA PEEK	77%
	750	750	665	Ti PVD PEEK	77%
	750	750	665	Ti	77%
	750	750	665	UHMWPE	77%

Table 1: Implant Configurations and Geometry (µm)

In the canine study, histologic review demonstrated robust bony ingrowth and vascularity in the 200µm and 400µm intra-pillar spacing implants in both PEEK and Titanium. There was little to no fibrous tissue present within the bone/implant interface. In contrast, the 100µm intra-pillar spacing showed immature bony ingrowth and reduced vascularization. Mechanical testing (Table 2) revealed a marked increase in push-out resistance at the 200µm and 400µm intra-pillar spacing with no difference between the PEEK and Titanium implants. The final results of the first study demonstrated extensive bony ingrowth into all pillar geometries and materials when the void volume surpassed approximately 50% as noted in Table 1.

Pillar Spacing (µm)	N/A	100	200	400	400
Pushout (N)	46	286	742	700	816

Table 2: Canine Mechanical Pushout

Histology in ovine study 1 demonstrated fully interdigitated bony ingrowth for all pillared implant groups at the final endpoint. Similarly, histomorphometry analysis showed over 80% bone in the available space. Mechanical testing demonstrated significantly higher push-out forces in all pillared implant groups compared to the grit blast control (Table 3). The 1000µm tall titanium pillars

revealed complete bony growth at 12 weeks with no fibrous tissue at the bone/implant interface (Figure 2).

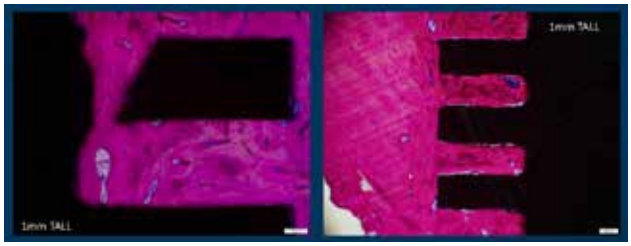

Figure 2: Histology, 12wk, 1000µm Tall Pillars, Ti

Pillar Height/ Spacing (µm)	N/A	500/ 400	1000/ 400	500/ 600
Shear (N/mm²)	4.2	24.3	28.3	29.9

Table 3: Ovine Study 1 Mechanical Pushout

In ovine study 2 the µCT revealed complete bony integration for all implant groups at the 12 week endpoint. Bone ingrowth into the pillared surface was extensive regardless of implant material. Cylindrical slice µCT sections were created (Figure 3, 1000µm PEEK) allowing for review of the circumferential bony interdigitation in a single image. Histology showed fully interdigitated ingrowth in intimate contact with the pillars with little to no intervening soft tissue encapsulation (Figure 4, 1000µm PEEK & PEEK). Mechanical testing (Table 4) revealed comparable shear stress resistance in all samples except for the UHMWPE. There was little to no fibrous tissue present in at the bone/implant interface and no inflammatory response was noted in any implant group.

Implant Material	1000µm PEEK	PEEK	HA PEEK	Ti	UHMWPE
Shear (N/mm²)	19.5	23.0	26.0	29.2	11.6

Table 4: Ovine Study 2 Mechanical Pushout

Discussion: The bone ingrowth potential of this morphology in PEEK, HA PEEK, Ti coated PEEK, and UHMWPE has been shown to be equivalent to that seen in Titanium. Little to no fibrous tissue was noted at the surface of the implants. Mechanical push-out testing demonstrated similar fixation in the PEEK, HA PEEK, and Ti Coated PEEK as compared to the Titanium samples. Comparing the 1000µm tall PEEK pillars in the third study with the same implant geometry in Titanium from the second study also demonstrated equivalent bony ingrowth as shown in both histologic analyses. Mechanical push-out testing revealed equivalent performance within the context of implant material physical properties. It is important to note that, per the testing protocol, the tibial defect size in the ovine studies was matched to the implant diameter at the top of the pillars. Hence, all bone in the pillar structure was new bone growth; a full 750µm to 1000µm of bone growth in all implant materials and pillar geometries.

This pillar concept turns the notion of a "porous" surface inside-out. In a traditional porous surface, the implant is in a continuous phase and the in-growing bone has to grow into the surface pores and voids in a discontinuous manner. In contrast, the pillared surface morphology inverts this notion by creating a surface topography which is discontinuous in nature; discrete pillar features extend from the bulk material. This opens the entire surface to continuous interconnected bone growth without restriction. This bone continuity results in improved vascularization, nutrient delivery and structural strength

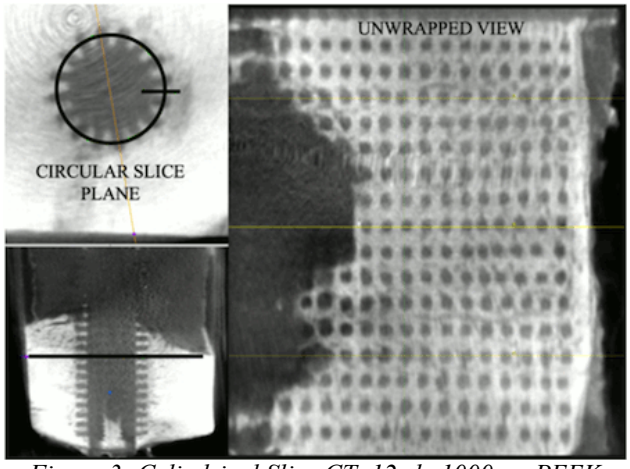

Figure 3: Cylindrical Slice CT, 12wk, 1000µm PEEK

The ability to control the surface morphology of the implant material enables tailoring the implant/bone interface in terms of biomechanical stiffness. Continuous bone surrounding discrete pillars enables the pillars to flex and bend more easily as compared to a continuous porous surface. This compliance may reduce stress shielding and more effectively transfer strain into the continuous, surrounding bone mass. Wolf's Law dictates that effective stress transfer from the implant into the surrounding bone is necessary for long-term implant stability and reduced osteolysis.

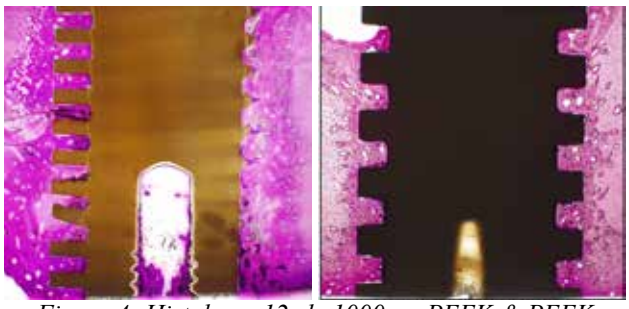

Figure 4: Histology, 12wk, 1000µm PEEK & PEEK

Summary: We have reviewed and confirmed, in three separate in-vivo studies utilizing two different animal species, the osseointegrative potential of a novel macro-scale surface morphology. Testing has yielded strong bony ingrowth with little to no fibrous encapsulation in PEEK based implants and has shown equivalence between PEEK and Titanium implants. The discontinuous pillar morphology has a number of benefits including robust bone ingrowth, an increased volume of available space for bone in the implant/tissue interface zone, solid ingrowth independent of implant materials, and the ability to tailor the biomechanics of the interface.

Characterization of PEEK filaments for Fused Filament Fabrication (FFF)

Garcia-Leiner, M[1]; Başgül, C[2]; Streifel, B[3]; Middleton, R[1]; Kurtz, S[1]
[1] Exponent, Philadelphia, PA, USA
[2] Drexel University, Philadelphia, PA, USA
[3] Exponent, Bowie, MD, USA
mgarcia-leiner@exponent.com

Introduction: Additive Manufacturing (AM), otherwise known as three-dimensional printing (3DP), is a growing technology area comprised of a spectrum of processes that allow production of solid objects of virtually any shape from information obtained from a digital object. These days, AM processes drive major innovations in engineering, manufacturing, art, education and medicine.

Polymers such as PEEK, PEKK, and PEKEKK are perhaps the most promising candidates for demanding engineering applications, and could revolutionize and enable the use of AM plastic parts in critical environments. Because of their extremely high thermal properties, some PAEK resins are suitable to be processed by extrusion-based approaches. Technologies such as Fused Filament Fabrication (FFF) have proven to be successful in incorporating a variety of PAEK polymers as raw materials. Among all the PAEK resins, PEEK is particularly suitable for extrusion-based processes and has captured the attention in recent years when it comes to FFF, FDM processes. In particular, PEEK allows for a larger processing range and represents the majority of the efforts in this area, with some developments also pursued in PEKK and other novel PAEKS. This study describes some of the structure property considerations for PEEK filaments used in extrusion-based AM processes, particularly FFF.

Methods and Materials: In this study, Polyetheretherketone (PEEK) filaments obtained from 4 different sources were used to produce 3D printed bars with rectangular cross sections using a commercially avaliable printer (Indmatec HPP 155/Gen 2) under similar conditions. Printed samples have the following dimensions: 40 mm in length, 10 mm in width, and 1 mm in thickness.

Thermal Characterization. Thermal properties of PEEK filaments in this study were analyzed using Differential Scanning Calorimetry (DSC). DSC experiments were performed using a TA Instruments Q2000 DSC using Helium as the purge gas. Materials were subjected to 20°C/min cycles from -100 to 375°C. The enthalpy of fusion (ΔH_f) and characteristic thermal transitions, including the glass transition temperature (T_g), melting temperature (T_m), and crystallization temperature (T_c), were measured in accordance with ASTM D3418.

Thermal Stability. Thermal decomposition behavior of PEEK filaments and printed parts in this study were analyzed using Thermogravimetric Analysis (TGA). TGA experiments were performed using a TA Instruments Q500 TGA. Materials were heated under a helium environment from room temperature to 600°C with a 20°C/min heating rate. At these conditions, the environment was switched to air and all the samples were subjected to an isothermal hold at 600°C for 20 minutes to evaluate potential oxidative decomposition before the test was finalized. Data was analyzed in general accordance to ASTM E1131.

Viscoelastic Properties. The viscoelastic behavior of PEEK filaments and printed parts in this study was analyzed using Dynamic Mechanical Analysis (DMA). Experiments were performed using a TA Instruments Discovery 850 DMA equipped with a Tension Clamp geometry. Temperature Sweep experiments were conducted to obtain dynamic moduli data (E' and E") from -100°C to 200 °C with a heating rate of 5 °C/min, using a deformational frequency of 1.0 Hz.

Results: As depicted in Figure 1, the thermal behavior of PEEK filaments for FFF was analyzed via DSC. All samples showed similar thermal properties, with Tg's around 143°C. Slightly lower melting temperature (Tm) was observed in the material from Manufacturer 1 (333.5°C) compared to that measured in filaments from Manufacturers 2 and 3 (336°C-337°C). Enthalpy of fusion is also similar for all materials in the range of 37-39 J/g, suggesting all materials have similar crystalline content.

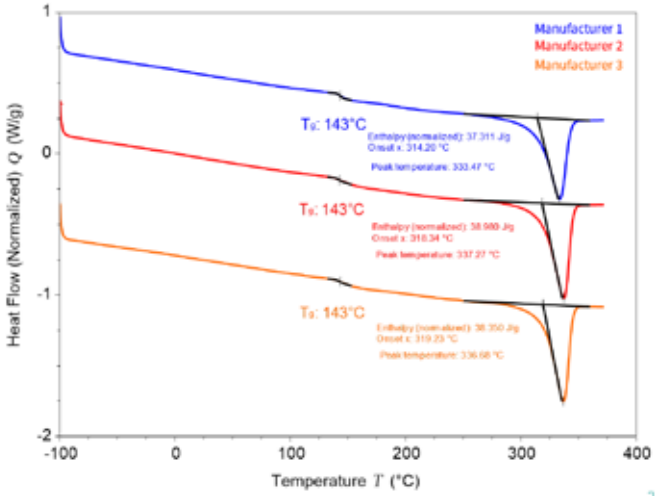

Figure 1 Thermal behavior obtained by DSC of various PEEK filaments included in this study.

Despite the similar thermal behavior of the parent filaments, the effect of printing conditions and filament

source was evident when analyzing the thermal stability and thermal decomposition process of various PEEK filaments and resulting 3D Printed parts. As depicted in Figure 2, all samples show a major thermal decomposition process at temperatures above 500°C. However, a lower thermal stability was observed in the material from Manufacturer 1 based on the earlier onset of thermal decomposition found in this sample compared to other PEEK filaments. In a similar way, processing effects on thermal stability are also evidenced through comparison of the filament and print material from the same source. As shown in this figure, lower thermal stability detected in the 3D printed sample from Manufacturer 2 compared to the parent filament.

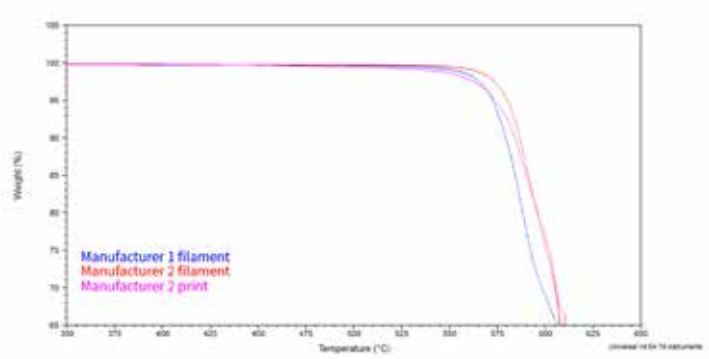

Figure 2 Thermal decomposition of PEEK filaments and a 3D printed parts obtained by TGA.

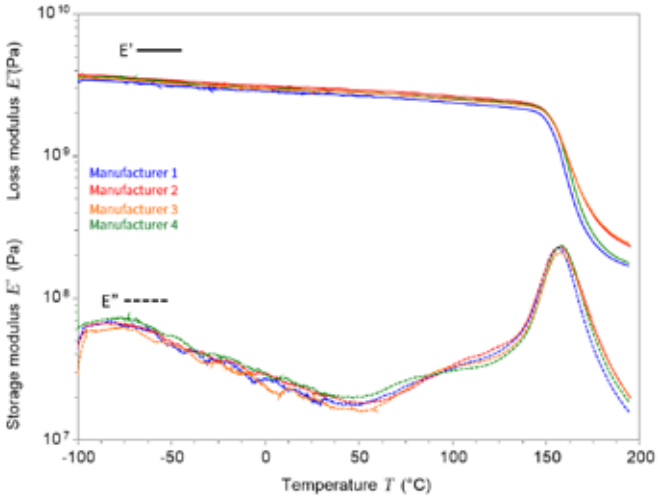

Figure 3 Dynamic Moduli obtained by DMA of PEEK filaments included in this study.

Consistent results were obtained through analysis of the viscoelastic behavior of PEEK filaments and AM parts printed at similar conditions. In this regard, oscillatory measurements at 1 Hz were performed to determine the viscoelastic response of these samples within a broad range of temperatures. Dynamic moduli (E' and E") of various PEEK samples were recorded as a function of temperature as shown in Figure 3. As shown, slight differences were noted among filaments from different sources. Compared to filaments from Manufacturers 2 and 3, material obtained from Manufacturers 1 and 4 have a more pronounced decrease in storage modulus (E') after Tg. In contrast, a relatively consistent dynamic response was observed in all printed parts. DMA data also suggests evidence of the effect of the printing process on the physical properties of PEEK parts. As shown in Figure 4, regardless of the filament source, compared to the parent filaments a decrease in T_g (max. in Tan δ) is observed after 3D printing. Contributions from both thermal and shear processes induced during extrusion are likely associated with these changes.

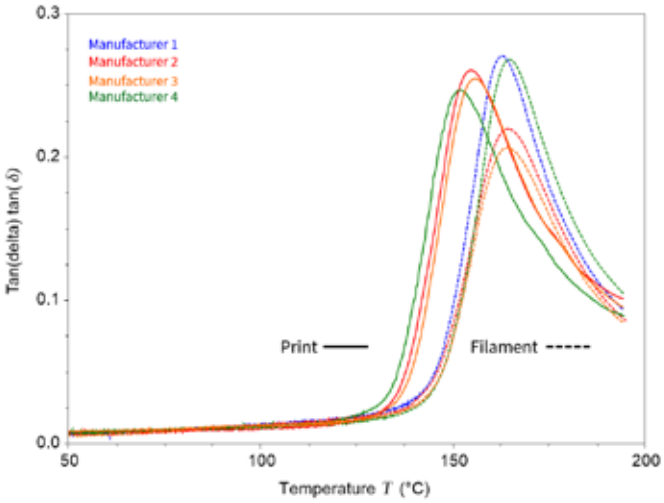

Figure 4 Tan δ (via DMA) of PEEK filaments and printed parts in this study.

Discussion: The conditions used in existing AM processes will have a definite effect on the structure and the properties of 3D printed parts, including those made of PEEK. Understanding the effects of process conditions is essential to predict the performance of these polymers in critical environments. In this study, we evaluated the physical and viscoelastic properties of a series of PEEK filaments and their resulting printed parts produced via FFF. Results suggest changes in the physical properties and viscoelastic behavior due to the printing process and the quality of raw materials.

Thermal and viscoelastic studies revealed that simple geometry parts produced via FFF display different thermal stability and viscoelastic behavior compared to their parent filaments despite the inherently superior properties expected in PEEK resins. Moreover, thermal stability and dynamic mechanical response data suggest different behavior in PEEK filaments from various sources, further suggesting that the inherent properties of raw materials used in FFF could play a significant role in the performance of a AM PEEK parts. These observations appear to be critical especially in high demanding

environments were PEEK (and other PAEK materials) could find a future application.

Developments in PAEKs for Additive Manufacture

Chaplin, A[1]
[1]Victrex Manufacturing, Thornton-Cleveleys, UK
achaplin@victrex.com

Introduction:

PolyArylEtherKetone (PAEK) polymers are increasingly being considered for Additive Manufacturing type processing techniques, where the high performance properties of he polymer are a good potential fit with Additive Manufacture and short, customized production runs. Laser Sintering and Filament Fusion are examples of Additive Manufacture techniques that may be used for processing PAEKs.

This work is intended to show what can be achieved through modification of the chemical backbone of a polymer such as PEEK to improve processability (in Additive Manufacture), whilst retaining the desirable aspects such strength and high purity.

With Laser-Sintering, known drawbacks with currently available materials include poor recycle potential of un-sintered powder [1] and the brittle failure (low elongation at break) of sintered parts. Improvement of both of these aspects was a primary aim of this work.

In Filament Fusion, highly crystalline polymers such as PAEKs have notoriously poor Z-direction strength, compared to the horizontal (XY) direction. Improved Z-strength of printed parts was therefore an objective. In both of these cases, the improvements would need to be achieved without adversely affecting the existing, desirable properties of the polymer such as its crystallinity.

Methods and Materials

PAEK materials were adapted for Filament Fusion by re-designing the polymer backbone, rather than by use of additives and modifiers. Like PEEK, the new polymers are fully aromatic, semi-crystalline PolyArylEtherKetones. They are free of additives and have a similar purity profile to PEEK. The polymers were made on a 50kg batch scale with a pilot scale polymerization plant, using similar polymerization technology to established PEEK.

The new polymers were designed to have a lower melting point than PEEK, of approximately 304°C (PEEK 343°C). In addition, the new polymers had reduced shear thinning and higher flow at low shear rates compared to PEEK. Another feature designed into the new materials was a much lower crystallization speed compared to conventional PEEK.

Results

A development grade for Laser Sintering (DEV-LS-B) was found to give a similar tensile strength to HP3 (a commercially available PAEK powder) of approximately 80 MPa, but with a much higher elongation-at-break of approximately 7%. It was also possible to demonstrate recycle of used powder at levels of up to 50% with no loss of properties.

With Filament Fusion, a Z-direction strength of 55MPa was achieved, against a typical baseline of <25 MPa for PEEK (using a conventional printer without heated chamber).

Discussion

With the Laser Sinter PAEK, the reduced melting point facilitated a lower bed temperature during processing and it is believed that this in turn resulted in a reduction in thermal degradation of the un-sintered powder compared to a polymer processed at higher temperatures. This would at least in part explain the ability to re-cycle this material without adversely affecting properties of sintered parts.

In filament fusion, it is believed that the slower crystallization of the polymer compared to PEEK, allowed the printed layer to remain amorphous for sufficient time for the next layer to be printed over it. This is believed to significantly improve inter-layer adhesion compared to printing onto a crystallised substrate. The improved rheology (better low-shear flow) could also have contributed to improved inter-layer adhesion.

In conclusion, improvements in PAEK materials for both Laser Sintering and Filament Fusion were achieved through modification of the polymer backbone at the polymerization stage.

This work was supported by Innovate UK funding. Victrex were lead party in a consortium that also included University of Exeter, EOS, South-West Metal Finishing, Airbus, E3D-Online, HiEta and 3T-RPD.

conclusion, PEEK might be the new resource required for future denture material.

[1] O.Ghita et al, Journal of Materials Processing Technology, 214 (2014), p969-978

Apium M220 medical device manufacturing machine

Popp, Uwe[1], Okolo, Brando[1]
[1]Apium Additive Technologies GmbH, Karlsruhe, Germany
Uwe.popp@apiumtec.com

Introduction: Only over the past 4 years has it been possible to process PEEK using commercially available Material Extrusion (ME) 3D Printing technology. Apium Additive Technologies GmbH, the first to introduce such a machine and a corresponding PEEK filament into the market for non-medical applications, has recently developed their technology for implantable medical device applications. Their 3D printing technology entirely relies on the quasi-isothermal deposition of melted PEEK filament onto a surface thermally conditioned at temperatures only slightly above the glass transition temperature (T_g) of PEEK. Apium's M220 3D printer operates under a stringent thermal management system ensuring that PEEK parts of the best possible quality are realized using the ME technology. In the development of the M220 machine, attention was given to the use of only materials certified for medical applications in all areas where there is a physical contact between the filament and the machine namely the bearings, guiding tubes for the filament, the nozzle and the print-bed. The software which manages the printing process has a general user interface architectured for easy navigation through the operating menu. A printing report is produced at the end of each print job where all essential information such as the readings from all thermal sources and sensors, the displacement of the print head, the amount of material used for the print-job, the loading/extrusion rate of the filament as well as all other regulated parameters associated with the printing process. An air filtration system included in the M220 printer ensures that stray/foreign particles (dust) are prevented from being incorporated into the material being printed. This is achieved through inlet air filtration and recirculation of ambient air in the printing chamber. While these precautions lend some credibility to the M220 machine, the most decisive aspect of the machine is the science-backed evidence that implant grade biocompatible PEEK filament processed on the M220 machine retain their biocompatibility with no additional chemical markers indicated in the as-printed PEEK part. Typically testing in accordance to international standards such as ISO 10993 as required by notified bodies are needed.
The basis of this presentation is on how the M220 3D printer works, its print-job documentation outline and the outcome of tests conducted as this machine goes to market.

Methods and Materials:
Testing for chemical species in the PEEK filament and as-3D printed PEEK parts were conducted using X-ray Photoelectron Spectroscopy (XPS).
Testing for mechanical properties in key printing orientations (based on a Cartesian space; where x and y are out of plane directions while z is the layer thickness direction) especially to determine the extent of layer bonding were conducted in bending mode and tensile mode.
Testing for dimensional accuracy was conducted using a statistical approach using a variation of square sizes. These squares have been printed, measured and compared to the desired dimensions.
Testing for bio-compatibility on the PEEK filament and the as-3D printed parts was conducted in accordance to ISO 10993.
The PEEK materials used were filaments extruded by Ensinger from Victrex 450 G and the i4 from Evonik.

Discussion: The chemical analysis tests showed that the chemical finger-print of the filament is reproduced in the 3D printed parts and that no additional chemical species were formed in the printed part as a result of the printing process.
The mechanical tests showed that the PEEK parts printed in the x and y directions had a tensile strength of up to 90% of the nominal strength of the material as provided by the PEEK material supplier. In the z direction, the bending strength was up to 60% of the value provided by the material supplier.
The dimensional accuracy of printed parts and print reproducibility tests revealed that printed parts are precise up to 0.05 µm of design specification while the print quality reproducibility is in the order of 90% certainty.
The biocompatibility tests were conducted for the organic as well as the inorganic cases on PEEK parts of standard geometry. These PEEK parts were 3D printed under clean-room ISO class 7 and non-clean room conditions. The tests revealed that the PEEK filament as well as the 3D printed PEEK parts do not contain germs in quantities suggestive of contamination. Also the tested PEEK samples had no indications of the presence of volatile organic compounds (VOC's).
These tests demonstrate the suitability of the M220 machine for use in the production of human implantable medical devices.

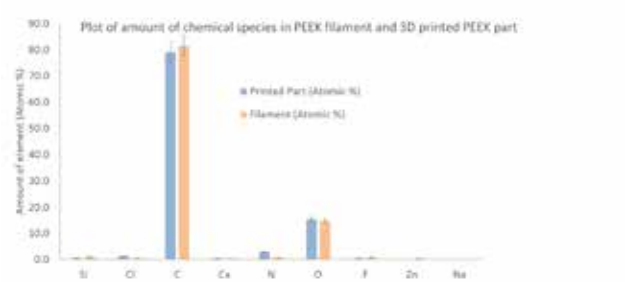

Plot obtained from XPS measurements of elements in PEEK filament and 3D printed PEEK parts.

3D Printing of Medical Products with PEEK Using FLM Technology

Stefan Leonhardt, Sebastian Pammer
Kumovis GmbH, Munich, Germany
stefan.leonhardt@kumovis.com

Introduction: Individualization respectively patient-specific medical products are of high advantage for patients and medical staff. Depending on the application, high performance plastics are often the preferred material for the products, due to radiolucency, low density, bone-like mechanics or biocompatibility. E.g. for patient specific implants, conventionally the polymer PEEK is processed by milling for individualized dental or cranial implants.

Methods and Materials: With a new 3D-printing technology from Kumovis (Munich, Germany) based on Fused layer manufacturing (FLM, also known as FDM), high performance plastics such as PEEK can be processed by additive manufacturing. Kumovis develops 3D printers, specially tailored to the requirements of regulated markets such as medical technology. The company focuses on the processing of high-performance plastics such as PEEK, which is already established in medical technology. With this technology a reproducible production of medical products via additive manufacturing is realized. Additive manufacturing enables the production of a new generation of implants:

- implants on demand
- economic production of patient individualized implants
- functionalized implants, for example with lattice structures that enable an improved bone ingrowth

To bring such innovative products from the lab to the patient specialized 3D printers are developed that fulfill the requirements to produce medical products.

Current issues are especially:

- size accuracy
- reproducibility
- mechanical properties (especially layer adhesion)
- suitable processes for the medical sector
- process monitoring (validation of processes)

The key element of Kumovis 3D-printers is their patented temperature management system. A laminar air flow cycle enables a constant and homogenous temperature distribution within the hole printing area. The air can be heated up to 250 °C, what enables the production of PEEK products in high quality. Furthermore, the air flow cycle can be equipped with a filter system that enables the production of medical products in a clean environment.

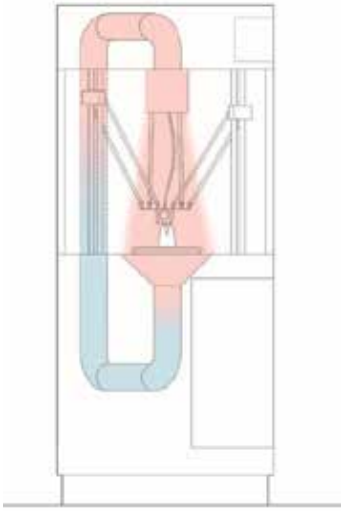

Figure 1: Temperature management system for printing high performance plastics, patented by Kumovis

Results: Several tests showed that the temperature management has a huge impact on the mechanical properties of the printed parts. Interlayer-adhesion and thus mechanical strengths is significantly improved by increased surface temperature. To print details or fine lattice structures an adjustable temperature management is essential to produce high quality products.

Discussion: An adjustable temperature management keeping the printed part on a certain temperature is a main reason for good mechanical results in combination with detail resolution.

Additive Manufacturing combined with the mechanical and biocompatible properties of PEEK, enable mass customization and small series production of medical products such as:

- 3D printed cranial implant
- 3D printed spinal cages
- 3D printed surgical guides

At the 4th International PEEK Meeting, Kumovis will show their technology in more detail and will present several use-cases.

Effect of Pore Size on Bone Regeneration of 3D-printed Porous PEEK Implant in Critical Size bone Defects

Kai Xie[1], Mengning Yan[1], Xuequan Han[1], Xu Jiang[1], Liao Wang[1], Xianming Dong[2], Chao Zeng[2]
[1] Shanghai Key Laboratory of Orthopaedic Implants, Department of Orthopaedic Surgery, Shanghai Ninth People's Hospital, Shanghai Jiao Tong University School of Medicine, Shanghai, China
[2] INTAMSYS Technology Co., Ltd.
mczt_x@163.com; yanmengning@163.com

Introduction: The ideal pore size of 3d-printed porous PEEK implant for the treatment of critical size bone defects still unclear. Therefore, 3D-printed porous PEEK implants with three different pore size (400μm, 600μm, 800μm) are prepared. The proliferation and mineralization of human bone mesenchymal stem cells (hBMSCs) on the surface of three different 3d-printed porous PEEK implants was evaluated *in vitro*. Moreover, the effect of pore size on bone ingrowth of 3d-printed porous PEEK implants was determined *in vivo* with critical size calvarial defects.

Methods and Materials:
The proliferation of hBMSCs on the surface of 3D-printed porous PEEK implants were evaluated by using a CCK-8 assay After 1, 3, 5, and 7-days incubation. The effect of pore size on the *in vitro* osteogenic differentiation of hBMSCs were evaluated by using alkaline phosphatase activity assay and alizarin red staining. Bone ingrowth into 3d-printed porous PEEK implants was evaluated with micro-CT, van Gieson staining, and double-fluorescence labeling at 4, 8, 12 weeks after implantation both qualitatively and quantitatively.

Results:
All three 3D-printed porous PEEK implants showed promising cytocompatibility *in vitro*. The cell viability increased in all samples with time. The *in vivo* evaluation indicated that the 3D-printed PEEK implant with pore size of 600μm exhibited significant higher bone formation and bone ingrowth compared to those of implants with a pore size of 400μm and 800μm.

Discussion:
The PEEK is considered as an ideal material for orthopedic implants with excellent cytocompatibility, mechanical property, and chemical resistance. However, the poor bone-implant osseointegration restrict the extensive use of PEEK implants. The pore structure could significant influence the biological behavior and bone-implant osseointegration performance of PEEK implants. However, the regular pore structure with large pore size on PEEK implant is difficult to fabricate in the past. Therefore, the ideal pore size of 3d-printed porous PEEK implant for the treatment of critical size bone defects remians unclear. The development of 3D printing provides a novel approach to fabricate porous PEEK implant with different pore size. The effect of pore size on bone ingrowth of 3d-printed porous PEEK implants was determined in current study. The result of our study indicates that the 3D-printed PEEK implant with pore size of 600μm exhibited significant higher bone formation and bone ingrowth compared to those of implants with a pore size of 400μm and 800μm, which supports the potential use of 3D-printed porous PEEK implant for the treatment of critical size bone defects.

Comparison of different FFF PEEK printer generations and nozzle sizes for FFF printed PEEK spinal cages

Cemile Basgul[1], Daniel W. MacDonald[1], Ryan Siskey[1,2], Steven M. Kurtz[1,2]
[1]Drexel University, [2]Exponent, Inc.
cb997@drexel.edu

Introduction: Polyaryletheretherketone (PEEK) has been commonly used for interbody fusion devices because of its biocompatibility, radiolucency, durability, and strength. While the technology of PEEK Additive Manufacturing (AM) is rapidly developing, comparison of 3D printed PEEK with different FFF PEEK printer generations is remains unknown. AM of PEEK has been challenging because of its high melt temperature (over 340°C) and requires specialized equipment that can reach high temperatures for FFF systems. A lumbar fusion cage design, used in ASTM interlaboratory studies, was 3D printed with a medical grade PEEK filament via Fused Filament Fabrication (FFF) with two different generations of FFF PEEK printers. Cages were then tested mechanically under compression to understand how the interlayer adhesion and porosity in 3D printed PEEK cages are possibly affected from different technologies.

Methods and Materials: We used a reference intervertebral lumbar cage design developed for ASTM interlaboratory studies. Cages were printed from a prototype medical grade PEEK OPTIMA LT1 (Invibio, UK) filament (1.75 mm) with two different nozzle sizes (0.2 and 0.4 mm) and under two different speeds (1500 & 2500 mm/min) using 3D printer customized for PEEK (P220-Apium Additive Technologies, Germany). According to ASTM F2077 [2], six cages for each cohort were tested under compression as the loading condition. Maximum load and displacement values were recorded for each test condition. In addition, three cages from each cohort were μCT scanned at 10 μm uniform resolution using a Scanco μCT 80 (Scanco, Switzerland) to determine the overall porosity. A control volume (5x5x2 mm^3) was created to measure the porosity from the scans. The results of P220 cages printed with the same nozzle diameter (0.4 mm) and same speed (1500 mm/min) were compared with the results from older studies where cages were printed with older FFF machine, HPP155 (Apium Additive Technologies, Germany). Statistical analysis was performed in SPSS 25. Different nozzle sizes with the newer FFF machine were compared using Two-way ANOVA. Independent Samples t-test was used to compare the newer and older versions of the FFF systems.

Results: Both nozzle diameter and number of cages printed at a time had a significant effect on the cages' maximum load before failure ($p<0.001$, for both), whereas printhead speed was not significant ($p=0.2$). Under slower print speed and bigger nozzle diameter, printing one cage at a time showed higher maximum loads than both printing four and eight at a time (mean difference=2396 & 2772 N, respectively, $p<0.001$ for both). Similarly, for higher print speed, while printing with bigger nozzle diameter, printing one cage at a time showed higher maximum loads than both printing four and eight at a time (mean difference=2752 & 2570 N, respectively, $p<0.001$ for both). Furthermore, for the same print speed, while printing with smaller nozzle diameter, printing one cage at a time showed higher maximum loads than both printing four and eight at a time (mean difference=1678 & 1552 N, respectively, $p<0.001$ for both). However, under slower print speed and the smaller nozzle diameter, both printing one cage at a time and eight at a time showed higher maximum loads than printing four (mean difference=1018 & 1376 N, respectively, $p<0.01$ for both). Furthermore, cages printed with a smaller nozzle showed lower maximum load than printed with the bigger nozzle size under five out of six conditions ($p<0.001$ for all). When comparing the printer generations, only cages printed once at a time with the newer version of FFF machine showed higher maximum load compared to six cages printed once at a time with the older version of the FFF system (mean difference=3090 N and $p<0.001$). However, there was not a significant difference when printing four and eight at a time with the newer printer versus printing six at a time with the older printer. In addition to the mechanical test results, cages printed with the newer FFF machine showed 0.57% porosity, whereas porosity observed with the older FFF machine was 3.82%.

Discussion: This study compares two FFF systems for PEEK as well as different features (different nozzle diameters) provided with the newer FFF system. It was observed that single prints achieved higher strength than multiple prints with the newer FFF machine for both features. In the same manner, only single prints with the newer FFF system failed under higher mechanical loads than multiple prints with the older FFF system. Although the porosity results were different, there was not a difference in cages strength between the newer versus older FFF systems while printing multiple cages. Thus, the failure mechanism is likely affected more by the interlayer adhesion which was poorer while printing multiple, since the cooling time of a layer is increasing. In addition, printing with the smaller diameter nozzle results in smaller layer height which dries quicker that leads to poor interlayer adhesion as well. The results of this study demonstrate the effect of different FFF printer generations on 3D printed PEEK cages. Our findings will lead researchers to further investigations on 3D printed implants and processing conditions.

References [1] Kurtz SM. PEEK Biomaterials Handbook. 2011. [2] ASTM F2077-14, 2014.

Acknowledgement: This study was supported by NIH-R01 AR069119. We would like to thank Invibio for

donating the filament and Apium for their helpful advice and fruitful discussions.

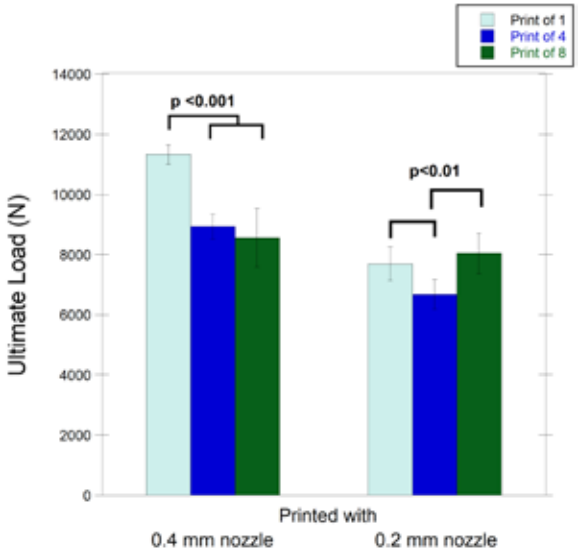

Figure 1. Ultimate load comparison of the cages printed with different nozzle diameters on the newer generation PEEK printer (P220) under slower speed.

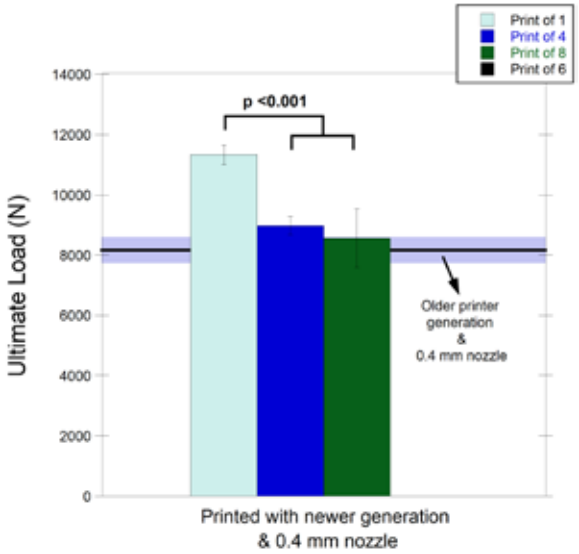

Figure 2. Ultimate load comparison of the cages printed with the newer generation (P220) versus older generation PEEK printers (HPP155) under slower speed.

PEEK laser sintered intervertebral lumbar cages: process and properties

R. Davies[1], Y.T. Shyng[1], P. McCutchion[1], T. Holsgrove[1], O.Ghita[1]
[1] College of Engineering, Mathematics and Physical Sciences, University of Exeter, North Park Road, Exeter, EX4 4QF, UK
o.ghita@exeter.ac.uk

Introduction:

PEEK material has been used in implants since the 1990s. Its unique characteristics such as biocompatibility, biostability, radiographic translucency, low abrasion and stress fatigue, mechanically tough with an elastic modulus similar to human bone, made PEEK the material of choice for cranio-facial implants [1, 2] as well as load bearing implants such as intervertebral lumbar cages and even knee replacements [3, 4, 5]. The growing use of PEEK 3D printing technologies in other industries and their continuous improvements over the last five years, brought the attention of the medical sector. Additive Manufacturing can allow manufacture of a wider range of implant sizes or patient specific implants, shorter lead time from design to manufacture and therefore support the growing and aging population. To date, the majority of studies on PEEK AM used extrusion deposition methods, known also as Free Form Fabrication (FFF) techniques [6, 7, 8, 9, 10]. Powder bed fusion, known as laser sintering, had only a few medically related studies [11] although it is the only AM technology commercially manufacturing medical implants with OXPEKK® material formulation [12]. There is very little known about the properties and behaviour of PEEK 3D printed implants under load conditions similar to those controlling the human body.

A drawback of some of the AM technologies, including FFF and LS, is the weaker layer to layer bonding which leads to a weaker mechanical performance in the vertical, as built direction (known also as Z direction) in comparison with the horizontal direction (X-Y directions).

This study presents mechanical properties of laser sintered lumbar cages and highlights the influence of various build directions on the sample performance. Where possible, a comparison with literature values is included.

Methods and Materials:

The material used for the manufacture of PEEK components is Victrex® PEEK 450PF. The material presents a glass transition temperature of 143˚C and a melting temperature of 343˚C. The powder was thermally treated for 24 hours before use in the EOSINT P800. The PEEK powder is not a laser sintering grade.

A standardized lumbar fusion cage design [6] was chosen for this investigation as shown in Figure 1.

Figure 1. Standardized intervertebral lumbar cage design [6]

Three build orientations were chosen to manufacture the cages: i) vertical, ii) oblique; iii) horizontal. The parts were manufactured in a reduced chamber configuration mode with laser power of 15W, a laser speed for 2550 mm s^{-1} and scan spacing of 0.2mm.

10 samples were manufactured and tested in compression for each orientation using a LLOYD EZ20 mechanical testing machine. The intervertebral body fusion devices were place between two flat metal blocks and tested in compression at 15mm/min using a 20kN load cell. The main external dimensions (height, depth and width) of all samples were measured using a digital caliper and compared against the STL file model.

For clarity, Figure 2 presents the printed and tested configurations.

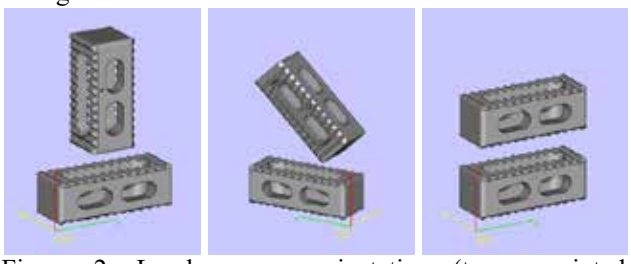

Figure 2. Lumbar cage orientation (top - printed orientation, bottom – tested orientation)

The SEM examination was performed using a Hitachi S-3200N scanning electron microscope. All samples were coated with 4 nm of gold coating in order to reduce the surface charging and the electron secondary imaging was set with an accelerating voltage of 25 kV.

Results:

Table 1 shows the variation in external dimensions of the manufactured samples.

Build orientation	Tested orientation			
	Height (mm)	Width (mm)	Depth (mm)	Overall cross-sectional area (mm^2)
STL file	10	10	25	250
Flat	10.05 ± 0.04	9.95 ± 0.03	25.84 ± 0.05	259.69
Vertical	9.75 ± 0.04	9.93 ± 0.05	26.31 ± 0.08	256.52
Oblique	9.88 ± 0.03	9.94 ± 0.07	25.90 ± 0.09	255.90

Table 1. External dimensions of the lumbar cages

It is well established that laser sintered samples develop a down and upper skin in the vertical orientation of the build. The down skin is formed by extra powder melted below the sintering layer which remains attached to the fabricated part, where the upper skin is the result of shrinkage. The depth of the parts used in the calculation of the cross-

sectional area, which represents here the vertical build position, shows an increase, of approx. 4 % in comparison with the original STL file. This is expected to result in errors when calculating the active cross-sectional area and subsequently the stress. The internal features are expected to introduce further errors. Although additive manufacturing processes allow printing of complex geometries, part resolution and accuracy of printed features can sometimes be distorted or over or under sized. This is particularly true in powder bed processes where the powder supporting the printed part fuses into the last printed layer.

Figure 3, 4 and 5 present three representative repeat traces of each batch tested. The results show good repeatability in the mode of failure of each batch.
The vertical and flat samples have a slower fracture behavior with several cracks propagating slowly through the structure.

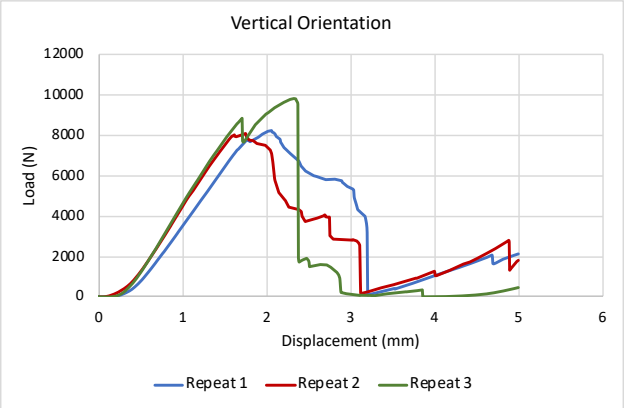

Figure 3 Load-displacement of a PEEK lumbar cage laser sintered in vertical orientation

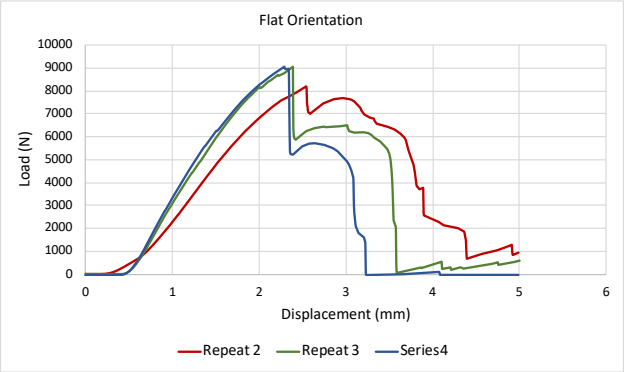

Figure 4 Load-displacement of a PEEK lumbar cage laser sintered in flat orientation

The flat load-displacement curves have similar patterns and show the first failure peaks taking place repeatedly in a specific displacement region: 2.2 and 2.6mm.
In comparison with the vertical and flat load displacement curves, the oblique traces show a sharp, single peak an indication of a major failure.

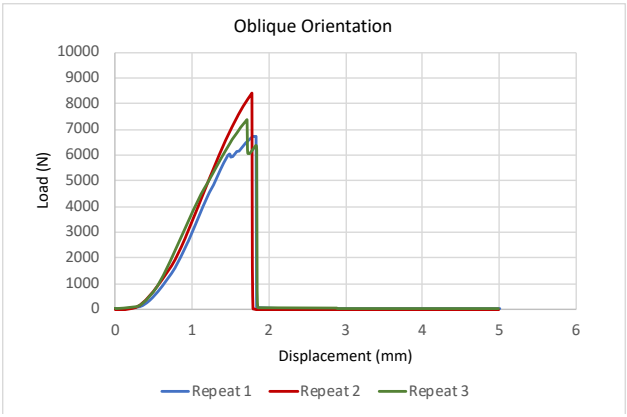

Figure 5 Load-displacement of a PEEK lumbar cage laser sintered in oblique orientation

Table 2 presents the average load, displacement and absorbed energy of the laser sintered samples fabricated in different orientation. The FFF and machined values were added for comparison [6]

	Max load (N)	Max displacement (mm)	Absorbed Energy (J)
Machined [6]	14229 ± 335	3.12 ± 0.4	-
FFF [6]	8964 ± 304	1.43 ± 0.2	-
LS Flat	9074 ± 476	3.8 ± 0.6	18752.2 ± 4780
LS Vertical	8738 ± 896	3.2 ± 0.4	14683.8 ± 2481
LS Oblique	8071 ± 1177	2.2 ± 0.4	6973.58 ± 2006

Table 2 Average load, average displacement and absorbed energy for each printed group.

Results in Table 2 show similar load values for laser sintered and FDM samples. The laser sintered samples recorded a 63% load of the machined cage. The displacement values of all LS cages were higher than those recorded from the FFF system and the cages built in flat and vertical configurations had higher displacement values than the machined ones. However, it is important to notice that the majority of traces show the main failure with a clear peak at a much earlier displacement than the max displacement value given in Table 2. As expected, the flat structure which is least influenced by the layer to layer bonding absorbed highest energy. The cages printed vertically had only a 21% drop in energy absorbed during the compression test where those printed oblique required very little work to produce total failure of the structure.
The maximum compression stress values for each orientation were also calculated, using the minimum cross-sectional area from the STL file, results are presented in Figure 6.

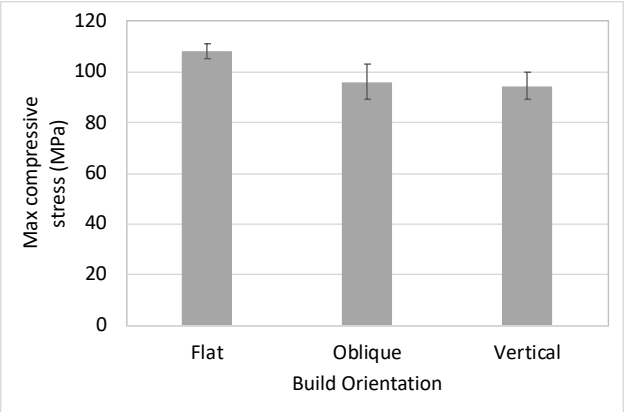

Figure 6 Maximum compressive stress of PEEK lumbar cages printed in different build orientation.

The cages printed flat seem to provide slightly higher strength than those printed oblique or vertical.
A close examination of the tested samples revealed that all batches break in the areas with the thinnest cross section regions as shown in Figure 7 and Figure 8.

Figure 7 (a) Key failure points of the lumbar cages.

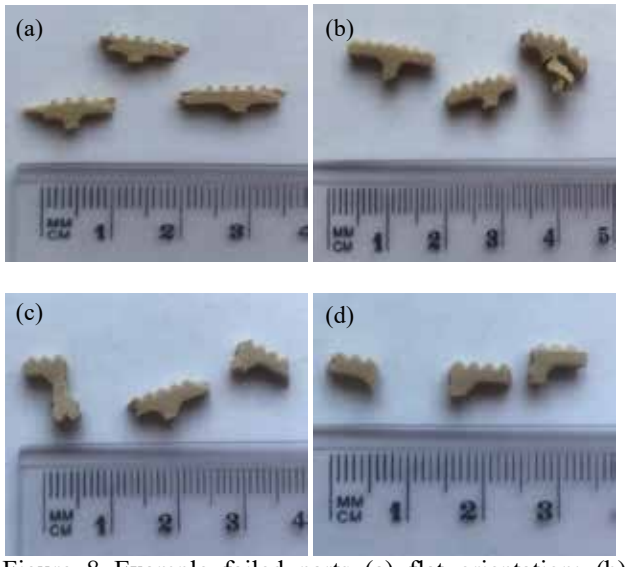

Figure 8 Example failed parts (a) flat orientation; (b) vertical orientation; (c) oblique orientation.

The flat and vertical lumbar cages had a more consistent and repeatable breaking pattern as noticed as well in the load-displacement curves, where the oblique samples were most unpredictable in the failure pattern.

The three types of fractured surfaces were examined using Scanning Electron Microscopy (SEM). Images are presented in Figure 9 (a) to (c).
Depending on the build orientation, the microstructure at the fracture interface had a different morphology. The flat and oblique orientations showed a brittle fracture through the entire cross section with the sintered layers clearly visible. The vertically built samples were significantly different, two types of fracture surfaces were observed: brittle region and granular region with a combination of brittle and ductile areas (Figure 10).

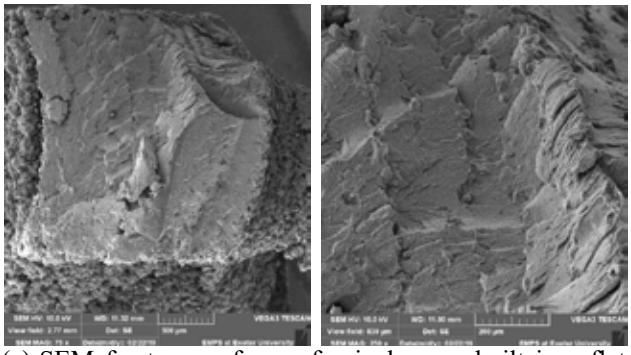

(a) SEM fracture surfaces of spinal cages built in a flat orientation

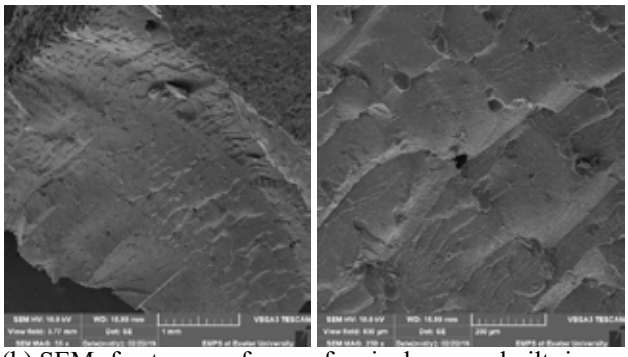

(b) SEM fracture surfaces of spinal cages built in an oblique orientation

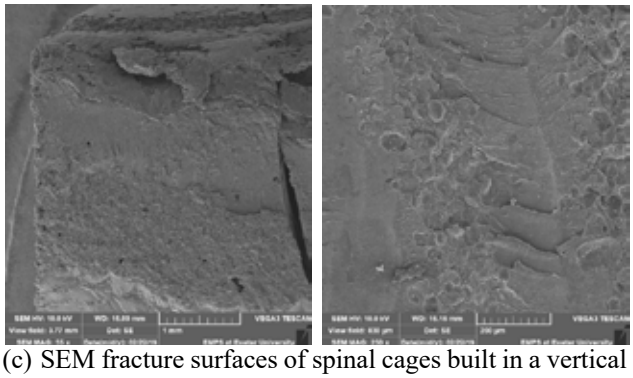

(c) SEM fracture surfaces of spinal cages built in a vertical orientation

Well-defined particles with a ductile interface or completely de-bonded particles were noticed across the fracture surface. These SEM images confirm the load-

displacement curves, where the crack propagates slowly through the sample, taking a more tortuous path as it reaches these two region types.

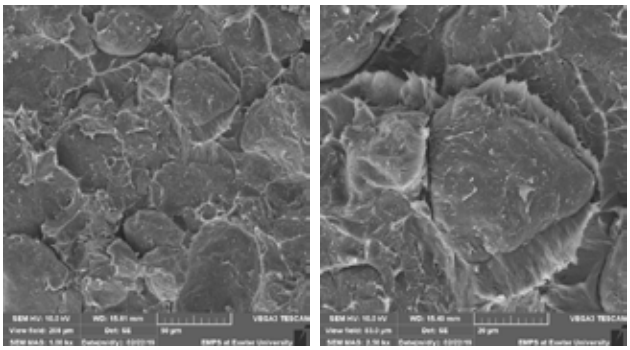

Figure 10 Close up SEM images of the granular regions of spinal cages built in a vertical orientation

Discussion: The results showed that laser sintered lumbar cages recorded similar loads and displacement values as the FFF cages. The lumbar cages printed flat absorbed most energy. Surprisingly, the differences between the cages printed vertical and flat were not as drastic as originally expected. The failure patterns of the oblique printed cages were significantly different than the vertically and flat printed samples. The SEM images highlighted specific undesirable features characteristic to the additive manufacturing processes. The examination of the tested cages highlighted the weak points of the design and the requirement for redesign for additive manufacturing, more specifically in this case laser sintering.

References:

[1]https://cmf.stryker.com/products/peek-customized-implant

[2] F. El Halabi, et al., Mechanical characterization and numerical simulation of polyether-ether-ketone (PEEK) cranial implants, *J. Mech. Behav. Biomed. Mater.,* vol. 4 (8) (2011) 1819–1832

[3]https://invibio.com/-/media/files/en/trauma/kneewhypeekknee105en.ashx

[4] N. T. Evans, F. B. Torstrick, et al., High-strength, surface-porous polyether-ether-ketone for load-bearing orthopedic implants, *Acta Biomater*., vol. 13 (2015) 159-167

[5] A. M. Diez-Pascual, A.L. Diez-Vicente, Nano-TiO_2 Reinforced PEEK/PEI Blends as Biomaterials for Load-Bearing Implant Applications, *ACS Appl. Mater. Interfaces,* vol. 7 (9), (2015), 5561-5573

[6] C. Basgul et al., Structure–property relationships for 3D-printed PEEK intervertebral lumbar cages produced using fused filament fabrication, *J. Mater. Res.,* vol. 33 (14), (2018).

[7] B. Valentan, et al., Processing poly(ether etherketone) on a 3d printer for thermoplastic modelling, *Materiali Tehnologije,* vol. 47 (6), (2013) 715- 721.

[8] C.Y. Liu, et al., Design and test of additive manufacturing for coating thermoplastic PEEK material, in: Proceedings of the IEEE International Conference
on Industrial Technology, 2016.

[9] M. Vaezi, S. Yang, Extrusion-based additive manufacturing of PEEK for biomedical applications, *Virtual Phys. Prototyp.,* vol.10 (3) (2015) 123-135.

[10] W. Wu, et al., Influence of layer thickness and raster angle on the mechanical properties of 3D-printed PEEK and a comparative mechanical study between PEEK and ABS, Materials 8 (9) (2015) 5834 - 5846.

[11] S. Berretta et al., Additive manufacture of PEEK cranial implants: Manufacturing considerations versus accuracy and mechanical performance, Materials and Design 139 (2018) 141-152

[12] http://oxfordpm.com/cmf-orthopedics

In Vitro Response to FFF Printed Porous PEEK Surfaces

Spece, H[1]; Yu, T[1], Law, AW[1], Marcolongo, M[1], Kurtz, SM[1,2]
[1]Drexel University, Philadelphia, PA
[2]Exponent Inc., Philadelphia, PA
Hgs29@drexel.edu

Introduction:

Clinical interest in polyetheretherketone (PEEK), an inert thermoplastic polymer, has been rapidly growing due to its modulus of elasticity similar to bone, natural radiolucency, and biocompatible wear debris [1, 2]. Though concerns have been raised about the bioinert nature of PEEK and its limited interaction with bone, the creation of porous networks has shown promising results for bone ingrowth [3, 4]. The interconnected pores of these networks create scaffolding that mimics bone morphology, provides anchorage for cell attachment, and allows for vascularization, thus exhibiting inherent osteoconductivity [5]. However, the structures are costly and difficult to produce by traditional machining methods. In this study, we therefore aim to manufacture porous PEEK structures via fused filament fabrication (FFF, 3D printing) and assess the effect of porous geometry on cell viability and activity. We hypothesize that the FFF printed porous PEEK structures will exhibit greater osteoblast viability and activity as compared to solid PEEK controls.

Methods and Materials:

Manufacturing and Characterization of Porous PEEK

Three different porous constructs (referred to as lattice, gyroid, and diamond) were designed to mimic the morphology of trabecular bone in their pore size and porosity. Printability of the geometries was also considered. The lattice structure is a simple network of cubic pores created by alternating layer deposition direction. The gyroid and diamond constructs were designed using triply periodic minimal surface (TPMS) models, which display periodicity in all three directions and are suitable for creating porous networks. The gyroid (Schoen Gyroid) and diamond (Schwarz Diamond) surfaces were selected from among all TPMSs for their pore interconnectivity and printability. Theoretical pore sizes and porosity were determined by analysis of the 3D models in Simplify3D (Cincinnati, OH).

The structures, along with solid PEEK samples for us as a control, were additively manufactured via fused filament fabrication using PEEK (PEEK 450G, Victrex, Lancashire, UK) filament. All samples, measuring 10mm x 10mm x 2mm, were manufactured with the same printer (Apium P220, Karlsruhe, Germany) and printing parameters. Following manufacturing, one sample of each geometry was μCT scanned using a Scanco μCT 80 (Nokomis, FL) to determine the resulting pore size and porosity.

In Vitro Cell Culturing

Prior to cell seeding, the PEEK constructs were washed and sterilized in UV light and 70% ethanol 3x for 30 minutes each. The PEEK constructs were then incubated in cell culture media overnight. MC3T3 E1 pre-osteoblast cells were seeded onto the porous PEEK constructs at a cell

t: solid, lattice, gyroid, and diamond.

density of 30,000 cells/construct for 7 and 14 days. Cell proliferation and alkaline phosphatase activity (ALP) were evaluated at each time point. Briefly, the MTT tetrazolium dye was added to each construct for 4 hours at 37°C and solubilized in dimethyl sulfoxide for 10 minutes. The solution was read in a TECAN at 540 nm (Niks M, J Immunological Methods, 1990). For ALP, p-nitrophenol phosphate was added (pNPP) was added to each construct for 1 hour at room temperature. The ALP enzyme secreted by the cells in culture dephosphorylates the pNPP reagent and turns to a yellow solution, which was read in a TECAN at 405 nm [6].

Additional constructs with cells cultured for 7 days (n = 4 for each design) and 14 days (n= 4 for each design) along with control constructs with no cells were imaged using a Zeiss Supra 50VP scanning electron microscope. Prior to imaging, samples were fixed with Karnovsky's fixative (2.5% glutaraldehyde and 2% paraformaldehyde) for 30 minutes, dehydrated in a series of increase alcohol concentration, and dried in hexamethyldisilazane for 4 hours. The constructs were sputter coated with platinum/palladium alloy. Micrographs were collected with a secondary electron detector at an accelerating voltage of 20 kV.

Results:

μCT imaging showed the pores in the PEEK constructs to be open and interconnected. The average pore size was 535 ± 92 μm for the lattice, 484 ± 237 μm for the diamond, and 669 ± 216 μm for the gyroid. Porosity was 71% for the lattice, 76% for the diamond, and 68% for the gyroid. The average error between the theoretical and actual values was -37.3 μm (standard deviation: 95.6) for pore size and -2.3 % (standard deviation: 6.7) for porosity.

ALP activity was normalized to the cell number at each time point to determine the ALP activity per unit cell. Normalized ALP activity of the three porous PEEK samples at 7 days were found to be significantly greater than the solid sample ($p < 0.05$ for lattice, $p < 0.005$ for gyroid, $p < 0.001$ for diamond). At 14 days, the same relationships were observed ($p < 0.001$ for all three designs). No difference between the three porous constructs was found (Figure 2).

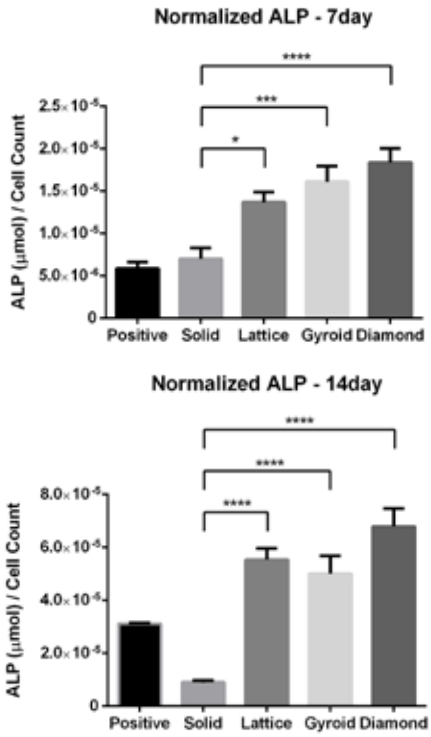

Figure 2. ALP assay of cells cultured on porous PEEK constructs for (top) 7 days and (bottom) 14 days. n = 6 for each design and timepoint combination.

SEM imaging of the 7-day samples revealed cells with flat, elongated morphology attached to the surface of the PEEK (Figure 3). The cells were distributed sporadically on the porous constructs with some instances of cell-to-cell interaction in the form of connecting cell extensions. At 14 days, the cells appeared to have proliferated well and further spread on the PEEK (Figure 4). More cell-to-cell interactions were observed, and in some instances a monolayer of cells could be found covering the PEEK surface.

Figure 3. SEM images of pre-osteoblast cell cultured on a gyroid porous PEEK structure for 7 days. Cells appeared attached to the PEEK surface and displayed a flat, elongated morphology.

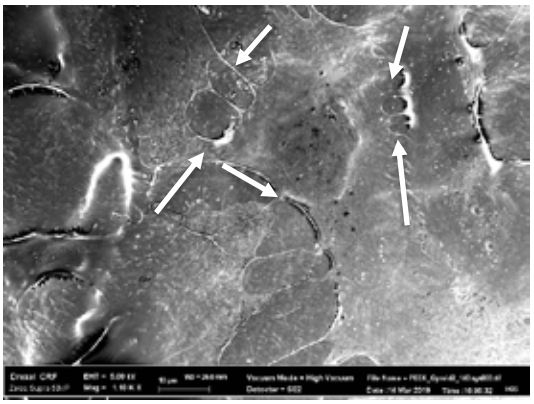

Figure 4. SEM images of pre-osteoblast cells cultured on the gyroid porous PEEK structure for 14 days. The cells have proliferated and spread, and cell-to-cell interactions (denoted by arrows) are apparent.

Discussion:

The fixation of orthopaedic components is greatly influenced by the biologic reaction at the bone-implant interface and, more specifically, by the ability of osteoblasts to survive and proliferate [19]. In this study, we demonstrated the ability of 3D printed PEEK surfaces to promote cellular processes necessary for bone-implant fixation. While all three porous structures showed promising results, more investigation into the material characteristics and osteogenic potential of each are necessary to determine which geometry may be most suitable for orthopaedic bone ingrowth surfaces.

Acknowledgement: This study was supported by NIH-R01 AR069119. We would like to thank Invibio for donating the filament and Apium for their helpful advice and fruitful discussions.

References:

1. Cowie, R.M., et al., *PEEK-OPTIMA() as an alternative to cobalt chrome in the femoral component of total knee replacement: A preliminary study.* Proc Inst Mech Eng H, 2016. **230**(11): p. 1008-1015.
2. Panayotov, I.V., et al., *Polyetheretherketone (PEEK) for medical applications.* J Mater Sci Mater Med, 2016. **27**(7): p. 118.
3. Honigmann, P., et al., *Patient-Specific Surgical Implants Made of 3D Printed PEEK: Material, Technology, and Scope of Surgical Application.* Biomed Res Int, 2018. **2018**: p. 4520636.
4. Kurtz, S.M. and J.N. Devine, *PEEK biomaterials in trauma, orthopedic, and spinal implants.* Biomaterials, 2007. **28**(32): p. 4845-69.
5. Karageorgiou, V. and D. Kaplan, *Porosity of 3D biomaterial scaffolds and osteogenesis.* Biomaterials, 2005. **26**(27): p. 5474-91.
6. Frohbergh, M.E., et al., *Electrospun hydroxyapatite-containing chitosan nanofibers crosslinked with genipin for bone tissue engineering.* Biomaterials, 2012. **33**(36): p. 9167-78.

Anterior Lumbar Interbody Fusion; A prospective, unmasked, non-randomized study of 240 patients utilizing a PEEK® Optima ALIF cage.

Matthew Scott-Young (MSSB, FRACS, FAOrthA.)[1] Laurence McEntee (MBChB, BHB, FRACS)[1] Mario Zotti (MBBS, FRACS, FAOrthA)[1] Emma Young (BSN, RN)[2]
[1]Gold Coast Spine, Australia[2] Prism Surgical Designs Pty Ltd, Australia

Introduction: Chronic low back pain can occur as a consequence of degenerative disc disease (DDD) and is a leading cause of work absenteeism, disability, and quality of life reduction, as well as having a significant impact on societal and health care expenditure. In patients with varying spinal disorders, the principle objective of treatment is often fusion accompanied by clinical improvements. Since the 1990s, polyethererketones (PEEKs) have been increasingly employed as the biomaterial of choice for spinal fusion interbody implants. The attractive qualities of PEEK are not limited to its inherently proven mechanical, radiological and functional properties. Unlike its Titanium counterpart, PEEK has a modulus of elasticity close to that of human bone, creating a mechanically stable and load sharing environment. Labelled as bio-inert and often negatively referred to as hydrophobic, PEEK has recently experienced engineering review by many companies and academic institutions, offering modifications to physical and mechanical properties, in an attempt to optimise the bone-implant interface. Surface technology for interbody fusion implants is an area of exponential growth within the spinal implant market where authentic innovation and invention has slowed down substantially. With many focusing on micro-, macro- and nanoscale textures, some on additive titanium or HA sprays, and others on 3D-printed and porous metal surfaces, these material advances are often not without valid concerns regarding the physical, radiological and mechanical compromise.

Methods and Materials:
Based on the 4 point principle or 'Diamond Concept' as defined by Giannoudis et al, a standard tissue engineering principle is adopted that embraces bone restoration and regeneration through the use of growth factors, scaffolds, mesenchymal stem cells and mechanical stability. All 4 points are equally acknowledged and each is essential for physiological bony healing. 240 patients were enrolled in a prospective, unmasked, non-randomised study. All participants suffered anterior lumbar spinal pathology at one or more levels and were unresponsive to non-operative or conservative care for a minimum period of 6 months. A diagnosis, with or without radicular pain, was established through clinical history, clinical examination, diagnostic imaging and patient reported baseline measurements. All participants underwent an ALIF at 1 or more levels between L2-S1. A meticulous surgical discectomy technique was employed. A mechanically reliable and rigid construct was crafted utilizing a unique design PEEK® Optima ALIF cage (Australis® Spinal System, Prism Surgical Designs P/L) supplemented with a 4 hole Titanium ALIF plate. Grafting material was comprised of a synergistic combination of osteoinductive and osteoconductive material; recombinant human bone morphogenic protein–2 (rhBMP-2) wrapped through and around pre-fashioned structural allograft (femoral head).

Visual Analog Pain Scale for the back and leg (right and left) were recorded along with the Oswestry Disability Index (ODI) and Roland Morris Disability Questionnaire (RMDQ) at 3 month, 6 month and 12 month intervals. Likewise, radiographic analysis of fusion was conducted by the operating surgeons at 3, 6 and 12 month intervals. Fusion acceptance criteria was defined as a confluence of bridging bone by fine cut CT imaging with 0° movement on flexion/extension films.

Results: A total of 240 patients were treated with anterior lumbar spinal fusion surgery utilising the Australis® Spinal System (PEEK-Optima®) between November 2013 and March 2017, in one independent centre with a follow up period of 12 months. Both statistically and clinically significant ($p<0.001$) reductions were seen in all patient reported outcome measures (PROMs) with median score improvements of 65.38% ODI, 86.04% RMDQ and 82.5% VAS Back respectively. Substantial clinical benefit in self- reported pain and function scores were also maintained at 12 months. Successful radiographic solid fusion was achieved in 96.67% (n = 240) of patients. No complications, re-operations of the primary site or revision surgeries were reported.

Discussion: Fusion is a complex physiological process. The results of this study indicate that solid fusion with substantial clinical improvements in both back and leg pain and function can be achieved utlising a PEEK-Optima® ALIF cage and ALIF plate for the anterior lumbar spinal fusion technique in equal combination with osteogenic cells supported by an osteoconductive scaffold. The clinical and radiographic outcomes of this study compare favourably against previous studies by reporting successful radiographic fusion at 12 months with statistically significant improvements in back/leg pain, disability, and quality of life[13]. Likewise, this study suggests that through the implementation of the Diamond Principle and meticulous surgical technique, PEEK possesses the required functional and mechanical qualities required. The pursuit of enhanced or modified PEEK may potentially be an overreach and may not result in improved clinical outcomes comparatively.

Effects of Toggling Loading on Pullout Strength of Modified Unilateral Spinal Constructs with PEEK and Titanium Rods

Uslan Y[1], Erbay Elibol FK[2], Dalgıç A[3], Işıtan E[3], Demir T[3]
[1] Department of Mechanical Engineering, TOBB University of Economics and Technology, Ankara, Turkey
[2] Department of Micro and Nanotechnology, TOBB University of Economics and Technology, Ankara, Turkey
[3] Department of Neurosurgery, Ankara Numune Health Training and Research Hospital, Ankara, Turkey
tdemir@etu.edu.tr

Introduction: Pedicle screw fixation is one of the most common methods to stabilize the spine by providing high stability [1,2,3]. Nonetheless, after the surgery, several complications such as vertebral fractures, screw loosening or cut-out may required revision surgeries [4-7]. Fixation strength is affected by various factors including bone density, pedicle anatomy, screw design, coating of the screw, insertion technique and cement augmentation [7-11]. Pedicle screws may come out in early stages of stabilization especially in osteoporotic and osteopenic bone densities.

Fixation strength of pedicle screws is determined by standardized (ASTM F543) pullout test [12]. Despite the fact that pullout is the most common test method to assess fixation strength, several studies and clinical results suggest that the main loading condition of the vertebrae is toggling and it is more likely to cause screw loosening than the pull out force [3,13-17]. In literature, toggling test were conducted by applying dynamic sinusoidal load through the longitudinal axis of the rod attached to the head of the screw [18-23]. However, aforementioned test setup cannot clearly represent physiological loading conditions in vertebrae. Hence, the purpose of this study was to develop an alternative test setup with realistic loading configuration and to determine effects of toggling loading on pull out strength of the pedicle screws.

Methods and Materials: 50 mm × 50 mm × 25 mm closed cell polyurethane (PU) blocks produced according to ASTM F1839 was used as bone model. Grade 5 (0.072-0.088 g/cm^3), Grade 10 (0.144 – 0.176 g/cm^3) and Grade 20 (0.289 – 0.353 g/cm^3) PU blocks represent osteoporotic, osteopenic and trabecular bone densities respectively [24-26]. The test blocks eliminates the disadvantages of the variability related to the human bone density [27].

Modified vertebrectomy models was designed based on ASTM F1717 [28]. PU test blocks were used as vertebral body model as opposed to ASTM F1717 defining polyethylene (PE) as vertebral body. Unilateral vertebrectomy model was constructed with pedicle screws (Ø4.5 × 35 mm; Osimplant, Turkey) and rods (Ø5.5 × 135 mm for polyether ether ketone (PEEK) rods, Ø5.5 × 130 mm for titanium (Ti) alloy rods; Osimplant, Turkey). Screws were inserted into 35 mm depth of the test blocks through Ø3 mm pilot hole located on the center of vertebral body model. The vertebrectomy models classified into six groups with different rod material and bone density (Grade 5 (G5), Grade 10 (G10) and Grade 20 (G20) with Ti rod and G5, G10 and G20 with PEEK rod). Each group comprises 9 samples. Besides, there were control groups of G5, G10 and G20 bone densities. The control group was not dynamically loaded before the axial pullout test. Dynamic test were conducted with a position control sinusoidal compressive loading with 3 mm peak-to-peak amplitude and 5 Hz frequency by using 2015EMY015 fatigue test machine (Labiotech, Ankara, Turkey) as shown in Figure 1. The amplitude value was selected to use maximum loading condition not causing to yield. To determine the effect of the dynamic toggling loading on pull out strength, 50.000, 100.000 and 1.000.000 cyclic loading was applied to each group. The run out cycles were determined considering an average daily spinal load is 7000 cycles. Therefore, effect of toggling was investigated for early post-op period (1 week (50k) and 2 week (100k)) and three to six months after the surgery (1m) since screw loosening occurs mostly in this period [29].

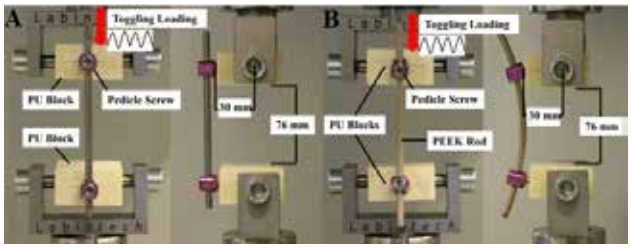

Figure 1: Dynamic test setup, modified vertebrectomy model with (A) Ti rod and (B) PEEK rod

Static axial pullout test was conducted by Instron testing machine (Instron 5944, 2kN, Norwood, MA, USA) for each sample after the dynamic toggling loading (Fig.2). Test blocks were placed to the apparatus and tensile load was applied to the samples with the constant rate of 5 mm/min via the handle according to ASTM F543 [12]. Load and displacement data was recorded and the ultimate load was defined as pullout force.

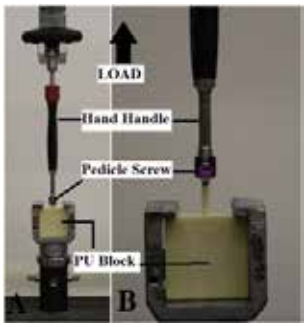

Figure 2: (A) Axial pullout test setup, (B) Tested Sample

Kruskal Wallis test was applied to compare pullout strengths of each group after toggling loading. P value less than 0.05 was considered statistically significant.

Results: The mean pull-out performance was 96.89 ± 34.91 N in Ti G5 group, 101.50 ± 27.91 N in Peek G5 group after 50 k cycle and 142.39 ± 5.96 N in control group. The mean pull-out performance was 560.03 ± 15.19 N in Ti G10 group, 541.81 ± 39.69 N in Peek G10 group after 50 k cycle and 572.15 ± 23.00 N in control group. The mean pull-out performance was 1728.02 ± 95.82 N in Ti G20 group, 1758.60 ± 92.00 N in Peek G20 group after 50 k cycle and 1802.74 ± 27.83 N in control group (Table 1). There was no significantly difference between Ti G5 and Peek G5, Ti G10 and Peek G10, Ti G20 and Peek G20 group for 50k cycle as (p=0.564, p=0.513, p=0.386, respectively (Table 2)).

Table 1: The mean and standard deviation values of axial pullout strength of the groups

Cycle		Ti G5 (N)	PEEK G5 (N)	Ti G10 (N)	PEEK G10 (N)	Ti G20 (N)	PEEK G20 (N)
Control	Mean	142.39		572.15		1802.74	
	STD	5.96		23.00		27.83	
50k	Mean	96.89	101.50	560.03	541.81	1728.02	1758.60
	STD	34.91	27.91	15.19	39.69	95.82	92.00
100k	Mean	95.60	100.32	542.21	525.99	1706.93	1703.34
	STD	20.32	9.05	33.36	39.16	46.56	0.01
1m	Mean	91.41	92.02	537.28	524.98	1586.94	1689.69
	STD	8.55	13.59	24.18	23.35	160.16	17.65

The mean pull-out performance was 95.60 ± 20.32 N in Ti G5 group, 100.32 ± 9.05 N in Peek G5 group, 542.21 ± 33.36 N in Ti G10 group, 525.99 ± 39.16 N in Peek G10 group after 100 k cycle. The mean pull-out performance was 1706.93± 46.56 N in Ti G20 group, 1703.34 ± 0.01 N in Peek G20 group after 100 k cycle. The differences between Ti G5 and Peek G5, Ti G10 and Peek G10, Ti G20 and Peek G20 for 100k cycle were not statistically significant (p=0.248, p=0.827, p=1, respectively (Table 2)).

Table 2: Comparison of the mean pullout strengths between groups for rod material

PEEK vs. Ti	P value	PEEK vs. Ti	P value	PEEK vs. Ti	P value
50k G5	0.564	100k G5	0.248	1m G5	0.773
50k G10	0.513	100k G10	0.827	1m G10	0.564
50k G20	0.386	100k G20	1	1m G20	0.480

The mean pull-out performance was 91.41 ± 8.55 N in Ti G5 group, 92.02 ± 13.59 N in Peek G5 group, 537.28 ± 24.18 N in Ti G10 group, 524.98 ± 23.35 N in Peek G10 group, 1586.94 ± 160.16 N in Ti G20 group and 1689.99± 17.65 N in Peek G20 group after 1m cycle. There was no significantly difference between Ti G5 and Peek G5, Ti G10 and Peek G10, Ti G20 and Peek G20 group (p=0.773, p=0.564, p=0.480, respectively (Table 2)).

There was also no statistically significant difference between 50k, 100k and 1m number of cycles for Ti G5, Peek G5, Ti G10, Peek G10, Ti G20 and Peek G20 (p=0.068, p=0.092, p=0.385, p=0.291, p=0.079, p=0.125 respectively (Table 3)).

Table 3: Comparison of the mean pullout strengths between groups for cycle of number

50k vs. 100k vs. 1m	Ti G5	PEEK G5	Ti G10	PEEK G10	Ti G20	PEEK G20
P value	0.068	0.092	0.385	0.291	0.079	0.125

Discussion: The material properties of human bone vary with age and gender. Compared to the tests conducted on human cadaver bones, it is found that PU test blocks provide rather more uniform and consistent density to overcome variability [8, 16]. Therefore, G5, G10 and G20 PU blocks were used for testing as a substitute for human osteoporotic, osteopenic, healthy vertebrae structure.

Despite there are several studies to determine the toggling effect, effect of number of cycle was not investigated. In this study, the effect of cycle number on the toggling was investigated with more realistic loading condition than the previous studies by taking flexion-extension movement into consideration, however it is found that there was not any statistically significant difference between the groups.

In the current study, Ti and PEEK rods were used in vertebrectomy models. Even though, titanium alloys are most common biomaterial for spinal fusion, recent studies centered on semi rigid fixation system with peek rods [30,31]. Our results show that there were no significant differences between Ti rod fixation and Peek rod fixation groups on pull out strength with toggling effect. So, Ti rod and Peek rod are provide same pull out strength after cyclic loading in osteoporotic, osteopenic and healthy bone structure.

Using only the trabecular bone model rather than two-layered bone structure is one of the constraints of this study. For further studies, models consisting of cortical cortex and trabecular core can be used to represent more realistic vertebrae models. The other constraint is number of cycle. The number of cycles can be increased in order to observe the effects of toggling on the longer process for future studies.

toughness and impact strength, which are important for their application as load bearing implants.

Effect of Porous Orthopaedic Implant Material and Structure on Load Sharing with Simulated Bone Ingrowth: A Finite Element Analysis Comparing Titanium and PEEK

Carpenter, RD[1], Klosterhoff, BS[2], Torstrick, FB[2], Foley, KT[3], Burkus, JK[4], Guldberg, RE[5], Gall, KA[6], Safranski, DL[7], [1]University of Colorado, Denver, CO, [2]Georgia Institute of Technology, Atlanta, GA, [3]University of Tennessee, Memphis, TN, [4]Hughston Clinic, Columbus, GA, [5]University of Oregon, Eugene, OR, [6]Duke University, Durham, NC, [7]MedShape, Inc., Atlanta, GA

David.safranski@medshape.com

Introduction: Osseointegration of load-bearing orthopaedic implants, including interbody fusion devices, is critical to long-term biomechanical functionality. Mechanical loads are a key regulator of bone tissue remodeling and maintenance, and stress-shielding due to metal orthopaedic implants being much stiffer than bone has been implicated in clinical observations of long-term bone loss in tissue adjacent to implants. Porous features that accommodate bone ingrowth have improved implant fixation in the short term, but long-term retrieval studies have sometimes demonstrated limited, superficial ingrowth into the pore layer of metal implants and aseptic loosening remains a problem for a subset of patients. Polyether-ether-ketone (PEEK) is a widely used orthopaedic material with an elastic modulus more similar to bone than metals, and a manufacturing process to form porous PEEK was recently developed to allow bone ingrowth while preserving strength for load-bearing applications. To investigate the biomechanical implications of porous PEEK compared to porous metals, finite element (FE) models were analyzed of the pore structure-bone interface using two clinically available implants with high (>60%) porosity, one being constructed from PEEK and the other from electron beam 3D-printed titanium (Ti). The objective of this study was to investigate how porous PEEK and porous titanium mechanical properties affect load sharing with adjacent bone and the mechanical stimulus transmitted to bone within clinically available porous architectures over time under relevant spinal load magnitudes.

Methods and Materials: One representative sample of porous PEEK (COHERE®, Vertera Inc., Atlanta, GA) and porous titanium (Ti; Tesera Trabecular Technology™, Renovis®, Redlands, CA) was scanned at a resolution of 17.2 and 24.3 μm, respectively using microCT (microCT 50, Scanco Medical, Brüttisellen, Switzerland). To characterize the pore morphometrics of each device, the full thickness of the porous structures were manually contoured and a threshold was applied to segment porous PEEK and porous Ti from their respective scan in a similar fashion to previous pore layer characterization. Both materials had high porosity (>60%) and interconnectivity (>99.9%). Strut spacing, an estimation of pore size, was twice as large for porous Ti compared to porous PEEK (Ti = 607 ± 277 μm vs. PEEK = 263 ± 73 μm, $p<0.05$), as was strut thickness (Ti = 277 ± 92 μm vs. PEEK = 99 ± 42 μm, $p<0.05$). The pore structure for porous Ti was approximately 50% deeper than porous PEEK (Ti =1263 ± 93 μm vs. PEEK = 829 ± 100 μm, $p<0.05$). After evaluation, thresholded images of a rectangular portion of each device including the underlying bulk solid were smoothed with a Gaussian filter (sigma=0.8, support=1) and exported as DICOM image stacks for mesh generation. The DICOM images were converted to finite element meshes using Simpleware ScanIP+FE software. Models were cropped to span approximately 8 pores along an edge, and a rectangular slab of simulated mature bone tissue was abutted to the porous surface. Four layers of tissue for simulating bony ingrowth were then created by dilating the external surface of the porous material by two voxels per layer in all directions (Figure 1). This resulted in a layer thickness of 52 μm for the PEEK geometry and a layer thickness of 141 μm for the titanium geometry. Each layer was assumed to represent 4 weeks of bony ingrowth, providing an equal number of time steps for both models. Bone, PEEK, and Ti were modelled as linear elastic, homogeneous, isotropic solids. Constant mechanical properties were assigned to PEEK (E=3 GPa, ν=0.33) and Ti (E=109 GPa, ν=0.33) at all modelling time points. At the first modelling time point, simulating the configuration immediately after implantation, the implant material and rectangular bone surface were included. Bone tissue formation within the porous structure was simulated by adding a new layer of bone at each 4-week time step, until the entire pore space was filled. From the second time point on, each layer of new bone tissue was sequentially assigned bone mechanical properties in discrete steps. To simulate mineralization and maturation within each layer of bone over time, microCT mineral density data of tissue ingrowth from a previous *in vivo* study evaluating porous PEEK in a rat femoral segmental defect was used. Once the mesh geometry and mechanical properties were established, the portion of load carried by either the bone or the implant was evaluated under compressive, tensile, or shear load. For all three load cases, a displacement equivalent boundary condition of 0.5% global strain was applied to the top surface of PEEK or Ti. Linear transformations were performed to determine strain values subjected to 5 MPa of applied stress for compressive, tensile, and shear cases.

Results: Porous PEEK substantially increased the load share transferred to ingrown bone compared to porous Ti under compression (i.e. at 4 weeks: PEEK = 66%; Ti = 13%), tension (PEEK = 71%; Ti = 12%), and shear (PEEK = 68%; Ti = 9%) at all time points of simulated bone ingrowth. The equilibrium load carried by mineralized bone at full ingrowth was 82.3% for porous PEEK and 42.2% for porous Ti (Figure 2). Applying PEEK mechanical properties to the Ti implant geometry and vice versa demonstrated that the observed increases in load sharing with PEEK were primarily due to differences in

intrinsic elastic modulus and not pore architecture (i.e. 4 weeks, compression: PEEK material/Ti geometry = 53%; Ti material/PEEK geometry = 12%). Local tissue energy effective strains on bone tissue adjacent to the implant under spinal load magnitudes were over two-fold higher with porous PEEK than porous Ti (i.e. 4 weeks, compression: PEEK = 784 ± 351 microstrain; Ti = 180 ± 300 microstrain, $p<0.05$; and 12 weeks, compression: PEEK = 298 ± 88 microstrain; Ti = 121 ± 49 microstrain, $p<0.05$) (Figure 3).

Discussion: In this study, high-resolution FE models of the porous implant-bone interface revealed that porous PEEK substantially increased load sharing with bone inside the pore structure compared to porous Ti in compression, tension, and shear. Importantly, the influence was demonstrated to be mediated primarily by differences in intrinsic elastic moduli between PEEK and Ti, as PEEK was observed to increase load sharing by at least 38% irrespective of the pore structure architecture or the level of bone ingrowth. The importance of load-sharing is a fundamental aspect of bone physiology and is clearly established in the bone remodeling literature, where removal of sufficient mechanical stimulation results in rapid bone loss, a phenomenon designated as "disuse-mode remodeling". To assess the local mechanical stimulus transmitted to the bone within the porous structures in this study, we computed the energy effective strain, a scalar description of the overall strain state, within the adjacent layer of bone tissue when a 5 MPa stress was placed on the implant. This stress corresponds to five-fold higher than the peak von Mises stress at the vertebral end plate-cage interface prior to bone ingrowth in a posteriorly instrumented lumbar spine of an adult standing up from a chair, as predicted by an experimentally validated FE model. In the context of bone adaptation, the strains produced in bone tissue within porous Ti corresponded with disuse-mode remodeling, whereas porous PEEK produced a more favorable mechanical environment for bone formation and maintenance. Importantly, the strains produced by the porous PEEK remained below thresholds where fracture, fatigue failure, or inhibition of new bone formation can occur (5000-10,000 microstrain). To summarize, porous PEEK was found to increase load sharing with adjacent bone compared to porous Ti, whereas porous Ti produced tissue strains that have been implicated in increasing the risk of bone resorption, regardless of the two pore architectures or levels of bone ingrowth investigated. The results of this study suggest that the lower intrinsic elastic modulus in porous PEEK structures may provide a more favorable mechanical environment for bone formation and maintenance under spinal load magnitudes than currently available porous 3D-printed Ti.

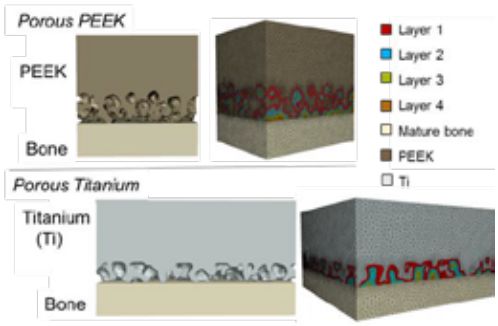

Figure 1. Finite element models of porous PEEK and titanium were generated from microCT imaging.

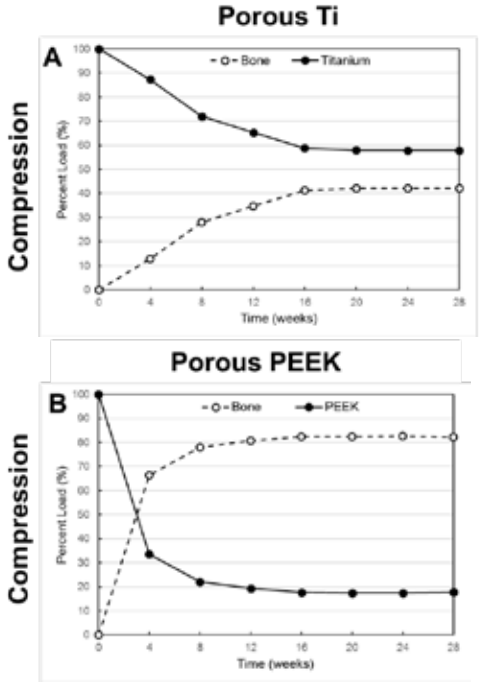

Figure 2. Time evolution of load sharing of (A) porous Ti and (B) porous PEEK under compressive loading.

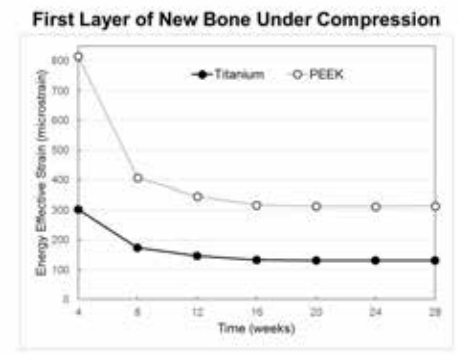

Figure 3. Mean energy effective strain in Layer 1 of bone ingrowth versus time under compressive loading for Ti and PEEK implants.

Impaction Durability of Porous PEEK and Titanium-coated PEEK Interbody Fusion Devices

Torstrick, FB[1], Klosterhoff, BS[1], Westerlund, LE[2], Foley, KT[3], Gochuico J[1], Gall, KA[4], Safranski, DL[5],
[1]Georgia Institute of Technology, Atlanta, GA, [2]St. Francis Spine Center, Columbus, GA, [3]University of Tennessee, Memphis, TN, [4]Duke University, Durham, NC, [5]MedShape, Inc., Atlanta, GA
David.safranski@medshape.com

Introduction: Interbody fusion devices are routinely used in spinal fusion procedures and are subjected to a variety of mechanical loading scenarios throughout their clinical lifetime. Interestingly, some of the highest loads experienced by a device can occur during its impaction and positioning within the disc space intraoperatively. More recent technologies have featured roughened or porous surfaces that allow for bone ongrowth and ingrowth to improve fixation through mechanical interlocking of bone with device. Despite the favorable osseointegration of these new technologies, the raised micro-scale features they display may be vulnerable to abrasion or delamination under impaction shear loads. While material delamination post-impaction is a concern primarily limited to coated devices (particularly titanium-coated device designs), the potential to compromise ingrowth surfaces during device impaction is relevant to all ongrowth or ingrowth surface designs and is a focus here. This is of substantive clinical relevance, as any compromise to the ingrowth surface has the potential to equally impede the intent of achieving a rapid and robust osseous union at the interbody reconstruction site. The goal of the current study was to investigate the impaction durability of a recently introduced porous PEEK cervical fusion device in comparison with titanium-coated PEEK (positive damage control) and conventional smooth PEEK devices (negative damage control).

Methods and Materials: Three groups of six cervical interbody fusion devices were used for this study: a conventional smooth PEEK device with ridges (Spinal Elements®, Crystal®, 11x14x12mm, 7°), a plasma-sprayed titanium-coated PEEK device with ridges (X-spine®, Calix PC®, 11x14x12mm, 7°), and a porous PEEK device without ridges (Vertera Spine®, Cohere®, 12x14x10mm, 0°). Following the method of Kienle et al., devices were impacted between two polyurethane blocks (40 PCF, Sawbones®) [1]. The blocks were cut to 50x45x40mm with a flat face and were mounted in a custom fixture with an attached pneumatic cylinder to apply a constant axial force of 200 N (Figure 1). This force was chosen to fall within the range of physiological compressive preloads for cervical and thoracic devices [2,3]. The posterior tip of the device was placed at the entrance of the polyurethane blocks and a guided one pound weight was dropped on the anterior face of the device with a maximum speed of 2.6 m/s to represent the strike force of a surgical mallet. Impacts were repeated until the device was fully impacted between the polyurethane blocks and the number of strikes to insert each device was recorded. The mass of each device before and after impaction was determined using a fine balance to calculate change in mass. The porous architecture (porosity, pore size, pore structure depth) of the leading edge of porous PEEK devices before and after impaction was characterized by micro-computed tomography (Scanco Medical, µCT50, 10 µm voxel size, 55 kVp, 200 µA) (n = 6). A Hitachi S-3700N VP SEM was used to image both surfaces of the smooth PEEK and titanium-coated devices before and after impaction (n = 8 images/side). Image analysis to threshold the titanium-coated area was performed using ImageJ. EDX was utilized to confirm SEM titanium-coating coverage based on elemental composition where a loss of titanium signal from the coating and a gain in carbon signal from the underlying PEEK indicated damaged areas.

Results: Upon macroscopic examination, there were minimal visual signs of damage to the porous PEEK or the smooth PEEK devices, yet titanium-coated devices showed substantial macroscopic damage, particularly on the lateral regions of the proximal and distal sides of the device. All six porous PEEK devices took one strike to fully impact between the polyurethane blocks. The smooth PEEK and titanium-coated PEEK devices took 2.2 ± 0.4 and 9.3 ± 0.5 strikes to fully impact, respectively. The porous PEEK, smooth PEEK, and titanium-coated PEEK devices exhibited mass changes of -0.6 ± 3.0, +0.1 ± 0.1, and -4.6 ± 1.0 mg of material, respectively. Titanium-coated device mass loss was significantly greater than porous PEEK and smooth PEEK devices ($p < 0.05$). µCT reconstructions of porous PEEK devices before and after impaction demonstrated that the overall pore structure was well preserved after impaction, although a slight densification could be observed upon close examination (Figure 2). Quantitative µCT analysis before and after impaction showed that the leading edge of the porous PEEK devices experienced a 1.0 ± 0.8% decrease in porosity, a 54.3 ± 24.5 µm decrease in pore depth, and a 12.4 ± 5.4 µm decrease in pore size ($p < 0.05$). Following impaction, titanium-coated PEEK devices exhibited macroscopic damage and demonstrated a 27.8 ± 3.6% decrease in titanium-coating coverage area as determined by SEM analysis ($p<0.05$) (Figure 3). SEM combined with EDX maps verified the damage seen on SEM by showing a loss of titanium signal and a gain in the carbon signal from the underlying PEEK in damaged areas (Figure 3). As expected, SEM images showed a lack of damage and only minor scratching near the ridges of the smooth PEEK devices.

Discussion: The current study adapted the impaction test setup by Kienle et. al. to evaluate the durability of porous PEEK in addition to titanium-coated PEEK and smooth PEEK devices during simulated cervical impaction. The

damage exhibited by titanium-coated devices in this study was comparable to those reported by Kienle et al. and provide further evidence that titanium-coatings may be at risk of wear and delamination under certain cervical and lumbar loading scenarios. There is a growing concern among surgeons regarding the delamination of titanium-coated interbody devices. These events are macroscopically visible, most typically noted at the edges of the device surfaces where impaction loads are highest. Unfortunately, these are the same surface regions that are in greatest contact with vertebral endplates and potentially most important in fostering favorable ingrowth from a clinical standpoint. In contrast to the titanium-coated cages, the porous PEEK devices only exhibited a 2 – 7% change to the porous structure following impaction depending on the pore metric evaluated. Importantly, the porous structure maintained a high porosity (>65%) following impaction that would be available for bone ingrowth. Consideration of the μCT structural metrics in conjunction with the minimal mass loss results of porous PEEK devices suggests that the porous PEEK structure is simply deforming, but not introducing loose particles into the surrounding tissue. These results suggest that porous PEEK may have an impaction durability that is more similar to conventional smooth PEEK devices than titanium-coated PEEK devices. The current study found porous PEEK devices to show minimal damage during aggressive cervical impaction, whereas titanium-coated PEEK devices lost a substantial degree of their initial titanium coverage.

References: [1] Kienle, et.al. The Spine Journal 2016. [2] ASTM F2077 2014. [3] Miura, et.al. Spine 2002.

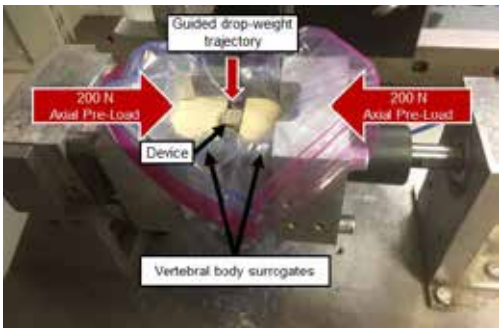

Figure 1. Impaction test setup for cervical interbody fusion devices.

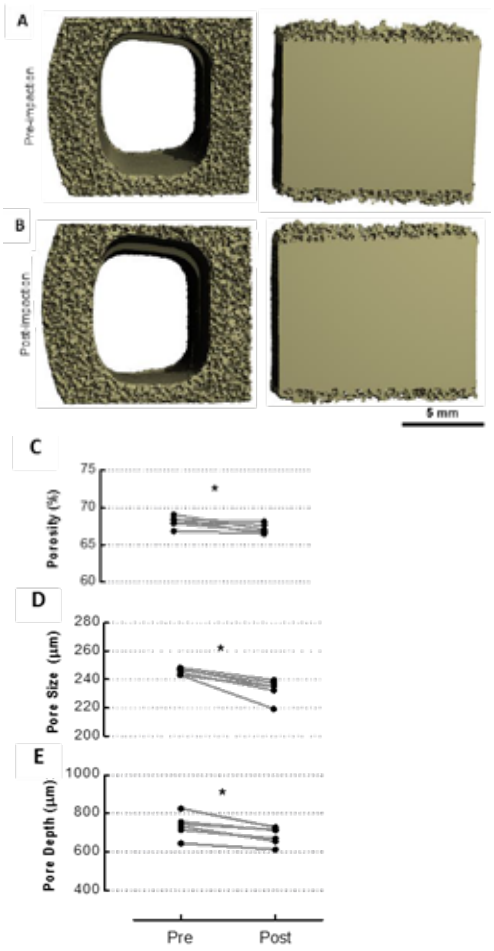

Figure 2. MicroCT reconstructions before and after impaction with porosity, pore size, and pore depth analysis.

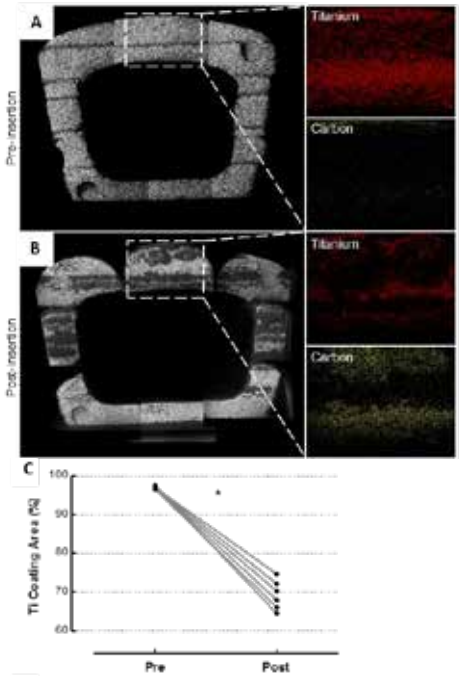

Figure 3. SEM and EDX analysis of Ti-coated PEEK before and after impaction.

ORTHODONTIC THERMOACTIVE ARCHWIRE - PEEK

Rodrigues, Alan[1]
Alaninvisible1@gmail.com

Introduction: Polyetheretherketone – PEEK is a semi-crystal thermoplastic with excellent resistance and mechanically has extreme properties of flexibility which enables all sort of shock absorption from the masticatory system.
Recent advances made by NASA (National Aeronautics and Space Administration) in the processing of this material has allowed the recovery of its memory shape behavior by mechanical reactivation.
The evolution of this technology and its perfect biocompatibility has rapidly spread throughout the medical field, and its use at present in orthopedics surgeries, in the dental area, is already using for implant-borne fixed and removable prosthetic which enable high precision, better implant survival rate, less bone loss, less peri-implantitis, with more comfort for the patient.
Dr. Alan Rodrigues[1] and his team developed for the first time a new orthodontic wire made from this entirely aesthetic PEEK material – Bio-PEEK - with thermoactivated properties in sizes of 0,017 x 0,025 and 0,019 x 0,025. That represent all the ideal characteristics to initiate complex tooth and dentoalveolar structure movement, by releasing very light and biological forces with complete control of both torque and rotation movements and able to recover the transverse dimension of the dental arches, preventing collateral damage of the teeth and supporting structures.
They are very flexible and release very light forces, significantly lower than even a 0,014 NiTi thermoactivated wire, the usual wires that are placed to start orthodontic treatment even in severe cases of clinical crowding. These characteristics allowed the professional to start the mechanics of dentoalveolar movement from any malocclusion case with 0.017x0.025 wire size offer since the beginning of the treatment full tri-dimension dentoalveolar movement control.
Another important feature of this wire is its natural aesthetic characteristic because it's metal free. Metals can sometimes be the cause of gingival inflammation due to an allergic reaction in some individuals.

Methods and Materials: Patients with SLIMCLEAR braces and Peek wires with every kind of malocclusion problems. Patients do a TC scan at the beginning and the end of treatment. The monthly clinical appointment is made to see treatment progression and photograph for later comparison and evaluation.

Results:
Clinical and CBCT Evidence
The 0,017 x 0,025 PEEK aesthetic thermoactivated polymer wire releases almost three times less force than the 0,014 NiTi thermoactivated wire providing an ideal amount of force, resulting in a quick and biologically safer way for dentoalveolar tooth movement, that we can see in treatment pictures.

Upper arches: Dentoalveolar movement sequence with only one 0.017 X 0.025 Bio-PEEK archwire in 6 Months of treatment.

Lower arches: Dentoalveolar movement sequence with only one 0.017 X 0.025 Bio-PEEK archwire in 6 Months of treatment.

CT images after treatment: The dentoalveolar movements are quickly and biologic safe and do not cause any root absorption or any kind damage for alveolar bone.

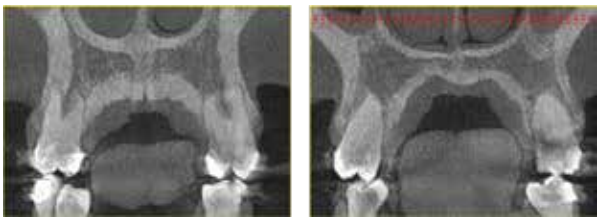

The TMJs are healthy and stabilized.

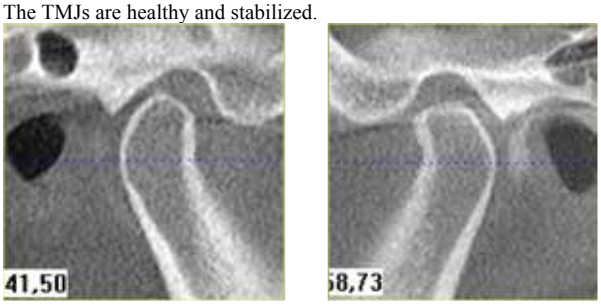

Sequence of Dentoalveolar movement with only one 0.017 X 0.025 Bio-PEEK archwire in 9 Months of treatment.

CT images after treatment: The dentoalveolar movements are quickly and biologic safe and do not cause any root absorption or any kind damage for alveolar bone.

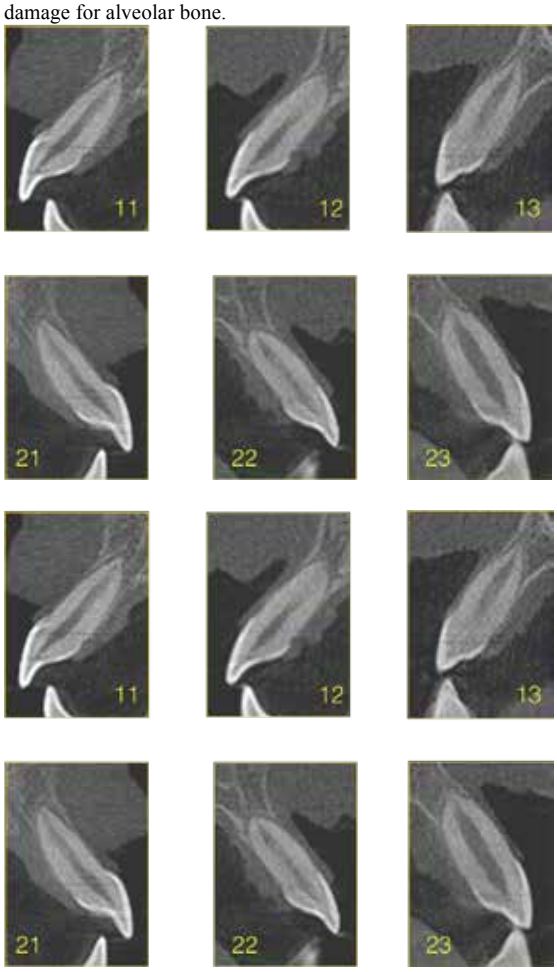

The TMJs are healthy and stabilized.

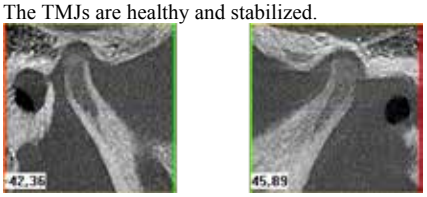

Four Months dentoalveolar movement sequence with only one 0.017 X 0.025 Bio-PEEK archwire

Discussion: PEEK wires are the evolution of all aesthetic wires already made for orthodontic use. This wire is completely biocompatible with thermal reactivation of its memory shape characteristics, even when it suffers significant changes in shape it returns to its natural shape only by a simple finger movement along the PEEK surface during appointments, avoiding the need to change the wire during orthodontic treatment.

Wear Performance of an All-Polymer Total Knee Replacement

Cowie, RM[1], Briscoe A[2], Fisher J[1], Jennings LM[1].
[1]Institute of Medical and Biological Engineering, University of Leeds, Leeds, UK. [2]Invibio Biomaterials Ltd, UK
r.cowie@leeds.ac.uk; abriscoe@invibio.com; l.m.jennings@leeds.ac.uk

Introduction: PEEK-OPTIMA™ (Invibio Biomaterials Ltd, Thornton Cleveleys, UK) has been considered as an alternative arthroplasty bearing material to cobalt chrome in the femoral component of total knee replacements (TKR) [1]. In this study, the wear performance of an all-polymer, PEEK-OPTIMA™-on-UHMWPE knee implant was assessed. Initial studies focused on assessing the wear performance in a simple geometry pin-on-plate configuration to understand the behavior of the UHMWPE-on-PEEK bearing couple and to investigate the most appropriate environmental conditions under which to further investigate this implant. Pin-on-plate wear simulation allowed the influence of individual variables on the wear of UHMWPE-on-PEEK to be considered. Namely, the environmental conditions in terms of the lubricant temperature as well as the influence of cross-shear and contact pressure. These simple geometry studies were carried out before moving into whole joint wear simulation of both the tibiofemoral and patellofemoral joints. For all the studies, the wear of the all-polymer combination was compared to a conventional metal-on-polyethylene couple of similar initial surface topography and geometry.

Methods and Materials:

Pin-on-plate wear simulation, influence of environmental conditions, contact pressure and cross-shear ratio

The pins used were GUR 1020 UHMWPE (conventional, non-sterile) and the plate material either polished cobalt chrome (initial mean surface roughness (Ra) <0.01µm) or PEEK-OPTIMA™, Ra ~0.03µm. Wear simulation was carried out using a 6-station multi-axial pin-on-plate rig. To study the influence of environmental conditions on wear performance, the contact pressure and cross shear conditions used reflected those in a TKR and studies were run at either room temperature as per standard practice at Leeds or at elevated temperature (~36°C) as in the ISO standard [2]. To investigate the influence of contact pressure, contact pressures from 2.1 to 80MPa were used and for the influence of cross-shear ratio, cross-shear ratios ranging from 0 (uniaxial motion) to 0.18, these tests were carried out at room temperature.

Influence of environmental conditions on the wear of the tibiofemoral joint (TFJ)

Six right mid-size, cruciate retaining PEEK-OPTIMA™ knee implants (collaboration partners Maxx Orthopedics Inc., Plymouth Meeting, PA, USA and Invibio Knee Ltd, Thornton-Cleveleys, UK) and six cobalt chrome femoral components (MAXX Orthopedics Inc.) of similar initial surface topography and geometry were tested against GUR1020 all-polyethylene tibial components (conventional, EO sterile) as shown in Figure 1. Experimental wear simulation was carried out using ProSim electropneumatic knee simulators (Simulation Solutions, UK) running Leeds high kinematics conditions (maximum anterior posterior displacement 10mm) [3]. Three of each implant type were tested under room temperature conditions (~27°C) for 5 million cycles; and three implants tested under elevated temperature (~33°C) conditions for 10 million cycles.

Patellofemoral joint (PFJ) wear simulation

Six right mid-size, cruciate retaining PEEK-OPTIMA™ knee implants and six cobalt chrome femoral components were tested against GUR1020 all-polyethylene 28mm diameter patellae components (conventional, EO sterile), Figure 1. Experimental wear simulation was carried out using ProSim electromechanical knee simulators running kinematic conditions to replicate a gait cycle [4]. The tests were carried out at room temperature.

For all the studies, the lubricant used was 25% bovine serum supplemented with 0.03% sodium azide. The wear of the UHMWPE components was assessed by their loss in mass measured by gravimetric analysis with two unloaded soak controls used to compensate for uptake of moisture. A minimum of 3 repeats was carried out for each condition.

Statistical analysis was carried out using ANOVA to compare the all-polymer to the metal-on-polyethylene bearing couple with significance taken at $p<0.05$.

Figure 1: Images of the all-polymer total knee replacement. Left: the PEEK femoral component coupled with an all-polyethylene tibial component, right: the patellofemoral joint

Results and Discussion:

Pin-on plate wear simulation

Influence of lubricant temperature

The wear of the UHMWPE pins is shown in Figure 2. When tested under room temperature conditions, there was no significant difference in the wear of UHMWPE-on-PEEK compared to UHMWPE-on-CoCr ($p>0.05$). Under elevated temperature conditions, the wear of UHWMPE-on-PEEK was lower, thought to be as a result of protein precipitation and deposition on the articulating surfaces [2].

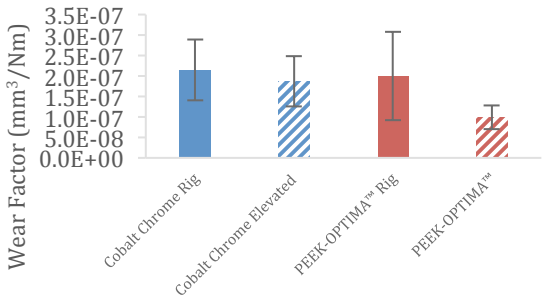

Figure 2: Influence of lubricant temperature on the wear of UHMWPE-on-PEEK and CoCr (n=6). [2]

Influence of contact pressure

With increasing contact pressure (Figure 3), there was a decrease in wear factor of the UHWMPE pins, this trend has previously been reported in UHMWPE-on-CoCr [5].

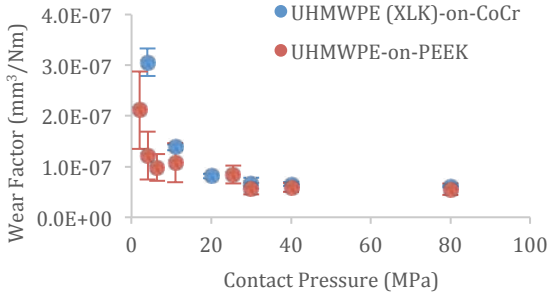

Figure 3: Influence of contact pressure on the wear of UHMWPE-on-PEEK and UHMWPE-on-CoCr [5].

Influence of cross-shear ratio

Under uniaxial motion, the wear of UHMWPE-on-PEEK was very low. Increasing the rotation of the pin increased the wear of UHMWPE. A similar trend has been reported for UHMWPE-on-CoCr [5] (Figure 4).

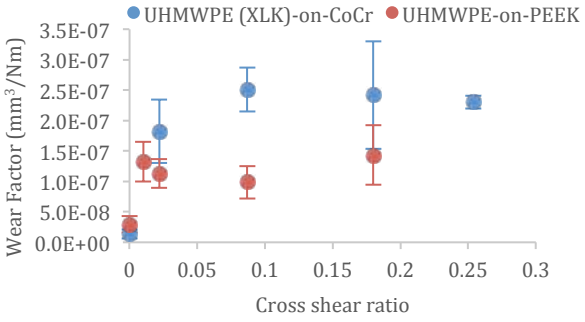

Figure 4: Influence of cross-shear ratio on the wear of UHMWPE-on-PEEK and UHMWPE-on-CoCr [5].

Wear simulation of the tibiofemoral joint

Under all conditions, wear of the UHMWPE tibial components was low (<5mm^3/MC). There was no significant difference (p>0.05) in the wear of the tibial components against PEEK or CoCr when tested at room temperature. Testing at elevated temperature reduced the wear rate for both material types (Figure 5).

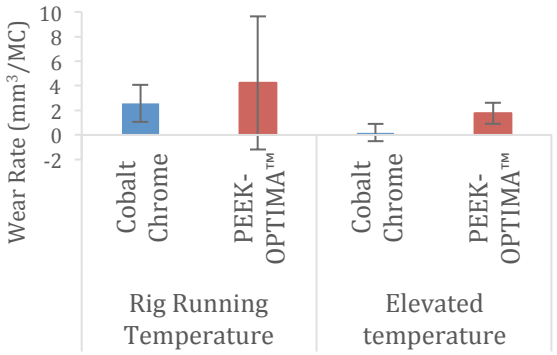

Figure 5: Wear of UHMWPE tibial components against PEEK and CoCr femoral components under rig and elevated temperature conditions, n=3.

Wear simulation of the patellofemoral joint

Wear of UHMWPE patellae was low (<1mm^3/MC) against PEEK and CoCr with no significant difference (p>0.05) in wear against the different materials (Figure 6).

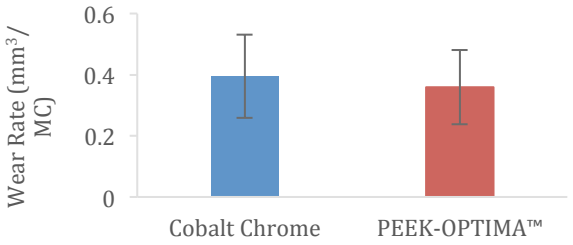

Figure 6: Wear of UHMWPE patellae against PEEK and CoCr femoral components (n=6).

Conclusions:

- Environmental conditions such as temperature influence wear performance
- Similar trends were noted in the wear of UHMWPE-on-PEEK and UHMWPE-on-CoCr with changing cross-shear and contact pressure
- Wear of the TFJ and PFJ was low and an equivalent rate of wear of UHMWPE was assessed against the two materials when tested at room temperature
- Experimental wear simulation of the all-polymer knee resulted in scratches on the articulating surface of the PEEK however, the magnitude of the scratches was not sufficient to influence the wear rate of the UHMWPE

References

[1] Cowie RM, et al. 2016. JEIM 230(11):1008-1015 [2] Cowie RM, et al. 2019. JMBBM 89: 65-71 [3] McEwen, H.M.J. et al. 2005 J Biomechanics, 38(2):357-365. [4] Maiti R., et al,2014.JEIM;228(2):175-181 [5] Abdelgaied A, et al. 2012. JEIM 227(1):18-26

The quantification and characterisation of the wear debris produced from Poly-ether-ether-ketone (PEEK) based bearing couples from a multi-directional motion pin-on-plate test rig

Chamberlain, K[1], Arnholt, C[2], Briscoe, A[3], Rankin, K[1], Deehan, D[1], White, J[4], Kurtz, S[2,4], Hyde, P[1]
[1]Newcastle University, UK [2]Drexel University, USA, [3]Invibio Biomaterial Solutions, UK, [4] Exponent Inc, Philadelphia, USA
Philip.Hyde@ncl.ac.uk

Introduction: Metal-on-polyethylene (MoP) remains the most frequently implanted bearing couple in both total hip and total knee arthroplasty, 59 % and 83 % respectively [1]. However, despite good clinical outcomes, wear from the ultra-high molecular weight polyethylene (UHMWPE) component has historically been a significant factor effecting the longevity of the joint replacements and, prior to the development of highly crosslinked UHMWPE, remains the main clinical burden for revision surgeries. Osteolysis, leading to aseptic loosening and failure of uncrosslinked MoP bearing couples, is directly related to the size, shape and morphology of the polyethylene wear debris produced [2]. Particles typically range from 0.01 – 10 μm, with particles between 0.1 – 1 μm classed as biologically active in terms of cytokine response [3]. Due to an increase in patient expectations and demand, alternative biomaterials have been investigated.

Poly-ether-ether-ketone (PEEK), currently used in spinal applications, is a biomaterial under investigation. More recently the prospect of an all polymer, PEEK-on-polyethylene (PKoPE) knee has been explored, which may benefit patients at risk of metal hypersensitivity [4, 5]. Despite preliminary studies on PEEK indicating favorable wear results and biocompatibility, it is important that both the wear and wear debris produced, especially under adverse conditions, of any new biomaterial under consideration be examined. There is limited data on the characterisation of the wear debris produced from unfilled, natural PEEK.

The aim of this study was to quantify the wear and characterise the wear debris produced from PKoPK and UHMWPEoPK bearing couples tested under different lubricant protein concentrations.

Methods and Materials: Injection moulded PEEK (Invibio Ltd) and uncrosslinked GUR-1020 ultra-high-molecular-weight-polyethylene (Orthoplastics) pins articulated on injection moulded PEEK plates in a four station multi-directional motion pin-on-plate (PoP) test rig. Both rotation and reciprocation were set at 1 Hz with a 20 mm sliding distance, applied contact pressure of 5.6 MPa and run to one million cycles. New born calf serum (BCS) at 1.28 mg/mL, 21 mg/mL and 64 mg/mL protein concentration (2 %, 33 % and 100 % dilution respectively) was used as the lubricant and changed, alongside gravimetric analysis with soak controls (to account for lubricant uptake), every 250, 000 cycles.

Post-test lubricant was stored at -18 °C until required, then thawed at ambient temperature. The aliquots were sonicated and vortexed to create a homogeneous representative sample, across the million cycles. Approximately 20 mL of serum was subject to an acid protein digestion following the method stated in ISO17853:2011, but not conforming to the serum/acid ratios stated therein. Briefly, hydrochloric acid and serum samples were mixed with a stirrer bar and heated at 50 °C for one hour. Samples of the digestion solution were then added to pre-determined amounts of methanol.

The remaining supernatants were sequentially filtered through 1 μm, 0.1 μm and 0.015 μm Cyclopore polycarbonate filter membranes (Whatman International Ltd). Sections of the filter membranes were cut and adhered to an aluminium stub with double sided carbon tape, and pt/pd splutter coated for analysis via a field emission gun scanning electron microscope (FEG-SEM, Zeiss SUPRA 50 vp, Fisher). Five random fields of view from each filter paper were analysed with 10 kV and a range of magnifications. The size and area of the particles were then analysed using ImageJ (National Institute of Health) with the equivalent circle diameter (ECD), form factor (FF), elongation, aspect ratio (AR), and roundness recorded as recommended by ASTM F 4 (1877). A minimum of 1000 particles per filter paper for each bearing combination were analysed. Data was then combined to obtain both frequency and volume distributions.

Statistical analysis was performed using a one-way ANOVA with Tukey post hoc test (Minitab) with significance at $p < 0.05$.

Results: The PKoPK (higher friction) bearing couple had the highest wear factor (Figure 2) across all three protein concentrations with a statistically significant ($p < 0.05$) decrease in wear factor with increasing protein concentration. This is in contrast to the UHMWPEoPK bearing couple where 33 % BCS had the highest wear factor with an insignificant decrease noted for both 2 % and 100 %, a similar trend to that of Cowie *et al* for UHMWPEoPK [4].

Visible wear scars were evident on PEEK plates from PKoPK tests with an increase of > 100 % in the number of wear particles observed compared to the UHMWPEoPK. Spherical, granular, fibril and roughened flake morphologies, as well as some agglomeration of particles was observed (Figure 1). At the time of writing, results exclude the 0.015 μm filtered debris therefore the percentage particle distribution graph (Figure 3) have a cut off at 0.1μm (100 nm).

Discussion: The wear results suggest that proteins present in test lubricants have a significant impact on the wear of PEEK self-mating bearing couples. The increased wear factor of PKoPK could be due to protein adsorption. At 2 % BCS there is not a sufficient amount of proteins present to adhere to the surface to form a protective boundary layer or biotribo-film. The results suggest that when testing PKoPK self-mating bearing couples, as used in spinal applications, a lower BCS concentration should be used to replicate adverse conditions.

The UHMWPEoPK bearing couple had a statistically insignificant ($p > 0.05$) increase in wear at 33 % BCS, similar to that observed in the current MoP bearings. As there was no statistically significant difference between the wear factors with varying protein concentration for the UHMWPEoPK bearing couples the current ISO protein concentration of 20 g/L, as stated in ISO 14243-1:2009, is still suitable for testing (for example) an all polymer knee.

For biomaterials under consideration for either a hip or knee replacement, a low wearing material combination which produces less wear particles between 0.1 – 1 µm is desired, reducing the risk of adverse bioactivity and consequential osteolysis. From the results it can be seen that under 100 % BCS the UHMWPEoPK bearing couple produced the least percentage of particles in this range. Under both 2 % and 33 % BCS there was no statistically significant difference ($p < 0.01$) between the percentage of particles in the 0.1 – 1 µm range for UHMWPEoPK and PKoPK. It should be noted that with the inclusion of the 0.015 µm filter paper these percentages will change.

Clinical Implications: As the protein concentration of peri-prosthetic synovial fluid differs from healthy synovial fluid, ranging between 15 – 55 mg/ml [6], these results show promise for the all polymer implant.

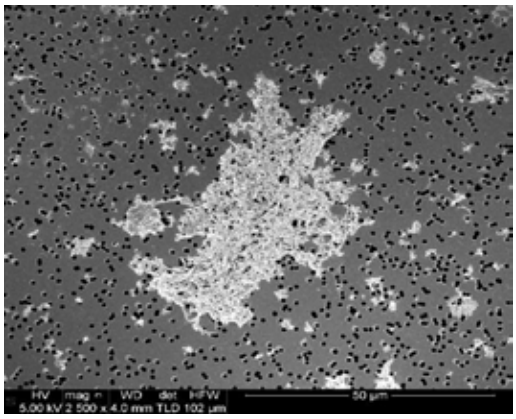

Figure 1: *Agglomeration of UHMWPEoPK particles isolated on a 1 µm filter with a, working distance of 4 mm, 5kV and 2,500 x magnification.*

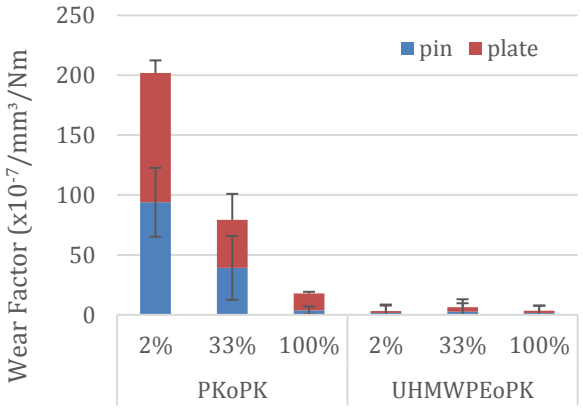

Figure 2: *Wear factors ($x10^{-7}$) mm^3/Nm for PKoPK and UHMWPEoPK bearing couples under 2 %, 33 % and 100 % BCS. Error bars represent ± SD.*

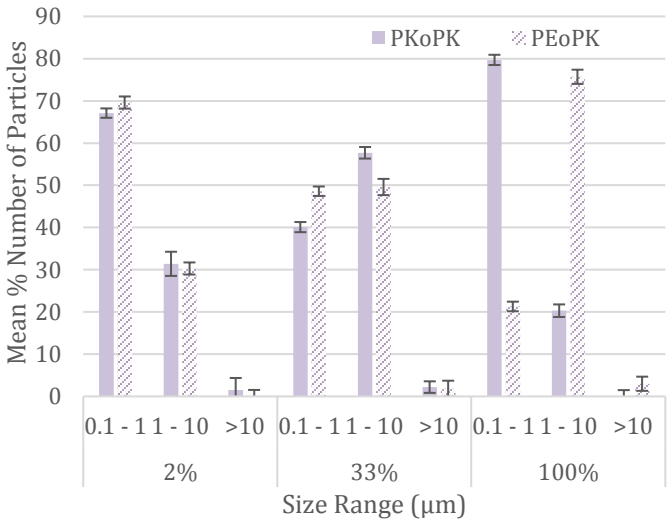

Figure 3: *PKoPK and PKoPE frequency distribution as a function of particle size generated from a multi-directional motion PoP rig with 2 %, 33 % and 100 % BCS protein concentration as the lubricant. Error bars represent ± SD.*

References

[1] NJR, 2017
[2] Ingram *et al.*, 2004
[3] Matthews *et al.*, 2000
[4] Cowie *et al.*, 2016
[5] Baykal *et al.*, 2016
[6] Saikko, 2003

Medical Imaging of an All-polymer Total Knee Arthroplasty

Janssen, D[1]; Briscoe, A[2]; Fascia, D[3]; Verdonschot, N[1,4]
[1]Orthopaedic Research Lab, Radboud umc, Nijmegen, The Netherlands; [2]Invibio Ltd, Thornton Cleveleys, UK; [3]Harrogate and District NHS Foundation Trust, Harrogate, UK; [4]TechMed Centre, Twente University, Enschede, The Netherlands
Dennis.Janssen@radboudumc.nl

Introduction: Polyetheretherketone (PEEK) has been proposed as an implant material for femoral total knee arthroplasty (TKA) components. Combined with an all-polyethylene tibial component, this allows for metal-free knee reconstructions. From a radiological point of view, a metal-free TKA opens up a range of opportunities, but it also requires a different approach for evaluating the images required by standard imaging modalities, such as radiographs, computed tomography (CT) and magnetic resonance imaging (MRI). One potential benefit of an all-polymer TKA is the early observation of adverse events, which may otherwise have been obscured by metal artefacts.
The objective of this study was therefore to evaluate imaging modalities for investigating all-polymer TKA reconstructions.

Methods and Materials: A pair of cadaveric knees (male, 92) was implanted by an experienced orthopaedic surgeon with a cemented PEEK Optima® Freedom Total Knee (right knee), combined with an all-poly tibial component (Maxx Orthopedics, Inc, USA). The left knee was implanted with a standard CoCr femoral component, and an all-poly tibial component.
After placing the components, the joint was irrigated with saline, after which the joint cavity was closed with sutures. Additional saline was then introduced in the joint cavity to simulate synovial fluid. Care was taken to prevent entrapped air in the joint cavity as much as possible.
Next, the reconstructions were analyzed using radiographs, CT, and MRI (PD, T1, T2, and STIR) scans, following previously established protocols.

Results: While the CoCr component obscured most of the femur on the radiographs, the radiopaque bone cement was clearly visible under the PEEK femoral component, due to its radiolucency (Figure 1). The PEEK implant itself was more difficult to discern on the radiographs.

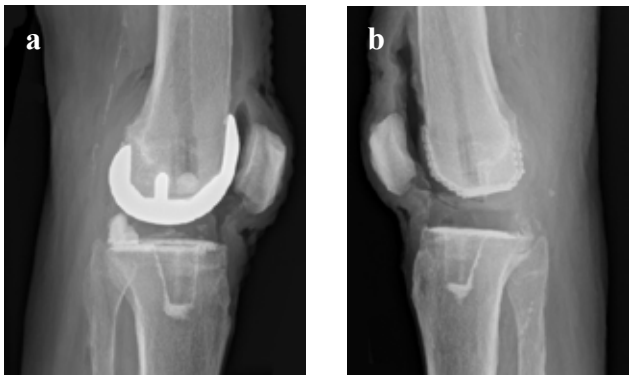

Figure 1 Mediolateral radiographs of the knees implanted with (a) the standard CoCr implant, and (b) the PEEK Optima femoral component. The PEEK component facilitated visualization of the radiopaque cement layer.

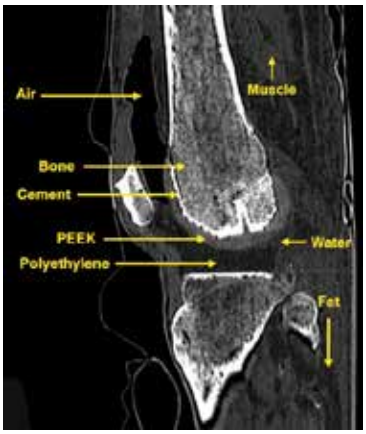

Figure 2 CT scanning of the reconstruction with the PEEK femoral component facilitated visualization of the femoral and tibial implant, cement, water, and entrapped air.

CT imaging of the PEEK component facilitated visualization of most of the structures around the knee joint, including the PEEK and polyethylene components, and the femoral and tibial cement mantles (Figure 2).
The CoCr femoral component caused significant distortions in the MRI images, which were absent in the images of the PEEK components (Figure 3). The PEEK component itself appeared as a black shape on the images, but was delineated by the surrounding fluids.

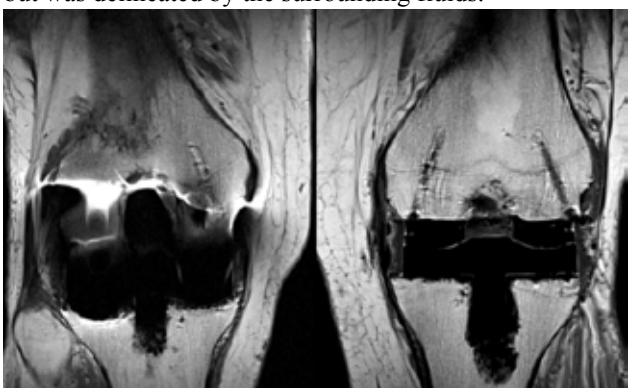

Figure 3 MRI images of the CoCr (left) and PEEK femoral components, with noticeable distortions around the CoCr implant.

Discussion: Orthopaedic surgeons often rely on medical imaging for the evaluation of implant performance. The use of a radiolucent PEEK femoral TKA component results in radiological images that are different from images of standard metal (radiopaque) implants. Due to the near total absence of artefact, PEEK opens up new horizons for imaging the previously shielded bone-cement-implant interface, potentially offering better follow up of implants and earlier detection of periprosthetic complications.

The Role of Contact Mechanics on the Fretting Corrosion Performance of PEEK-Metal Taper Junctions

Stephanie Smith[1], Jeremy L. Gilbert, Ph.D.[1]
[1]Department of Bioengineering, Clemson University, Charleston, SC 29425
ss6@clemson.edu

Introduction: Fretting corrosion, or mechanically-assisted crevice corrosion (MACC), of metallic orthopedic implants is a well-documented process that may have detrimental effects on the surrounding biological environment in vivo. Previous studies of modular head/neck taper seating mechanics[1] fretting corrosion performance on a low-modulus, low-hardness PEEK composite[2] at the modular taper junction of total hip replacement devices has shown significant reductions in fretting corrosion damage to the contacting metal surfaces in vitro. This raises the potential to effectively protect alloy surfaces and minimize the damage associated with MACC using low hardness polymer gaskets. The goal of this study is to evaluate PEEK's ability to minimize fretting corrosion damage and alter the contact mechanics under stress conditions relevant to modular taper junctions in vivo.

Methods and Materials: A custom *in vitro* pin-on-disk fretting test setup[2] was used to test couples made from PEEK pins (Vitrex 381G) and Ti6Al4V disks, a commonly used implant alloy. Each sample was tested in a variable-load pin-on-disk fretting test where 100 seconds of cyclic fretting motion (<100 μm, 1.25 Hz) was applied, between subsequent rest periods, under incrementally increasing normal loads (0.5-50 N). Pin displacement, normal and tangential forces, and coefficient of friction (COF) were collected every 50 s. Nominal contact area was measured before testing and true contact area measured after, both microscopically. Sticking forces (i.e. the lowest applied normal force that minimizes displacement and fretting currents), system setup stiffness, and work done per fretting cycle were calculated from the data collected. Three replicates were tested, using separate pins and disks. One- and two-way analyses of variance with post- hoc Bonferroni-corrected student t-tests were performed on all parameters to determine significant differences between the samples tested and controls (Ti6Al4V pins and disks of comparable dimensions, $p < 0.05$).

Results: Sticking forces, pin stiffness, and system stiffness were significantly lower for PEEK pins tested, compared to Ti6Al4V controls (Fig. 1, $p < 0.05$). Average displacement during fretting dropped in a more consistent manner than controls, decreasing immediately after approximately 0.5 N compared to a more gradual decline seen in controls (Fig. 2). Work of fretting (WOF), the amount of mechanical energy dissipated during one fretting cycle, were approximately 3.5-5 times lower than those of Ti6Al4V couples at comparable loads (data not shown). COF values at each normal load were approximately 2-4 times lower for PEEK tests than Ti6Al4V, on average (Fig. 2). Fretting currents remained at baseline levels throughout testing (Fig. 3), regardless of applied normal load, indicating no measurable surface abrasion on disk samples occurred.

Discussion: Lower sticking forces seen in PEEK pins are largely caused by its increased compliance, governed primarily by modulus and pin geometry. Pin compliance is also partly responsible for the disparities in WOF measurements of both groups, as a more compliant pin will elastically bend more as it is loaded during fretting, reducing the overall pin displacement (Fig. 2). PEEK effectively reduced COF of the interface compared to controls and kept it more consistent over the testing period. This is likely due to the creation of oxide debris at the interface resulting from surface abrasion, which caused COF to drop off at around 6N in controls (Fig. 3). The altered contact mechanics and lack of surface damage caused by PEEK pins, as well as the material properties itself are likely responsible for these discrepancies. Fretting currents that are recorded during testing as a means of quantifying the surface damage that results from induced fretting corrosion, which is dependent on oxide film disruption and electrolyte exposure. Therefore, the lack of fretting current (regardless of normal load), as well as negligible post-fretting surface damage observed on both pins and disks compared to controls suggests that the unique properties of PEEK may be responsible. The relatively low hardness of the polymer does not allow it to disrupt the oxide film of the metal surface, and its low modulus allows for more elastic sticking displacement prior to sliding, creating a more compliant interface. Combined, these material factors limit the observation of fretting corrosion damage.

Conclusion: The use of PEEK in the above study indicates minimal oxide film disruption of Ti6Al4V surfaces can be achieved under typical in vitro fretting corrosion conditions. This is likely attributed to the material properties of PEEK, mainly its hardness and modulus, creating a less abrasive, more compliant interface that prevents sliding motion during fretting. The use of PEEK in this way can effectively insulate metal surfaces from fretting corrosion damage at stresses comparable to those imparted on modular taper junctions, and may be viable in design modifications that mitigate the associated risks of MACC in current modular taper junctions while preserving their innate advantages. Future work includes testing similar PEEK pins on CoCrMo disks, as well as long-term tests using PEEK composites as an interfacial thin film between metal surfaces.

References: 1. Pierre et al. J Arthop, in process. 2. Ouellette and Gilbert, Clin. Orthop. Relat. Res. 3. Swaminathan and Gilbert, Biomaterials, 2012.

Pin Type	Sticking Force (N)	Pin Stiffness (N/m)	System Stiffness (N/m)
PEEK	4.67 (0.94)	9.15E+03 (6.6E+02)	2.94E+04 (4.0E+03)
Ti6Al4V	7.17 (0.24)	6.44E+08 (1.9E+07)	1.29E+06 (8.9E+04)

Figure 1: Average sticking forces, pin stiffnesses, and system stiffnesses for PEEK pins and control titanium pins, both tested on titanium disks. Standard deviation in parentheses. Each parameter was significantly different than controls ($p < 0.05$).

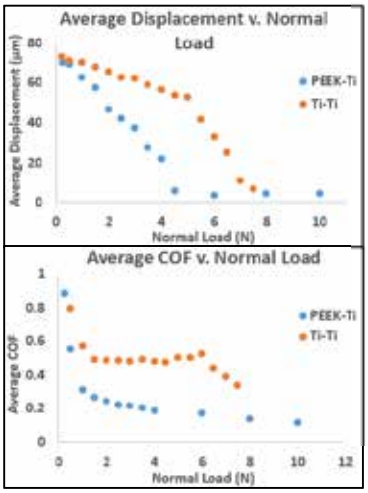

Figure 2: Average displacement and COF v. normal loads for PEEK and control pins (n = 3).

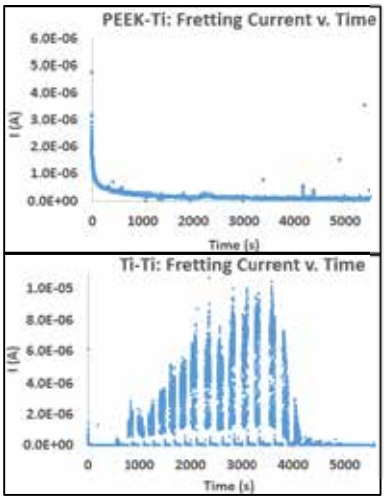

Figure 3: Fretting current v. time plots for one sample of PEEK-Ti6Al4V pin/disk couple (top) and Ti6Al4V-Ti6Al4V couple (bottom). Each 100-second current spike occurred at increasing normal loads in-between 100-second rest periods, allowing the current to recover.

Does Annealing Improve the Interlayer Adhesion and Structural Integrity of FFF 3D printed PEEK Lumbar Spinal Cages?

Cemile Basgul[1], Tony Yu[1], Daniel W. MacDonald[1], Ryan Siskey[1,2], Michele Marcolongo[1], Steven M. Kurtz[1,2]
[1]Drexel University, [2]Exponent, Inc.

Statement of Purpose: Polyaryletheretherketone (PEEK) has been commonly used for interbody fusion devices because of its biocompatibility, radiolucency, durability, and strength. Although the technology of PEEK Additive Manufacturing (AM) is rapidly developing, post-processing techniques of 3D printed PEEK remain poorly understood. AM of PEEK has been challenging because of its high melt temperature (over 340°C) and requires specialized equipment which was not commercially available until recently. A lumbar fusion cage design, used in ASTM interlaboratory studies, was 3D printed with a medical grade PEEK filament via Fused Filament Fabrication (FFF) under two different print speeds. Cages were then annealed at two different temperatures to understand whether annealing helps with undesired porosity and interlayer adhesion in 3D printed PEEK cages. **Methods:** We used a reference intervertebral lumbar cage design developed for ASTM interlaboratory studies. Cages were printed from a prototype medical grade PEEK OPTIMA LT1 (Invibio, UK) filament (1.75 mm) with two different speeds (1500 and 2000 mm/min) using a 3D printer customized for PEEK, HPP155 (Apium Additive Technologies, Germany). They were then annealed at above PEEK's glass transition temperature, at 200°C or 300°C. [1] According to ASTM F2077 [2], six cages for each cohort were tested under compression and torsional loading conditions. Maximum values were recorded for each test condition and stiffness values were calculated. SEM images were captured both before and after annealing from the cages' surfaces of each cage cohort to visualize the pores. In addition, three cages from each cohort were μCT scanned at 10 μm uniform resolution using a Scanco μCT 80 (Scanco, Switzerland) to determine the overall porosity. A control volume (5x5x2 mm^3) was created to measure the porosity from the scans. Statistical analysis was performed in SPSS 25 using Two-way ANOVA. **Results:** Under compression, there was not a significant main effect of speed on cages' ultimate strength ($p=0.49$), as well as annealing ($p=0.1$). Interaction between the effects of annealing and print speed on ultimate strength was not significant either ($p=0.86$). For stiffness on the other hand, although the main effects of speed and annealing were not significant ($p>0.05$), there was a significant interaction between the effects of annealing and speed ($p<0.01$). Cages' stiffnesses annealed at 200 ºC were higher than non-annealed and annealed at 300ºC cohorts under slower speed ($p=0.03$ & $p<0.01$, respectively). Neither main effect nor the interaction between the main effects were significant for maximum displacement. Under torsion, the main effect of annealing was significant on cages' both ultimate torque and stiffness values ($p<0.01$ & $p<0.01$, respectively). Additionally, the interaction between speed and annealing for both was significant as well ($p=0.02$ & $p=0.03$, respectively). Annealed cages at 300ºC and non-annealed ones showed higher ultimate torque compared to cages annealed at 200ºC under slower speed ($p<0.01$ & $p<0.001$, respectively). However, non-annealed cages' stiffness was decreased by both annealing conditions for printed cages under slower speed ($p<0.01$). Neither the main effects of annealing and speed, nor the interaction between the speed and annealing were significant on maximum angle cages failed under torque ($p>0.05$). SEM images showed the pores on the surface of the cohorts. According to the μCT scans, neither the main effects (annealing and speed) nor their interaction was significant on the porosity difference in cages before and after annealing ($p>0.05$). **Conclusions:** To the authors' knowledge, this is the first study to investigate annealing as a post processing method on 3D printed PEEK cages, as well as both the mechanical properties and microstructure of the cages. It was observed that annealing effect was more dramatic and significant on cages printed with slower speed, indicating printing in higher speeds, by not jeopardizing the undesired porosity in cages, might enhance the interlayer adhesion. Moreover, higher ultimate strength in cages annealed at higher temperature might be the indication of improved interlayer adhesion. Although the structure of the pores changed after annealing, annealing conditions examined here as a post-processing method were not able to decrease the undesired porosity formed during the 3D printing process. The results of this study demonstrate the effect of a post-processing method on 3D printed PEEK cages to investigate the deficiencies which were detected in the previous study. Our findings will lead researchers to further investigations on 3D printed implants and processing conditions. **References** [1] Kurtz SM. PEEK Biomaterials Handbook. 2011. [2] ASTM F2077-14, 2014. **Acknowledgement:** This study was supported by NIH-R01 AR069119. We would like to thank Invibio for donating the filament and Apium for their helpful advice and fruitful discussions.

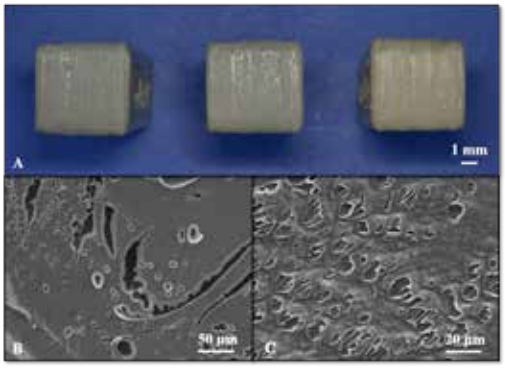

Figure 1. (A) 3D Printed cages; non-annealed, annealed at 200°C and 300 °C, from left to right. (B-C) SEM images showing porosity of a non-annealed (B) and annealed (C) cage surfaces at 300°C.

Relative effect of topography and chemistry on osseointegration

F. Brennan Torstrick[1], Angela S.P. Lin[2], Ken Gall[3], Robert E. Guldberg[2]
[1]Georgia Institute of Technology, Atlanta, GA, [2]University of Oregon, Eugene, OR, [3]Duke University, Durham, NC
brennan@gatech.edu

Introduction: Nearly 500,000 spinal fusion surgeries are performed each year in the U.S. Interbody fusion devices have been used for decades to facilitate fusion across the disc space, yet debate continues over the optimal material and structure used for these devices. Current cages are primarily made from PEEK due to its radiolucency and bone-like stiffness. However, current smooth PEEK cages are often associated with fibrous encapsulation and implant migration. This poor response is often attributed to inherent material properties of PEEK. However, the smooth surface of conventional PEEK surfaces may equally impede osseointegration, particularly when considering that rough and porous surfaces of various non-PEEK materials elicit more favorable osseointegration compared to smooth surfaces.

Methods and Materials: Porous PEEK implants were created as described previously [1]. Rough surfaces were created by soda-blasting PEEK surfaces and smooth surfaces maintained an as-machined surface finish. Half of each group was coated with a ~30 nm thick layer of TiO2 using atomic layer deposition (ALD) while the other half maintained their native PEEK chemistry. Sterile implants were implanted into the proximal tibial metaphyses of skeletally mature male Sprague Dawley rats [2]. At 8 weeks, animals were euthanized and bone-implant interfaces were subjected to µCT analysis (n=12), histology (n=4), and biomechanical pullout testing (n=8). All data were reported as mean±SE. Comparisons between groups were calculated using a 2-way ANOVA followed by a Tukey multiple comparisons test.

Results: Quantitative µCT analysis demonstrated that mineralized tissue ingrowth was 38.9 ± 2.8% for porous PEEK and 30.7 ± 3.3% for porous titanium ($p = 0.07$). µCT tomograms and matching histological sections showed bone ingrowth in porous titanium surfaces primarily consisted of thin bone shells that conformed to the pore walls, leaving the center of pores devoid of bone. In contrast, bone ingrowth within porous PEEK was greater in the center of pores with periodic contact with pore walls. Greater bone-implant contact was observed for titanium compared to PEEK surfaces. Histological and µCT observations were corroborated by biomechanics outcomes. Across all groups both surface chemistry and topography had a significant overall effect on pullout force ($p < 0.05$), but topography accounted for 65.3% of the total variance for pullout force ($\omega^2 = 0.653$), whereas surface chemistry accounted for 5.9% ($\omega^2 = 0.059$). Porous PEEK and porous titanium exhibited increases in pullout force compared to smooth and rough implants regardless of surface chemistry ($p < 0.05$).

Discussion: The poor osseointegration of conventional PEEK implants may be linked more to their smooth surface topography rather than their material composition. The effect of surface topography (specifically porosity) dominated the effect of surface chemistry in this study and could lead to further improvements in orthopaedic device design.

References: [1] Evans, Acta Biomater, 2015; [2] Agarwal, Biomaterials, 2015

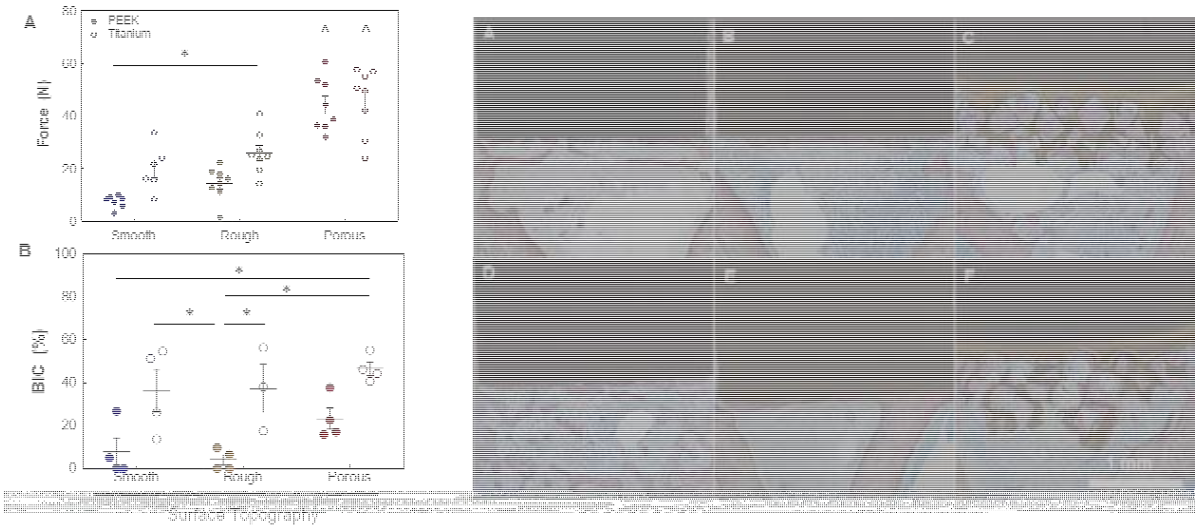

Figure 1: (A) Pullout force and (B) bone-implant contact of smooth, rough and porous PEEK possessing PEEK or titanium surface chemistry at 8 weeks. *p<0.05; ^p<0.05 versus smooth and rough groups, two way ANOVA, Tukey, n = 7). Mean ± SE.

Figure 2: Representative histological sections of the bone-implant interface at 8 weeks for smooth (A, D), rough (B, E), and porous (C, F) surface topographies. Each topography was implanted possessing its native PEEK surface chemistry (A, B, C) or TiO2 ALD surface chemistry (D, E, F). Bone appears pink. Length scale bar is 1 mm.

The effect of annealing and surface texture of 3D printed PEEK on MC3T3 E1 behavior

Cemile Basgul[1], Tony Yu[1], Sofia Escobedo[1], Daniel W. MacDonald[1], Michele Marcolongo[1], Steven M. Kurtz[1,2]
[1]Drexel University, [2]Exponent, Inc. Philadelphia, PA

Statement of Purpose: Polyaryletheretherketone (PEEK) has been commonly used for interbody fusion devices because of its biocompatibility, radiolucency, durability, and strength. Since the technology of PEEK Additive Manufacturing (AM) is rapidly developing, AM of PEEK has attracted much attention in the field of biomaterials. However, cell interactions of 3D printed PEEK remain poorly understood. AM of PEEK has been challenging because of its high melt temperature (over 340°C) and requires specialized equipment which was not commercially available until recently. 3D printed constructs were designed in this study using experimentally developed medical grade PEEK filament via Fused Filament Fabrication (FFF). Annealed 3D printed PEEK surfaces were also investigated. It was hypothesized that the rough and annealed surface texture of 3D printed PEEK would promote ALP activity of pre-osteoblast cells. **Methods:** PEEK constructs (10*10*1 mm^3) were developed for cell studies. PEEK surfaces were 3D printed from a prototype medical grade PEEK OPTIMA LT1 (Invibio, UK) filament (1.75 mm) with a 3D printer customized for PEEK, HPP 155 (Apium Additive Technologies, Germany). PEEK surfaces were divided into two group according to their position to the heated bed (100°C). Surfaces interacting with the heated bed were considered as smooth, whereas the top surfaces were considered as rough. Surfaces were then annealed at above PEEK's glass transition temperature, at 300°C. [1] The PEEK constructs were sterilized via UV light and 70% ethanol 3x for 30 minutes each. Samples were immersed in culture media overnight (Alpha-MEM, 10% fetal bovine serum, and 1% penicillin/streptomycin). MC3T3 E1 osteoblast-like cells (ATCC) were seeded onto the templates in 24-well plates at $3x10^5$ cells/well. Cells were evaluated at 7-day time point for MTT (Invitrogen), ALP (Abcam), and SEM. SEM samples were fixed with Karnovsky's solution (EMS), dehydrated in a series of ethanol concentrations, and then dried with hexamethyldisilazane overnight. For the MTT assay, the tetrazolium dye MTT was added to each sample for 4 hours. The formazan was then solubilized in dimethyl sulfoxide (Sigma) and read in the TECAN at 540 nm [2]. In the ALP assay, p-nitrophenyl phosphate (pNPP) was added to each sample for an hour. The secretion of ALP from the cells cleave the pNPP, which turns yellow when dephosphorylated. The solution was read in the TECAN at 405 nm [3]. Two-way ANOVA with Tukey post hoc multiple comparison analyzes were performed on MTT and ALP activity to determine statistical significance ($p<0.05$) among the different groups. **Results:** The PEEK constructs were printed on a heating bed, which resulted in two distinct surface roughnesses. The top side had a roughness of 3.20 μm and the bottom side had a roughness of 0.401 μm. Cells seeded on the rough side seemed to be more integrated with the PEEK surface as illustrated in the SEM images. On the other hand, the cells on the smooth surface were attached but not integrated. The cell and surface integration on the rough side of the PEEK constructs increased ALP activity by 66% and 33% compared to the cells on the smooth side of the non-annealed and anneal samples, respectively. Interestingly, the smooth side resulted in 20% higher cell proliferation than the rough side, indicating that the amount of ALP enzyme secrete per cell on the rough side was ~2x higher compared to the smooth side of the non-annealed samples. Similarly, on the annealed samples, the cells on the rough side increase in ALP per cell by ~1.3x of the cells on the smooth side. Surprisingly, there was no statistical difference in MTT or ALP between non-annealed and annealed samples. **Conclusions:** Although annealing PEEK constructs under these conditions did not influence cell metabolic activity, increased surface roughness increased production of the bone protein, ALP, while reducing cell proliferation compared to smooth surfaces.

References: [1] Kurtz SM. PEEK Biomaterials Handbook. 2011. [2] Niks, J Immunol Methods. 1990:12(149-151). [3] Frohbergh, ME. Biomaterials. 2012:33(9167-9178). **Acknowledgement:** This study was supported by NIH-R01 AR069119. We would like to thank Invibio for donating the filament and Apium for their helpful advice and fruitful discussions.

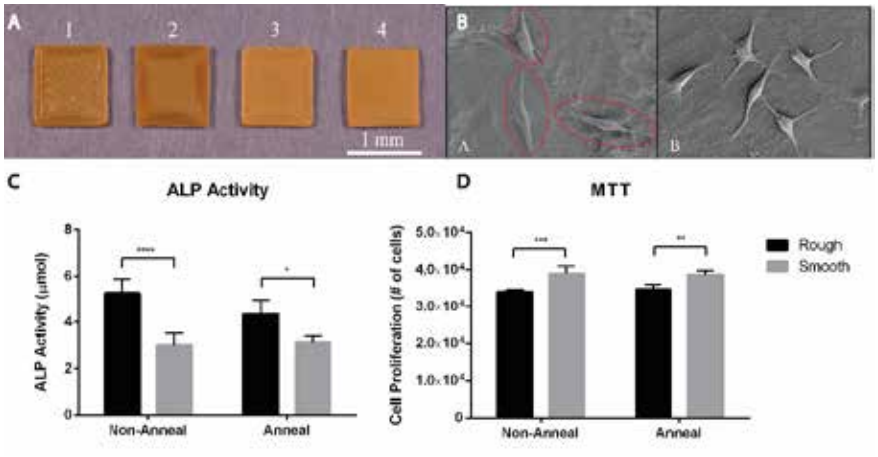

Figure 1: A) Images of PEEK constructs: 1. Non-annealed, rough; 2. Non-annealed, smooth; 3. Annealed, rough; 4. Annealed, smooth. B) SEM of MC3T3 E1 cells seeded on PEEK

constructs: a. Non-annealed, rough; b. Non-annealed, smooth. C) ALP activity of cells seeded on PEEK constructs. D) Cell proliferation of MC3T3 E1 cells seeded on PEEK constructs. * ($p<0.05$), ** ($p<0.01$), *** ($p<0.005$), **** ($p<0.001$) statistically significant.

Interim Report of Clinical Outcomes for 1 & 2 level ACDF utilizing the STALIF C and STALIF C-Ti Integrated Interbody device(s): A Prospective, Non-Randomized Study

Jad Khalil, MD[(1);] Rick Sasso, MD; [(2)] Ryan Snowden, MD[(2)]; Brad Webb, DO[(1)]; Sheetal Vinayek, M.Sc., CCRP[(2)]; Lisa Motowski, RN, BSN, CCRP[(1)]

[(1)]Michigan Orthopedic Institute, Southfield, MI 48033; [(2)]Indiana Spine Group, Carmel (Indianapolis), IN 46032

jad.khalil@beaumont.org

Introduction: Anterior cervical discectomy and fusion (ACDF) is an effective, reliable, and safe treatment modality for the treatment of cervical disc disease. However, there is very little in the literature concerning outcomes data on "stand-alone" cervical devices. This study presents our results from the first prospective, non-randomized evaluation of patients undergoing 1 and 2 level anterior cervical fusions with an integrated interbody device (STALIF C & STALIF C-Ti – Centinel Spine, West Chester, PA).

Methods and Materials: 53 patients approved by the IRB were included into the study for the treatment of anterior cervical discectomy and fusion (1 and 2 levels) with an integrated interbody device. All patients reached a minimum of 12 months of follow-up. We obtained baseline clinical exams, Neck Disability Indices (NDI), Visual Analog Scores (VAS) and EAT Dysphagia score on all patients at the following time points: preoperative, 6 weeks, 3 months, 6 months and 12 months postop. EAT-10 was considered abnormal if greater than 3.

Results: All patients underwent 1 and 2 level ACDF procedures. Of the 53 total patients, 41 patients underwent single level fusion, and 12 patients underwent two level fusion. Average surgical times were 48 minutes and 68 minutes for 1 and 2 levels, respectively. There was no significant blood loss, and average length of stay was less than 24 hours. The average NDI scores were 54 preoperatively and were significantly improved at each following time-point ($<p=0.001$). VAS scores were 72/48/48 for neck/right arm/left arm pain pre-operatively, and showed significant improvement at each following time-point ($<p=0.001$) (FIGURE 1). Nine patients had abnormal EAT-10 scores at the 6 week postop visit; with the average score of 2.3. All patients with dysphagia improved and the highest EAT Score at 12 months was 4. The average EAT-10 score improved from 2.3 to 0.295 ($p=0.001$) at 12 months (FIGURE 2). There were no hardware failures or adverse surgical outcomes.

Conclusion: Successful anterior cervical fusion is dependent upon many factors. In the age of value based healthcare delivery, it is important to mitigate the potential complications of healing. This study is the first to show the successful, prospective outcomes of an integrated interbody device in a cervical spine fusion model. It shows patient reported outcomes consistent with previously reported results and rates of dysphagia consistent with, or lower than reports of standard ACDF.

FIGURE 1

	Time Point				
	PreOP	6 weeks	3 month	6 month	12 month
Outcome Score					
NDI	54.3	36	29.9	25.9	26.9
VAS NECK	71.9	33.7	30.9	29.5	26.9
VAS RIGHT ARM	47.6	25.5	19.8	17.3	26.3
VAS LEFT ARM	47.8	19.9	19.9	16.8	22.6

All time points were significantly improved from preop, p<0.05

FIGURE 2

	Time Points				
	PreOP	6 weeks	3 month	6 months	12 months
EAT-10	1.75	2.31	1.59	2.2	0.29^
Total Patients with abnormal EAT-10*	5	9	7	4	2

*** EAT-10 >3 considered abnormal**

^ p<0.5

Critical analysis comparation of TMJ PEEK prosthesis and Conventional TMJ Prosthesis

Wladimir Genovesi, Iara Cristina Comenale, Glaucia Faro

Introduction: The aim of this study is to show the difference between the PEEK LTI 20%Ba TMJ total joint prosthesis and conventional titanium TMJ prostheses—like: TMJ Concepts, Lorenz Biomet, Cristhensen and others. A new material, Polyether ether Ketone (PEEK), is a polymer derived from petroleum (Invibio, UK). It is thermoplastic, biocompatible, and inert and exhibits high stability and resistance. PEEK is successfully used as the material of choice for orthopedic and spine implants. This study demonstrates the feasibility of a custom TMJ prosthesis PEEK, a with protocol development for reconstruction of TMJ while comparing the results between PEEK and conventional prosthesis.

Methods and Materials: Twelve patients with PEEK TMJ prosthesis were compared with two patients with conventional titanium TMJ prosthesis. In 2012 Genovesi developed a TMJ prosthesis, after many laboratory, tests it was concluded that it would be perfect for use it in a human body. 6 years 8 months after the first surgery there were 12 patients with 19 surgeries. 7 patients had bilateral surgeries and 5 had unilateral operations. All procedures used PEEK ON PEEK prosthesis. For the comparison, this study included 2 patients that underwent bilateral surgeries, using titanium TMJ prosthesis (Lorenz, Biomet). 4 surgeries were done. All patients were followed for a period for 36 months. The patients were followed up and evaluated for criteria such as: mouth opening, lateral movements and protrusion. Plain radiography and CTs were also done during this period, in all patients. The surgeries were performed between 2012-2018. All patients had a TMJ problem, such as multiple TMJ surgeries, fibrous ankyloses and bone degeneration. The Mean age was 38 years. The surgery technique for PEEK LTI20%Ba prosthesis is less traumatic than the conventional surgery prosthesis. Making eminectomy, flatted with 90º. In the ramus, the osteotomy must be at the imaginary line in the sigmoid notch, with 15mm from the ankyloses mass or 15mm of the condylar articular surface, maintaining 90º with the long axis of the ramus. Also by the tunnelization of the prosthesis over the ramus. If necessary, a little incision of 1cm, in the posterior region of the mandible must be done to place the inferior screws.

After conducting studies on CT scans of 50 TMJs, 25 Male 25 Female, which measured the size of the Mandibular Ramus, from the Sigmoid Notch to the angle of the jaw, it was concluded that the average length is 470 mm. In the glenoid fossa, an average of 0.8 mm concave radius and length of lateral / medial 19 mm was obtained. The customized prosthesis was developed in PEEK LTI20%Ba, The screws were also developed in PEEK. This system of a customized TMJ (temporomandibular joint) prosthesis constructed in PEEK LTI20%Ba, was submitted for laboratories tests, to 2 different laboratories. The tests were performed by Lab Mat and Cenic Lab -authorized by ANVISA-, and had result of 100% effectiveness of the prosthesis model developed.

Discussion: Understanding that all TMJ prosthesis systems may help patients that need a joint replacement, but is known that the conventional 'titanium systems-UHMWP', have a short period of use. The PEEK LTI20%Ba prosthesis lets patients become more comfortable. It has a greater, shelf life and preserves all mandibular movements. The future is now, all materials in PEEK will substitute Titanium and UHMWP for hip prosthesis, knee and TMJ, as mini plates.

4TH International PEEK Meeting

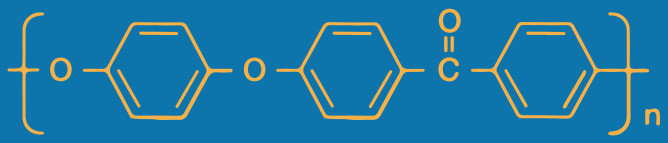

Thank you!

ORGANIZED BY

IRC IMPLANT RESEARCH CENTER

Exponent®

SPONSORED BY

Invibio BIOMATERIAL SOLUTIONS

Invibio
BIOMATERIAL SOLUTIONS

Advancing the Science of Implantable Devices

Invibio works closely with medical device manufacturers and healthcare professionals on innovations that make a positive impact on patient quality of life.

500+ PEEK-OPTIMA™ Devices FDA Cleared in the US alone

~9M PEEK-OPTIMA Devices Implanted Worldwide

15+ Years of Clinical History

EMERGING MEDICAL
(Craniomaxillofacial (CMF) and more)

DENTAL
(Restorative and prosthetic dentistry)

SPINE
(Spinal disorders)

ORTHOPEDIC TRAUMA
(Fracture fixation)

ORTHO
(Joint arthroscopy and arthroplasty)

Invibio.com

Copyright © 2019 Invibio Ltd. INVIBIO™, PEEK-OPTIMA™, JUVORA™, INVIBIO BIOMATERIAL SOLUTIONS™ are trademarks of Victrex plc or its group companies. All rights reserved.

a victrex company